EXPLORATION OF THE SOLAR CORONA BY HIGH RESOLUTION SOLAR DECAMETRIC OBSERVATIONS

R. V. BHONSLE, H. S. SAWANT, and S. S. DEGAONKAR
Physical Research Laboratory, Ahmedabad-380009, India

(Received 13 December, 1978)

Abstract. In this review, current state of knowledge of high resolution observations at decameter wavelengths of the quiet Sun, the slowly varying component (SVC), type I to V bursts and noise storms is summarized. These observations have been interpreted to yield important physical parameters of the solar corona and the dynamical processes around $2R_\odot$ from the photosphere where transition from closed to open field lines takes places and the solar wind builds up. The decametric noise bursts have been classified into (i) 'BF' type bursts which show variation of intensity with frequency and time and (ii) decametric type III bursts. The angular sizes of noise storm sources taking into account refraction and scattering effects are discussed. An attempt has been made to give phenomenology of all the known varieties of decametric bursts in this review. Available polarization information of decametric continuum and bursts has been summarized. Recent simultaneous satellite and ground-based observations of decametric solar bursts show that their intensities are deeply modulated by scintillations in the Earth's ionosphere. Salient features of various models and theories of the metric and decametric noise storms proposed so far are examined and a more satisfactory model is suggested which explains the 'BF' type bursts as well as conventional noise storm bursts at decametric wavelengths invoking induced scattering process for $l \rightarrow t$ conversion. Some suggestions for further solar decametric studies from the ground-based and satellite-borne experiments have been made.

Contents

Space Science Reviews **24** (1979) 259–346. 0038–6308/79/0243–0259$13.20.

1. Introduction

Solar radio noise storms at meter, decameter and longer wavelengths constitute perhaps one of the most spectacular manifestations of the complex plasma processes in the solar atmosphere. Noise storms have been extensively investigated by many workers using a variety of observational techniques. Different models of the noise storm sources have been proposed in order to arrive at better understanding of the physics of the noise storm sources; their birth, development and subsequent decay of their activity. Historically, the solar noise storm radiation was discovered accidentally by Hey in 1942 at meter wavelength. Through subsequent research efforts, it is now known that an enhanced emission from the Sun known as the solar radio noise storm lasting from hours to days occurs quite often during periods of high solar activity and its spectrum extends from decimeter to decameter wavelengths. With the advent of satellites in 1960's, the existence of noise storms comprising type III bursts in hectometer and kilometer wavelengths at 1 AU is also established. Even though the noise storm radiation was discovered as early as 1942 by Hey, their source size measurements were obtained only after the establishment of Nancay interferometer at 169 MHz in France in 1956. As early as 1958, attempts were made to determine the source size of decametric noise storm centers. Mean source sizes determined at 65 MHz and 45 MHz were 6′ and 10′ of arc respectively (Wild and Sheridan, 1958). Source sizes at decameter wavelengths decrease with increasing frequency and the decrease is faster as compared to that at meter wavelengths (Gergely and Kundu, 1975). Many reviews of noise storms have appeared in the literature (for example:

Wild *et al.*, 1963; Kundu, 1965; 1971; Zheleznyakov, 1970; Wild and Smerd, 1972; Fainberg and Stone, 1974; Newkirk, 1974; Elgaroy, 1977; Sawant, 1977). However, the present review paper is based on experimental observations and theoretical work done in the decametric region in which lot of new information has accumulated in the recent past both from ground-based and satellite-borne instruments.

2. Noise Storm Phenomena at Decametric Wavelengths

A metric and decametric storm consists of a smooth continuum radio emission, on which are superimposed narrow band short-lived type I bursts at metric wavelengths and type III bursts with or without fine structure at decameter wavelengths. Brightness temperature of the continuum and the burst may exceed 10^9 K. Obviously, thermal processes that are known to exist near the Sun cannot account for such high brightness temperatures. Gyrosynchrotron and plasma radiation processes are believed to be the nonthermal sources for such radiations. Both the continuum and superimposed bursts are circularly polarized in the same sense or in opposite sense. A high degree of circular polarization suggests the presence of strong magnetic fields up in the corona. Newkirk (1971) and Dulk and McLean (1978) have reviewed the current status of information on coronal magnetic fields based on calculations and inferences derived from radio and optical measurements. Noise storm centres are found to be associated with visible optical regions on the Sun's disk while some others seem to occur independently. In general, it is known that noise storm activity and flare activity are two aspects of a center of activity on the Sun though they may occur independently of each other.

Decametric noise storms are almost always associated with metric storms (Boischot *et al.*, 1970). The decametric noise storm continuum may be looked upon as a large number of type III bursts occurring in quick succession. Occasionally, varieties of fine structure in frequency and time are encountered. Earlier reviews on type III bursts can be cited for more detailed information (Wild and Smerd, 1972; Mattoo, 1973; Solar Radio Astronomy Group, Utrecht, Correspondent: de Groot, 1974; Smith, 1974).

Gergely and Kundu (1975) studied the characteristics of a decametric noise storm with the help of 65 to 25 MHz swept frequency interferometer at the Clark Lake Radio Observatory in U.S.A. They found two kinds of type III bursts, namely, 'On-fringe' and Off-fringe' types as shown in Figure 1. The 'On-fringe' type III bursts coincide in position with that of the associated continuum source. Starting frequencies of these bursts were below 50 MHz. They are generally weak in intensity and not associated with flares and occur over a frequency range of 30–20 MHz. Further properties of these bursts have been investigated by Aubier *et al.* (1978) and they have shown that these bursts are associated with type I activity and are more strongly polarized than normal type III bursts ('Off-fringe' bursts) with the sense of polarization same as that of related type I burst. 'Off-fringe' type III bursts are

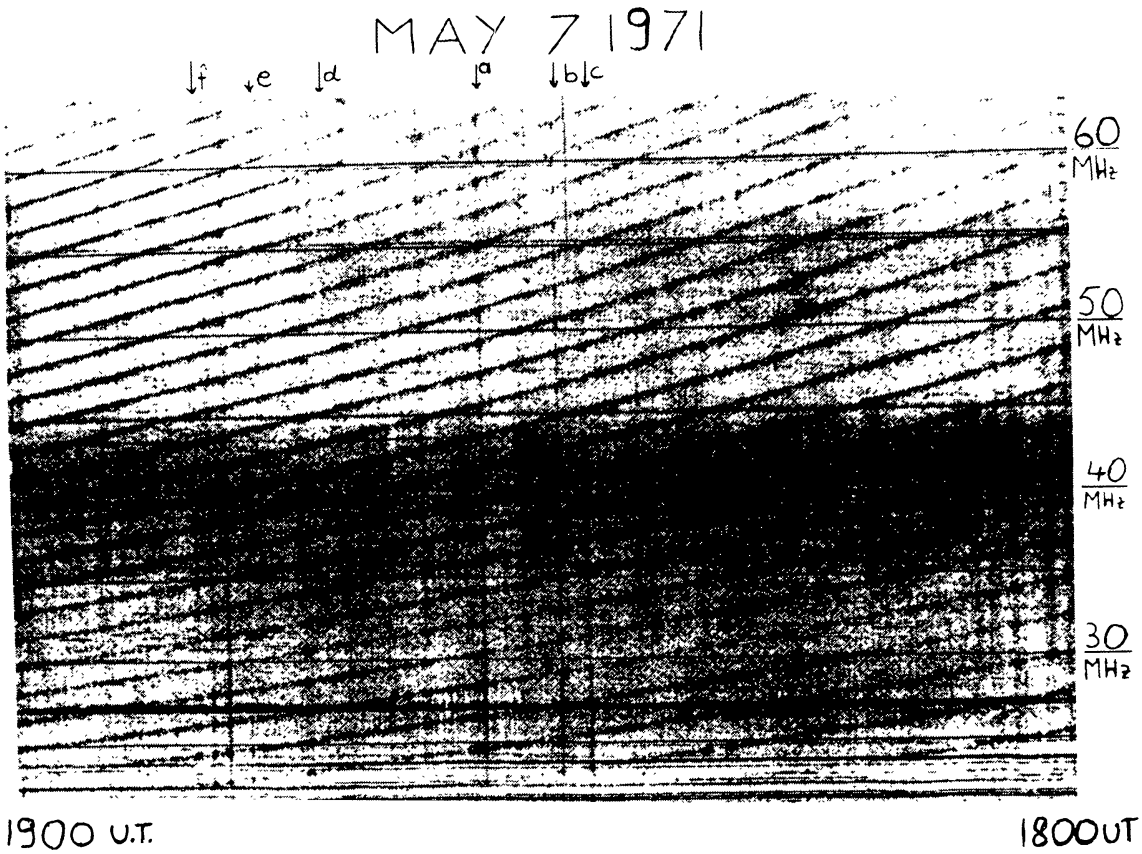

Fig. 1. 'On-fringe' and 'Off-fringe' type III bursts observed with the sweep frequency interferometer at Clark Lake Observatory, U.S.A., on 7 May, 1971, during decametric noise storm, *a*, *b*, and *c* are 'On-fringe', *d*, *e*, and *f* are 'Off-fringe' bursts (from Gergely and Kundu, 1975).

displaced from the position of the continuum by $0.1R_\odot$ to $0.5R_\odot$. Most of them are intense, generally associated with flares and appear all over the frequency range of 62–25 MHz.

Gergely and Kundu (1975), taking into account the effect of refraction and scattering (Fokker, 1965; Leblanc, 1973), determined the height and source sizes in the range 65 to 25 MHz. Figure 2 shows the distribution of source sizes obtained by Gergely and Kundu (1975). Mean source sizes were found to be $0.5R_\odot$ and $1.3R_\odot$ at 65 MHz and 30 MHz respectively. The heights were determined, by applying least square analysis method and assuming constant rotational rate of the source, which at 40 MHz and 30 MHz turned out to be $(1.9 \pm 0.5)R_\odot$ and $(2.3 \pm 0.25)R_\odot$ respectively. The variation of the source size with frequency is shown in Figure 3. It can be seen from the figure that the source size increases more rapidly in the decameter range than in the meter range. One of the characteristics of decametric noise storm sources is that the size of the source is not constant but changes over a short period of time. Moreover, changes in size at nearby frequencies are usually not correlated. Like the metric noise storm continuum, decametric noise storm continuum is found to have more directivity at the centre of the disk. The east–west asymmetry as observed in the metric band is also observed in the decametric band (Gergely and Kundu, 1975). A

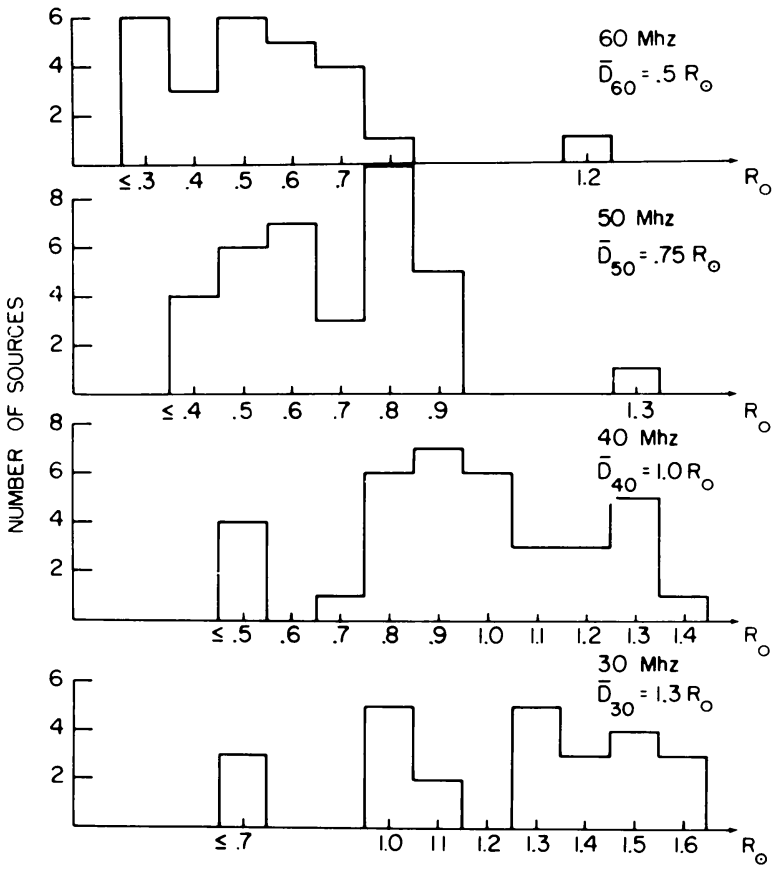

Fig. 2. Distribution of decametric source sizes at 60, 50, 40, and 30 MHz. Average source size at each frequency is indicated on the right. Note that the source size increases as the frequency decreases (from Gergely and Kundu, 1975).

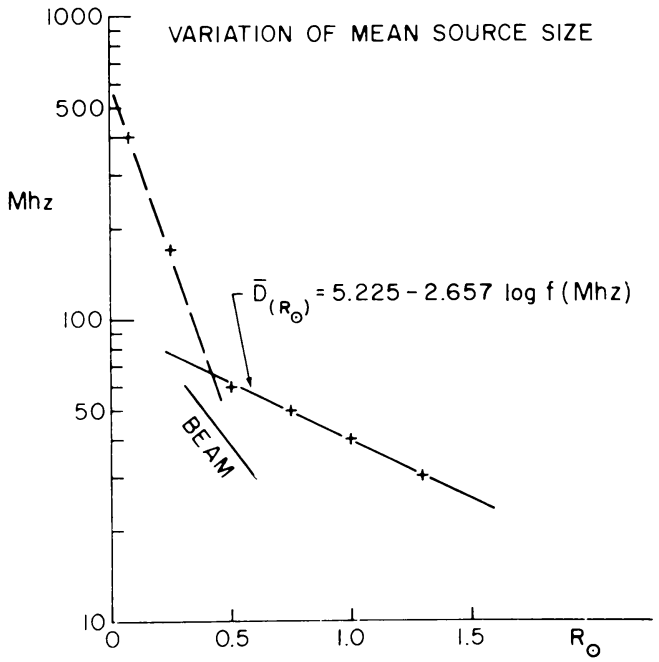

Fig. 3. Variation of mean source sizes as a function of frequency in the decimeter–meter and decameter ranges. Thick continuous line indicates the size of the beam in the 65–20 MHz range (from Gergeley and Kundu, 1975).

comparison with the model of Newkirk (1967) and other models (see Figure 4) obtained from radio observations (Wild *et al.*, 1959; Weiss, 1963; Malitson and Erickson, 1966) shows that the storms originate in moderately low to high density regions. Although directivity information of the decametric noise storms are becoming available only recently (Steinberg, 1977), polarization information of the decametric noise storms are very scanty.

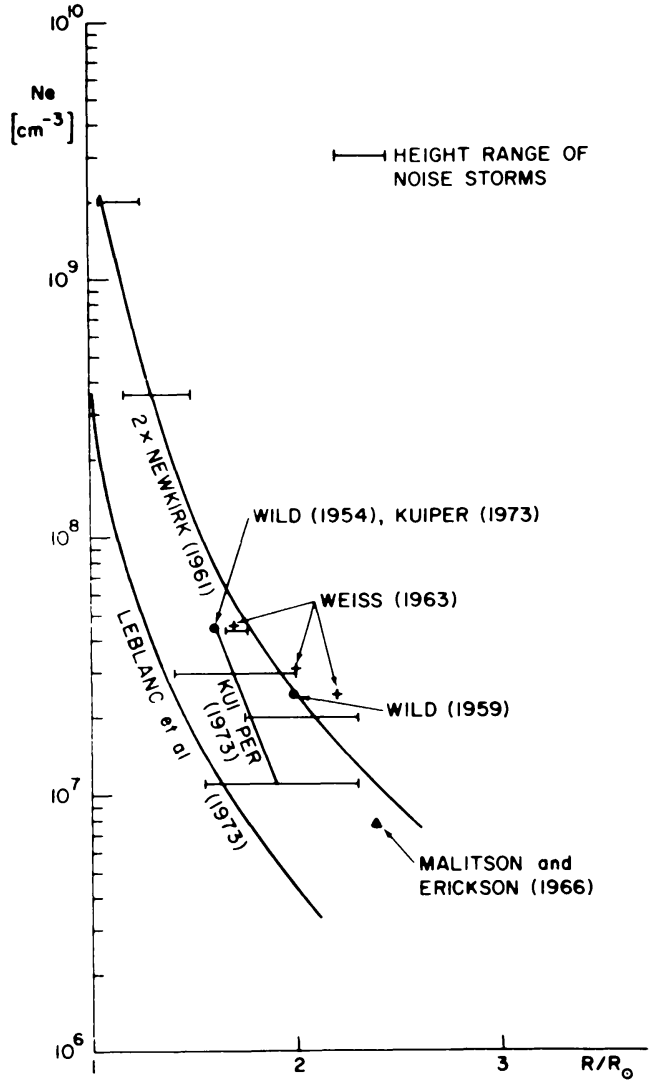

Fig. 4. Different electron density models of the corona. Heights where the decametric storms originate are shown by horizontal bars (from Gergely and Kundu, 1975).

Resolution in time and frequency comparable to that observed in metric band was not realized in the decameter band till late 1960's. Ellis and McCulloch (1966) initiated high resolution (simultaneously in time (20 ms) and frequency (30 kHz)) observations in the range 36–28 MHz. High sensitivity observations in the decametric range were initiated by de la Noë and Boischot (1972) along with high resolution in time (10 ms) and frequency (60 kHz).

TABLE I

The low frequency radio spectrum of the quiet Sun, determined during July, 1976[a]

Frequency (MHz)	Assumed Tau A flux (Jy)	Uncorrected solar flux (10^3 Jy)	Assumed solar diameter (arc min)	Visibility	Visibility correction				
					(a) Gaussian		(b) Uniform disk		
					Peak brightness temp. (10^6 K)	Corrected solar flux (10^3 Jy)	Visibility	Disk brightness temp. (10^6 K)	Corrected solar flux (10^3 Jy)
109.0	1800	18.6±1.3	35′	0.68	0.93	27.4±1.9	0.86	0.73	21.6±1.5
73.8	2000	8.5±1.2	40′	0.78	0.62	10.9±1.5	0.92	0.52	9.3±1.3
57.7	2300	5.5±0.5	44′	0.85	0.49	6.4±0.5	0.94	0.44	5.8±0.5
38.1	2500	1.5±0.3	48′	0.90	0.24	1.6±0.4	0.96	0.22	1.5±0.3
25.8	2900	1.4±0.3	50′	0.96	0.44	1.5±0.3	0.98	0.43	1.5±0.3
19.0	3700	1.1	55′	0.98	0.50	1.1	0.99	0.49	1.1

[a] From Erickson *et al.* (1977).

2.1. The quiet sun decametric radiation and isolated type III bursts

Measurement of flux density and brightness distribution of the quiet Sun provides a very useful method in obtaining the information of density and temperature of the corona. Because of instrumental limitations, the quiet Sun observations in decameter wavelengths are scanty (O'Brien, 1953; Aubier *et al.*, 1971). Aubier *et al.* (1971) carried out these measurements with the large Arecibo dish at 29.3, 36.9, and 60 MHz. The observed fluxes were 0.33, 0.40, and 1.03 solar flux units (1 sfu = 10^{-22} W m^{-2} Hz^{-1}). The coronal temperatures deduced from these fluxes are of the order of 0.5×10^6 K. They have explained these low temperature values as due to the effect of scattering by an irregular corona.

Erickson *et al.* (1977) have accurately determined the decameter wavelength spectrum of the quiet Sun in the range 109–19 MHz. Their results for flux and brightness temperature at various frequencies are given in Table I. The flux of the

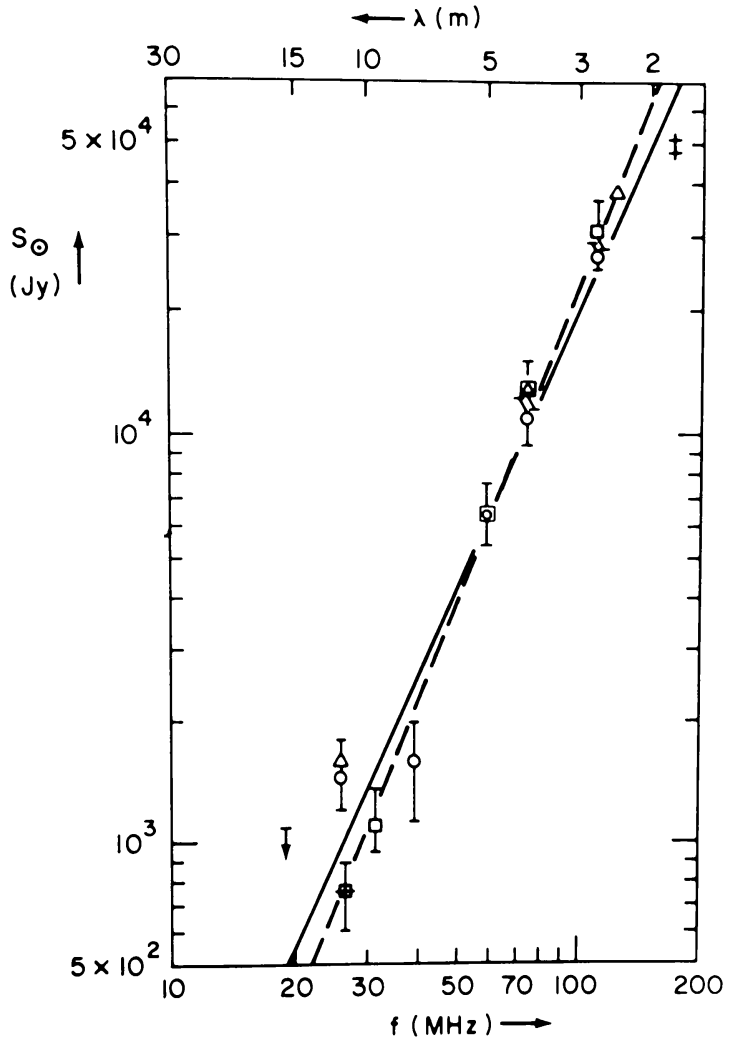

Fig. 5. Spectrum of the quiet Sun obtained from various observation at low frequencies. Full line represents best fit to all data points. Spectral index is about +2.3. The dashed line represents best fit neglecting the higher values obtained at 25.8 MHz (from Erickson *et al.*, 1977).

Sun has been compared with that of strong decametric sources Taurus A and Virgo A. Assuming a gaussian shape for the solar brightness distribution at decameter wavelengths, the flux density spectrum obtained by them is shown in Figure 5. The equation to the best fit (full line) to all data points is given by

$$\log S_0 = -0.2(\pm 0.21) + 2.25(\pm 0.12) \log F, \tag{1}$$

where S_0 is the solar flux in Jansky (1 Jy = 10^{-26} W m^{-2} Hz^{-1}) and F is in MHz. The spectral index of the quiet Sun at solar minimum in the frequency range 109–19 MHz is found to be about +2.3.

Kundu *et al.* (1977) made use of the meter and decameter observations of the quiet Sun on a few quiet days in 1975 and 1976 using the E–W and N–S arms of the large array at Clark Lake to obtain solar brightness distribution. From the observed total fluxes and half-power diameters, they derived the peak brightness temperatures of the solar disk and also of sources of the slowly varying component. Figure 6a shows

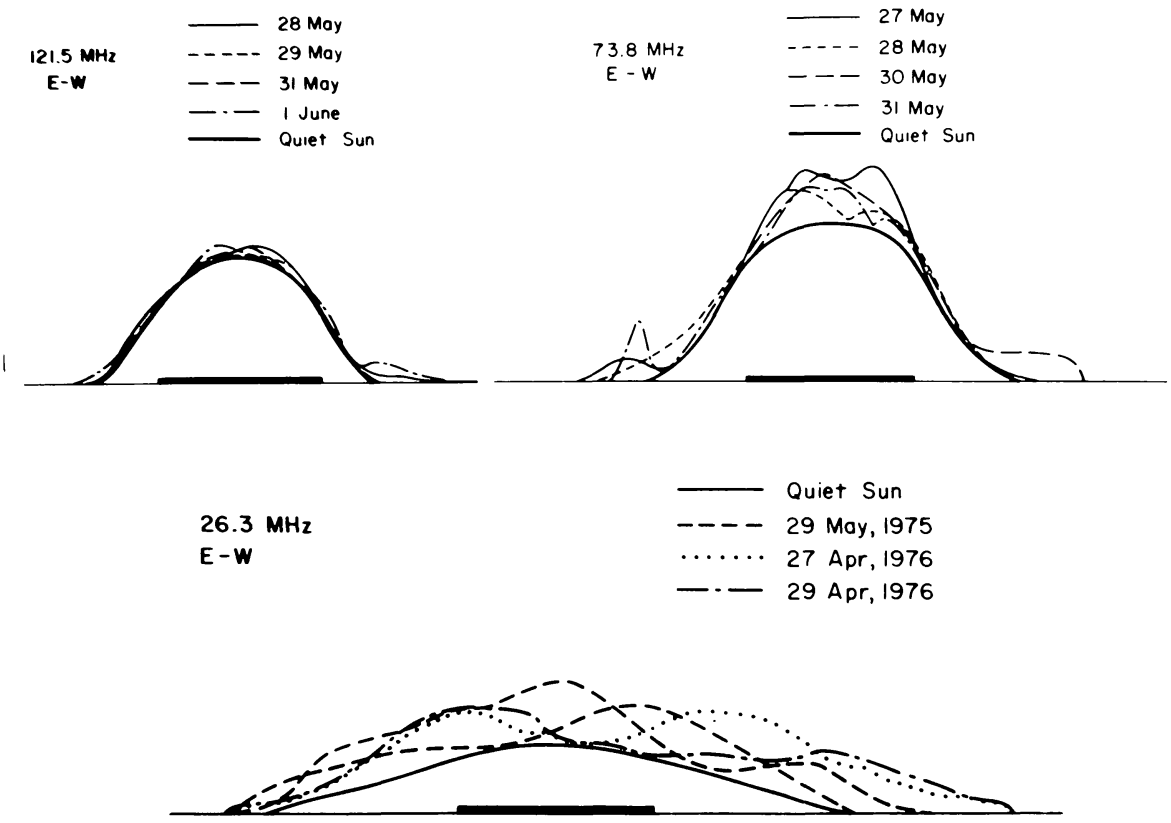

Fig. 6a. Brightness distributions of the Sun along east-west direction at 121.5, 73.8 and 26.3 MHz are shown. The lowest envelope shows the quiet Sun brightness distribution. The extent of the optical disk is shown by heavy horizontal line (from Kundu *et al.*, 1977).

the scans of brightness distribution of the Sun in the E–W direction at 121.5, 73.8, and 26.3 MHz. The lowest envelope shows the quiet Sun brightness distribution and the extent of the optical disk is shown by heavy horizontal line. The day to day

variability in brightness distribution in the decametric range is much more than that seen in the metric wavelengths. The limb brightening observed in the centimeter and decimeter wavelengths is found to be absent in the decameter range as in the metric range. Figure 6b shows similar curves in the N–S direction.

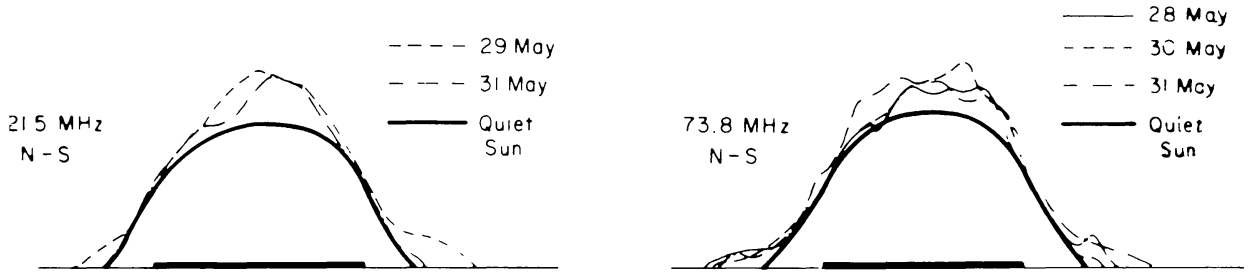

Fig. 6b. Similar curves as shown in Figure 6(a) in north-south direction at 121.5 and 73.8 MHz (from Kundu *et al.*, 1977).

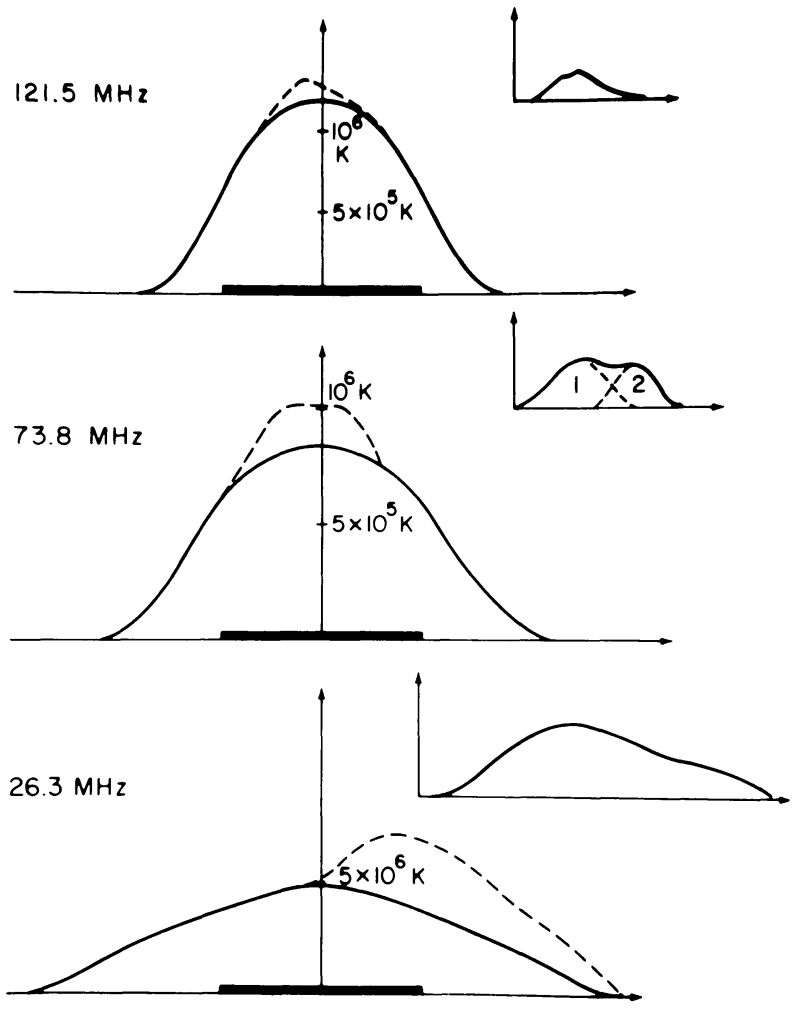

Fig. 7. One dimensional brightness distribution scans at 121.5, 73.8, and 26.3 MHz are shown by continuous line and the SVC part by the dotted line. Thick horizontal line shows the extent of the optical Sun. The inset curves show only the SVC component which in the decametric range is observed for the first time. The SVC component at 73.8 MHz appears to be made up of two sources (from Kundu *et al.*, 1977).

Apart from the quiet Sun brightness distribution, source of the slowly varying component (SVC) is identified for the first time in the decametric range (Kundu *et al.*, 1977). This is shown in Figure 7 along with its metric counterpart. The details of the source fluxes, half-power diameter, etc. are given in Table II. The sources appear to

TABLE II

Sources of the slowly varying component[a]

Frequency (MHz)	121.5	73.8		26.3
		Region 1	Region 2	
Half-power diameter (arc min)	11′.2	8′.3	5′.1	19′.4
Total flux ($W\,m^{-2}\,Hz^{-1}$)	1.4×10^{-23}	6.4×10^{-24}	3.6×10^{-24}	5.4×10^{-24}
Peak brightness (temperature (K))	7.2×10^{5}	8.4×10^{5}	1.3×10^{6}	1.0×10^{6}
Confusion limit ($W\,m^{-2}\,Hz^{-1}$)	1.0×10^{-25}	2.0×10^{-25}		6.0×10^{-25}

[a] From Kundu *et al.* (1977).

be meter–decameter wavelength extensions of SVC of solar radio emission observed at cm–dm range. Chiuderi *et al.* (1972) and Dulk *et al.* (1977) have pointed that the temperatures and densities derived from EUV observations are consistently higher by three times than those derived from radio brightness measurements. This discrepancy persists even with the accurate measurements obtained by Erickson *et al.* (1977).

Above the quiet Sun background, isolated weak type III bursts at 60, 36.9, and 24.3 MHz have been observed by Aubier and Boischot (1972). From the observed time profiles, they obtained the average values of exciter function duration at the three frequencies as 3.9, 6.2, and 7.5 s respectively and the average decay time constant of 2.0 s at all the three frequencies. A relationship was established between the duration and the decay time constant of type III bursts. It was shown that the coronal temperatures derived from the decay time constant of type III bursts at 29.3 MHz, with the assumption of collisional damping of the plasma waves, were $\sim10^5$ K which is lower by an order of magnitude than those deduced from optical observations, while from decay time constant at 60 MHz leads to coronal temperature $\sim10^4$ K. By using an improved method, but with less sensitivity, similar results were obtained in the range 36 to 15 MHz by Barrow and Achong (1975) and by Achong and Barrow (1975). Hence, the validity of the assumption of collisional damping to be operative in the corona appears doubtful. It should be noted that observations of spectral features with high resolution and high sensitivity render valuable information such as:

(a) Plasma irregularities in the corona around $2R_\odot$ (Takakura and Yousef, 1975; Melrose, 1975; Sawant *et al.*, 1976).
(b) Longitudinal dependence of noise storm bursts for studying the propagation effects (de la Noë, 1975; Sawant, 1977).

(c) Scattering effects in the corona and nature of exciter responsible for bursts (Boischot *et al.*, 1970).

2.2. Association of noise storms with solar activity

Noise storms have been found to be associated with sunspots. But the 27-day cycle which is observed in the case of active regions (or sunspots) is not necessarily observed in the case of noise storms. The noise storms often appear to be related to certain phases of development of active regions. The storm activity does have correlation with the number of major sunspots on the disk but it is found that complex large sunspots are almost always associated with noise storm activity. While studying the association of meter wavelength noise storms with sunspots, Fokker (1965) found that the noise storm activity increases with the area as well as with the magnetic field strength of the sunspot. Similar results were also obtained previously by Payne-Scott and Little (1951) and Malinge (1963). However, noise storm centers are not radially situated above the optical centers of activity. There is enough observational evidence to show that the decametric noise storms originate in non-radially oriented coronal structures (Malinge, 1963; Stewart and Labrum, 1972). The dependence of some of the storm characteristics in meter wavelength region such as mean intensity, number of storms per year, etc. on the 11-year solar cycle has been established (Korolev, 1974). He has shown statistically that the intensity as well as the number of noise storms at 169 MHz follows the solar cycle variation as shown in Figure 8. Further, he found that the probability of occurrence of noise storms increases with the increase of the area of sunspots above 600 million part of the solar disc in high solar activity year and above 200 million part of the solar disc in low solar activity year.

Most noise storms are found to occur after the onset of a solar flare within an hour (Malinge, 1963) and within 30 min if the flare is a large one. Similar studies carried out in sunspot minimum rule out the association of noise storms with flares by chance. However, studying the association of decametric noise storms with flares,

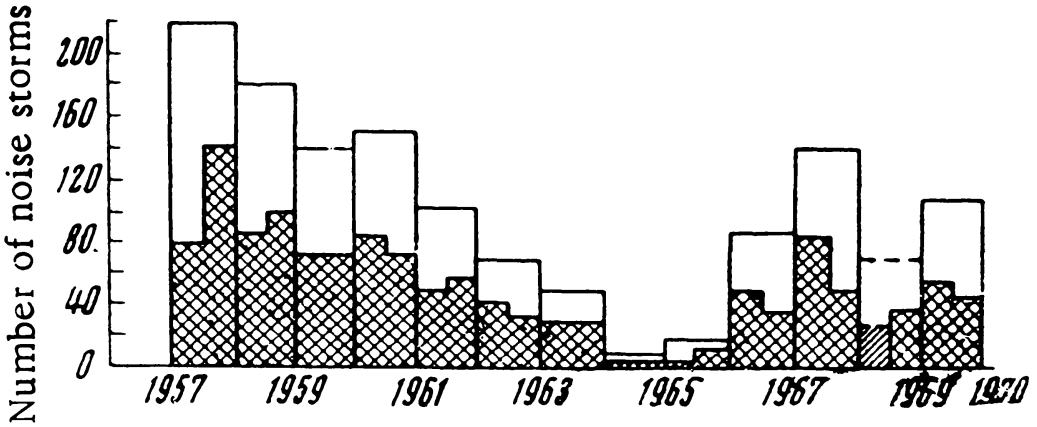

Fig. 8. Number of noise storms (days) at 169 MHz per year from 1957 to 1969. Crossed hatched portion represents the distribution of storms for each half-year (from Korolev, 1974).

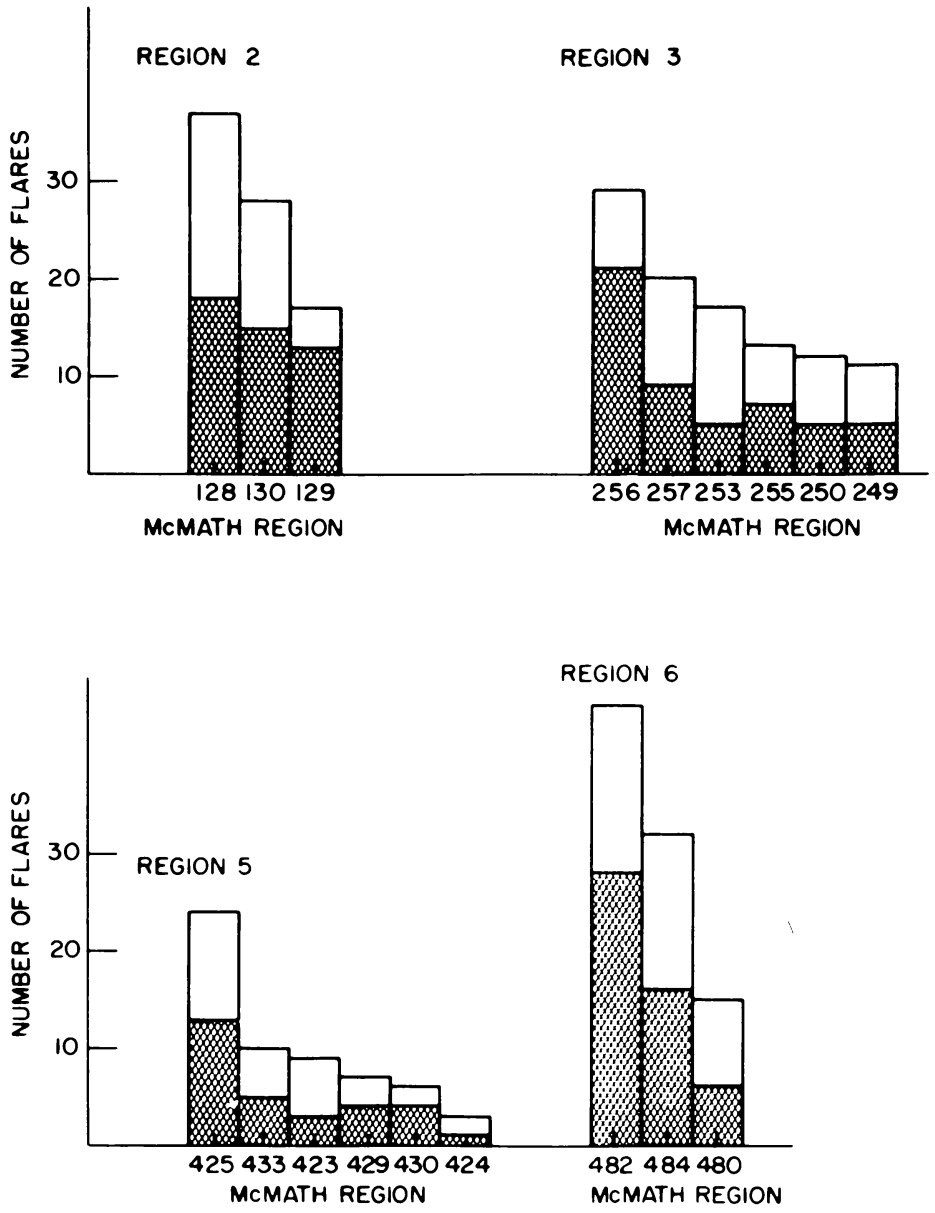

Fig. 9. Histograms showing number of flares observed during the noise storms against the active regions on the Sun. Hatched portion indicates the probable number of flares that would have been observed in the absence of noise storms (from Gergely and Kundu, 1975).

Gergely and Erickson (1975) found that intensification or onset of decametric storms does not directly relate with flares; but during the storm, several active regions are present on the disk and a number of subflares are observed in these active regions (see Figure 9). These active regions appear to form a complex at the chromospheric level and all decametric storm centers are associated with these active regions which interact with each other. The X-ray pictures obtained during SKYLAB mission show complex inter-connections among several regions (Vaiana *et al.*, 1973). This interaction can be evidenced by the occurrence of sub-flares following a sub-flare in some other region. A technique developed by Gergely and Kundu (1975) for studying the

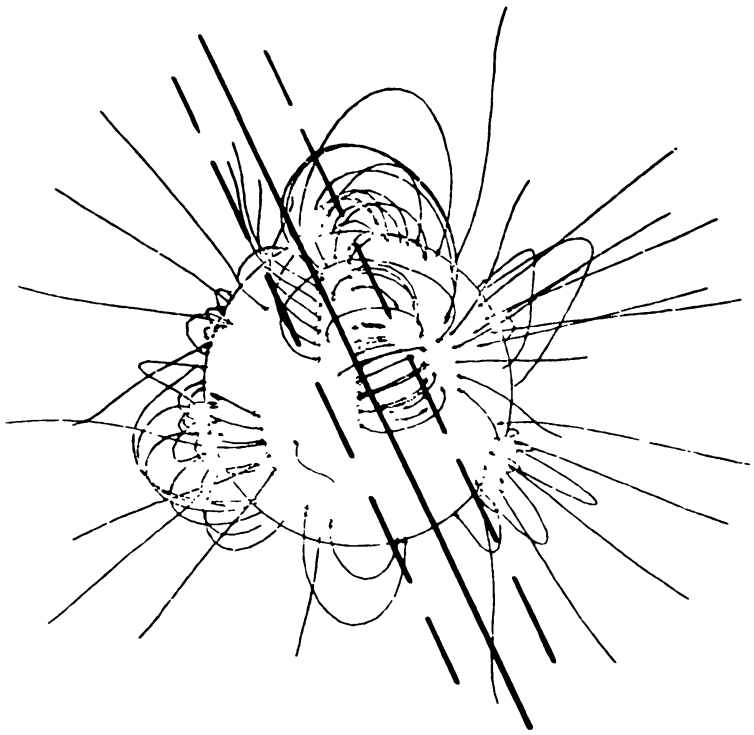

Fig. 10. Magnetic fields related to decametric source. The centroid of the source is indicated by the solid line, its size by the two dashed lines. Magnetic map by courtesy of Mrs. D. P. Trotter, High Altitude Observatory, Boulder, Colorado (from Gergely and Kundu, 1975).

association of a flare in distant active regions showed that simultaneously observed flare frequency, when the noise storm is in progress, turned out to be twice the number expected on the basis of random occurrences. Simultaneous studies of calculated potential coronal fields around the CMP date and positions of decametric noise source showed that magnetic structures associated with storm sources were found to be either on higher or lower magnetic arches (see Figure 10). The position of the decametric continuum source frequently coincided with the filaments or chains of filaments.

Systematic studies of association of the optical activity of the Sun with hecto- and kilometer noise storms are scarce. However, Sakurai (1971) has shown that hectometer and type I noise storms were associated with the active region McMath 9597 on the disk in the August 1968 storm.

Thus, in view of the lack of definite association of the storms with the large magnetic sunspots and a poor correlation between the largest sunspot of a group and the intensity of the noise storm radiation, there appears to be yet another condition for the generation of noise storms, other than only the presence of high magnetic fields, such as the availability of energetic electrons.

2.3. High resolution studies of noise storm sources

As noted earlier, the noise storm consists of a continuum radiation (Kruger, 1972) and an enormous number of short duration bursts having narrow bandwidths.

Understanding of these bursts and their relation, if any, to the continuum radiation is facilitated through high resolution observations. By observing temporal and spectral variation of solar radio emission with high resolution techniques, it is possible to distinguish between phenomena intrinsic to the source and subsequent propagational effects in the overlying medium (de la Noë and Boischot, 1972; Sawant *et al.*, 1976; Sawant, 1977). As an evidence for the directivity of the noise storm, it is worth noting that the decametric noise storm observed at 25 MHz at Ahmedabad during the now well-known August 1972 events had 3 db beamwidth centered around CMP of about 40° (Bhonsle *et al.*, 1973).

Type I, type III and drift pairs are the predominant spectral features observed in the metric storms over and above the continuum. Type I bursts are characterized by short duration 0.15 to 0.5 s and narrow bandwidths 3 to 6 MHz. Some of these bursts show frequency drifts and high degree of circular polarization. These bursts are observed within the range of 400 to 50 MHz and have brightness temperature of the order of 10^{10} to 10^{11} K (Elgaroy, 1965, 1977). These bursts often appear singly in the frequency-time plane. Also there is a tendency for them to cluster together in tens or hundreds to form what are called narrow band 'chains' of type I burst (Wild, 1957; Elgaroy, 1961; Hanasz, 1966; de Groot *et al.*, 1976). Whether type I burst appears singly or in chains, there is no difference in their properties (Hanasz, 1966) except that the chains slowly drift in frequency. Most chains are found to occur below about 300 MHz (Elgaroy and Ugland, 1970), which is the high frequency cut off for noise storms (Kundu, 1965). The observations show that weak type III bursts grow out of 'chains' of type I bursts (or even isolated type I) which appear almost parallel to the time axis on the dynamic spectra, sometimes indicating the band splitting phenomenon (Hanasz, 1966) as shown in Figure 11a. This transition from type I to type III usually occurs in the range 60–40 MHz (Malville, 1962; Hanasz, 1966; Stewart, 1972; Gergely and Kundu, 1975) as can be seen from Figure 11b.

The stereo experiment carried out by Caroubalos and Steinberg (1974) determined the radiation power pattern of type I and type III bursts. Same solar events observed at 169 MHz simultaneously from the Earth and with a distant Soviet space probe Mars-3 have shown 3 dB beamwidth smaller than 25° in the ecliptic plane. These observations also showed that: (i) sources of type I as measured from the space probe are smaller than that seen from the ground and are situated in overdense fibres or arches which extend up to $0.8R_{\odot}$ above the photosphere, (ii) angle of radiation with the magnetic field is less than 40°, (iii) the lower corona above the active region is full of fibres and arches and random scattering in that medium accounts for all the observed properties of type I burst, and (iv) type III bursts are less directive compared to type I burst and there is enough evidence for the presence of large scale dense structures.

Observations obtained with Culgoora Radioheliograph and spectrograph combined with optical data suggest that type I sources are located on multiple strong field loops and the sources of sporadic type III burst on widely diverging field lines (Kai and Sheridan, 1974). The Culgoora observations show that no significant

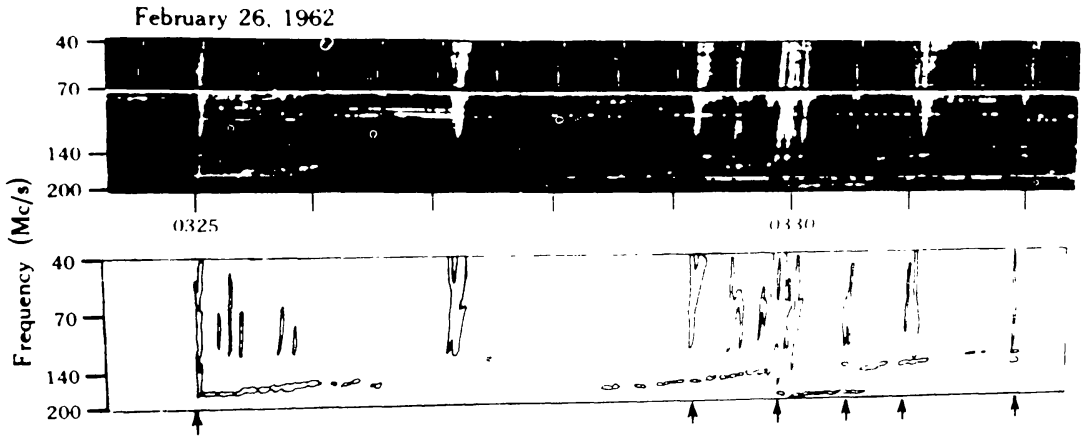

Fig. 11a. Shows weak type III bursts growing out of type I chains. The lower figure shows the schematic of the above dynamic spectra. The arrows indicate weak type III bursts growing out of chains (from Moller-Pedersen, 1974).

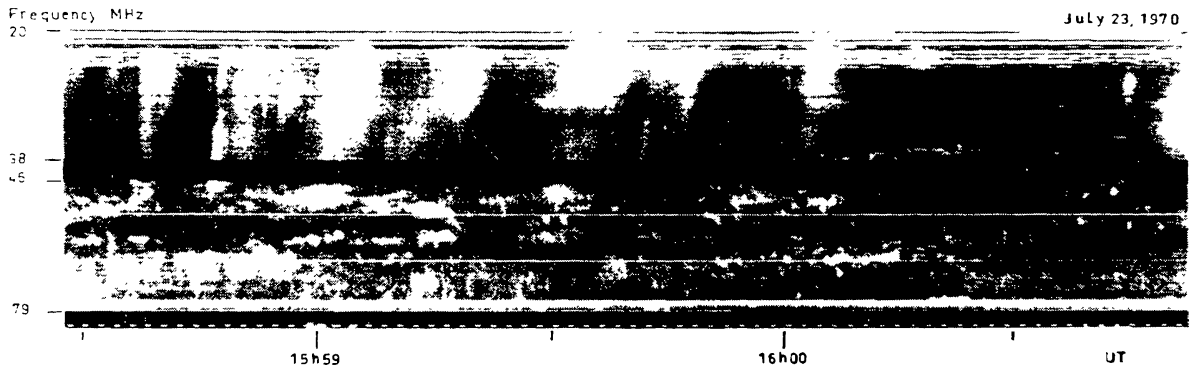

Fig. 11b. Simultaneous type III storm and type I storm in decameter range on 23 July, 1973 (from Moller-Pedersen, 1974).

difference was found between the position of type IIIb and the following type III burst. The angular size of type IIIb and associated type III burst at 80 MHz occurring as a pair turns out to be about 15′ to 20′ of arc at the same position in the corona as shown in Figure 12.

Abranin *et al.* (1976) have determined the angular size of sources in 25 to 12.5 MHz range. The size of individual stria can be less than 10′ of arc in 26–24 MHz band. Angular sizes of diffuse traces which are probably second harmonic are 20′ and 40′ of arc at 25 and 12.4 MHz respectively. No significant change in the sizes of the sources of the second harmonic was obvious during the lifetime of a type IIIb burst. The entire region of emission is usually no larger than the source of the second harmonic (type III) and coincides with it in position. Further work by Abranin *et al.*

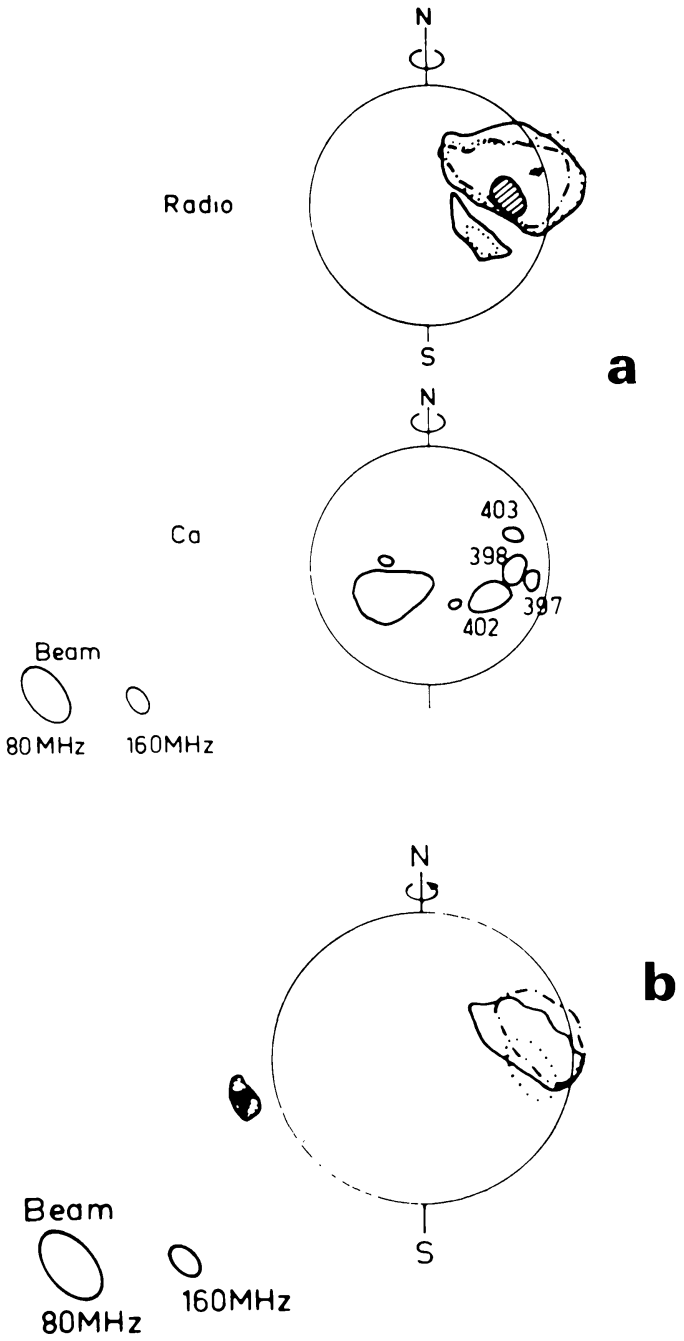

Fig. 12. Contours of radio sources of both the fundamental and the second harmonic in type IIIb–III harmonic pair at 0.35 times the maximum beam brightness (a) *Solid contour*: type IIIb precursor observed on June 28, 1978 at 23:27:46 at 80 MHz, polarization 4% LH. *Dot dash contour*: Transition between type IIIb and type III at 80 MHz, observed at 23:27:47, polarization 15% LH. *Dotted contour*: type III burst at 80 MHz 23:27:48, polarization 5% RH. *Hatched pattern*: type III burst at 160 MHz, observed at 23:27:49, polarization 0%. *Bottom*: Ca plage map at 15:00 UT. (b) *Solid and dot-dash contours*: 80 MHz R and L circular polarization respectively of type IIIb fundamental observed on 28 June, 1973 at 23:29:24.0 UT, polarization 46% LH. *Dotted contours*: 160 MHz, R and L circular polarization of type III second harmonic observed on the same day at 23:29:25.0 UT, polarization 0%. *Hatched and solid contours*: 160 MHz, right handed and left handed circular polarization respectively of a continuing type I storm (from Takakura and Yousef, 1974).

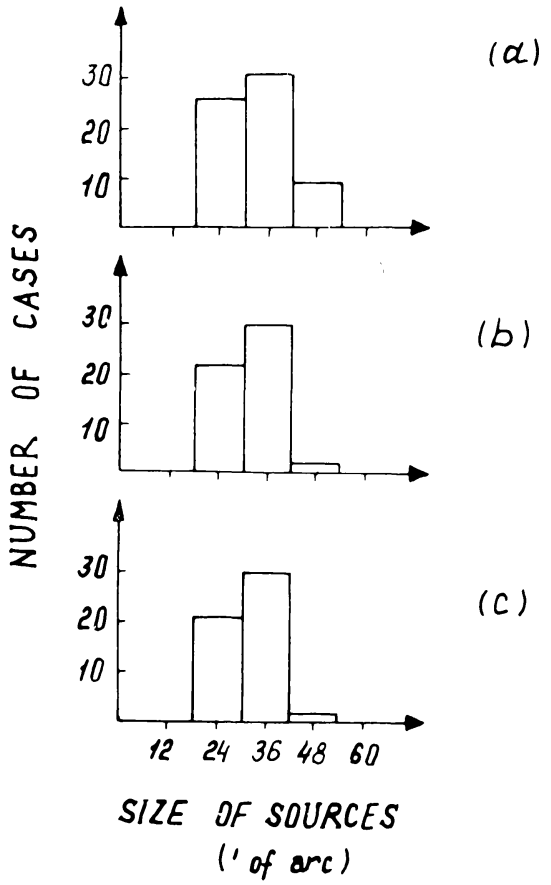

Fig. 13. Distribution of decametric burst source sizes. (a) Stria bursts in the range 26–24 MHz. (b) Stria bursts at 25 MHz. (c) For type III bursts at 25 MHz (from Abranin *et al.*, 1978).

(1978) has given source sizes of stria bursts between 20′ and 40′ of arc in the range 26–24 MHz as shown in Figure 13. These source sizes are the same as type III bursts in the same frequency range (Wild *et al.*, 1959; Shain and Higgins, 1959). The observed large source sizes of 20′ and 40′ of arc are difficult to explain on the basis of radio wave scattering in the corona (Steinberg *et al.*, 1971; Riddle, 1974; Kundu and Erickson, 1974; Chernov, 1976). But in view of the results obtained by Poquerusse and Steinberg (1978), there appears to be substantial scattering and refraction in the Earth's ionosphere at lower frequencies. Interpretation of source sizes at low frequencies should be attempted taking into account ionospheric scintillations and the possibility of existence of multiple compact sources in the corona (Gergely and Kundu, 1975; de la Noë and Gergely, 1978).

The two dimensional evolutions of sources of type II, III, IV, and V at 26.4 MHz with multiple baselines and time sharing interferometer system is derived by Chen and Shawhan (1978). The average source parameters observed are given in Table III. For all types of bursts it can be seen that the overall average core size is $10' \pm 4'$, the halo size is $31' \times 29'$, the power ratio between the core and halo is 1.0 ± 0.4. Details of source evolution with time vary from burst to burst and the general characteristics for type III and type IV bursts are shown in Figure 14. In general, it may be noted that for

TABLE III

Source sizes and velocities for solar bursts of spectral type II, III, IV, V observed at 26.4 MHz[a]

Spectral type	Number of events	Half-power diameter in arc min			P_C/P_H [b]	A_H/A_C [b]	Apparent velocity	Remark
		Core	Halo					
			E–W	N–S				
III	20	8±3	30±9	28±15	1.0±0.3	8%	$0.1c$ [c] → $0.5c$	There are 3 type
V	10	12±4	42±16	27±12	1.6±1.1	8%	$0.1c \rightarrow 0.5c$	III, V pair bursts included separately in the group of type III and type V events
II	2	8±2	26±2	32±3	1.1±0.2	7%	$\sim 2.2\times10^3$ km s^{-1}	Event B75042
		6±2	29±8	41±9	1.2±0.2	3%	$\sim 2.2\times10^3$ km s^{-1}	Event B75043
IV	3	14±8	43±34	28±17	0.5±0.3	33%	Phase information was corrupted by ionosphere; not reliable	Event B75010, mostly single source strucutre
		14±4	24±3	17±5	0.6±0.4	80%	velocity could be deduced	Event B75011
		5±2	24±5	31±5	1.3±0.3	3%	~stationary	Event B75044

[a] From Chen and Shawhan (1977).
[b] P_C/P_H = core to halo power ratio, A_H/A_C = halo to core intensity ratio.
[c] c = speed of light $\cong 3\times10^5$ km s^{-1}.

type III bursts, the core decreases in size and starts to expand just before the intensity reaches to its peak value in E–W direction. The halo in N-S direction follows the behaviour of core size but that in E–W remains the same. For type V bursts, the behavior of the halo in E–W and N–S directions closely follows that of its core, which is different from halo variations of type III burst.

2.4. Polarization Studies of Noise Storms

Systematic studies of polarization behavior of noise storms at metric wavelengths have been made by Cohen (1958, 1959), Fokker (1960), and Suzuki (1961) around 200 MHz, and by Harvey and McNarry (1970) at 74 MHz. No systematic polarization measurements of noise storms at decameter and longer wavelengths are currently available. Nevertheless, some polarization data at decameter wavelengths are available. (Bhonsle *et al.*, 1967; Warwick and Dulk, 1969; Ellis, 1969; Chin *et al.*, 1971; de la Noë and Boischot, 1972; Dodge, 1972; Sastry, 1972; Boischot and Lecacheux, 1975; Sawant *et al.*, 1976; and Sawant, 1977).

Weakly polarized or unpolarized storms have also been observed but their positions are found to be higher than those of the polarized storm (Kundu, 1965, and

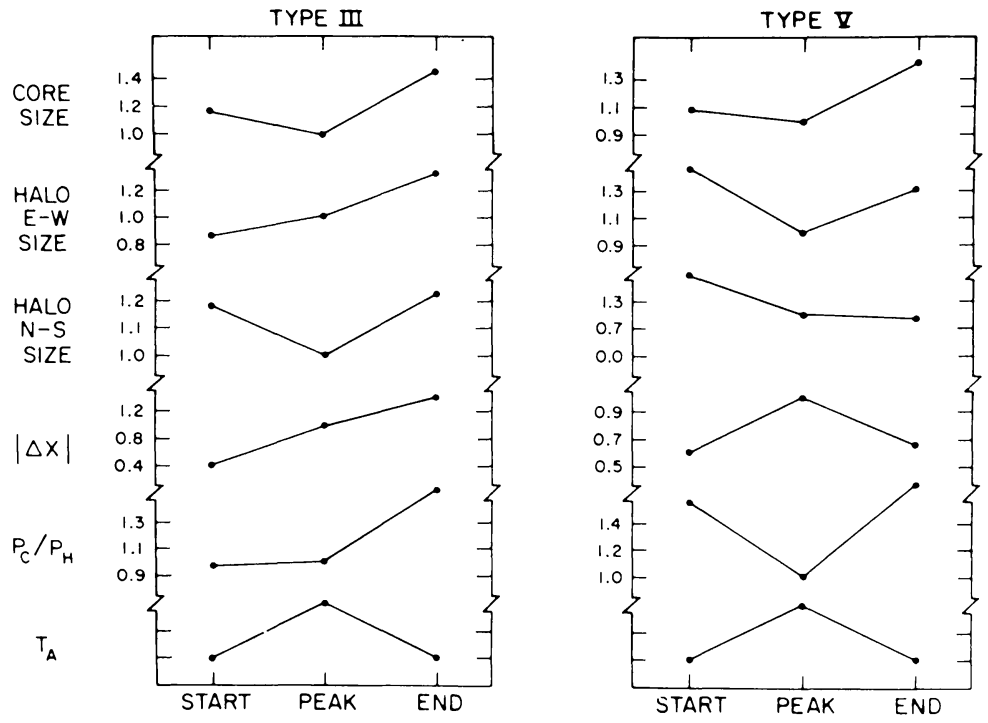

Fig. 14. Normalized and averaged temporal evolution of source parameters for the observed type III and type V bursts. Δx is the E–W position difference between the halo and the core. P_C/P_H is the power ratio between the core and the halo. T_A in dB above 6×10^{-21} W m^{-2} Hz^{-1} (from Chen and Shawhan, 1978).

references therein). Both the continuum emission and the radio bursts at decameter wavelengths are sometimes circularly polarized in the opposite sense of rotation (Mattoo *et al.*, 1975). The polarization characteristics of the continuum and superimposed bursts at 25 MHz have been studied by Mattoo (1973) and Mattoo *et al.* (1975). It was observed by Mattoo *et al.* (1975) that following the solar flare on 14 July, 1969 at 08:13 UT, the degree of polarization of the continuum radiation was nearly 80% in the left handed sense in contrast to the superimposed intense type III bursts which were strongly polarized in the right handed sense. Figure 15 shows the detailed characteristics of polarization observed on 14 July, 1969 at Ahmedabad. The general trend in the time variation of the net degree of polarization is to increase when the total intensity of emission decreases and vice versa. This means that the continuum radiation and the type III burst radiation were incoherent with each other and were separately generated in different source regions pervaded by opposite magnetic field polarities.

The sense of polarization of the noise storm radiation is related to the polarity of magnetic field of the associated center of activity and is related to the leading sunspot in the group. It is well known that the spot polarity is opposite in the two hemispheres and reverses at each sunspot cycle (Thiessen, 1952; Babcock, 1959).

The noise storms at meter wavelength (17–23 May, 1969 and 7–13 June, 1969) were studied by Chernov *et al.* (1972) with simultaneous high resolution observations of spectrum, flux density and polarization. They found that same sense of

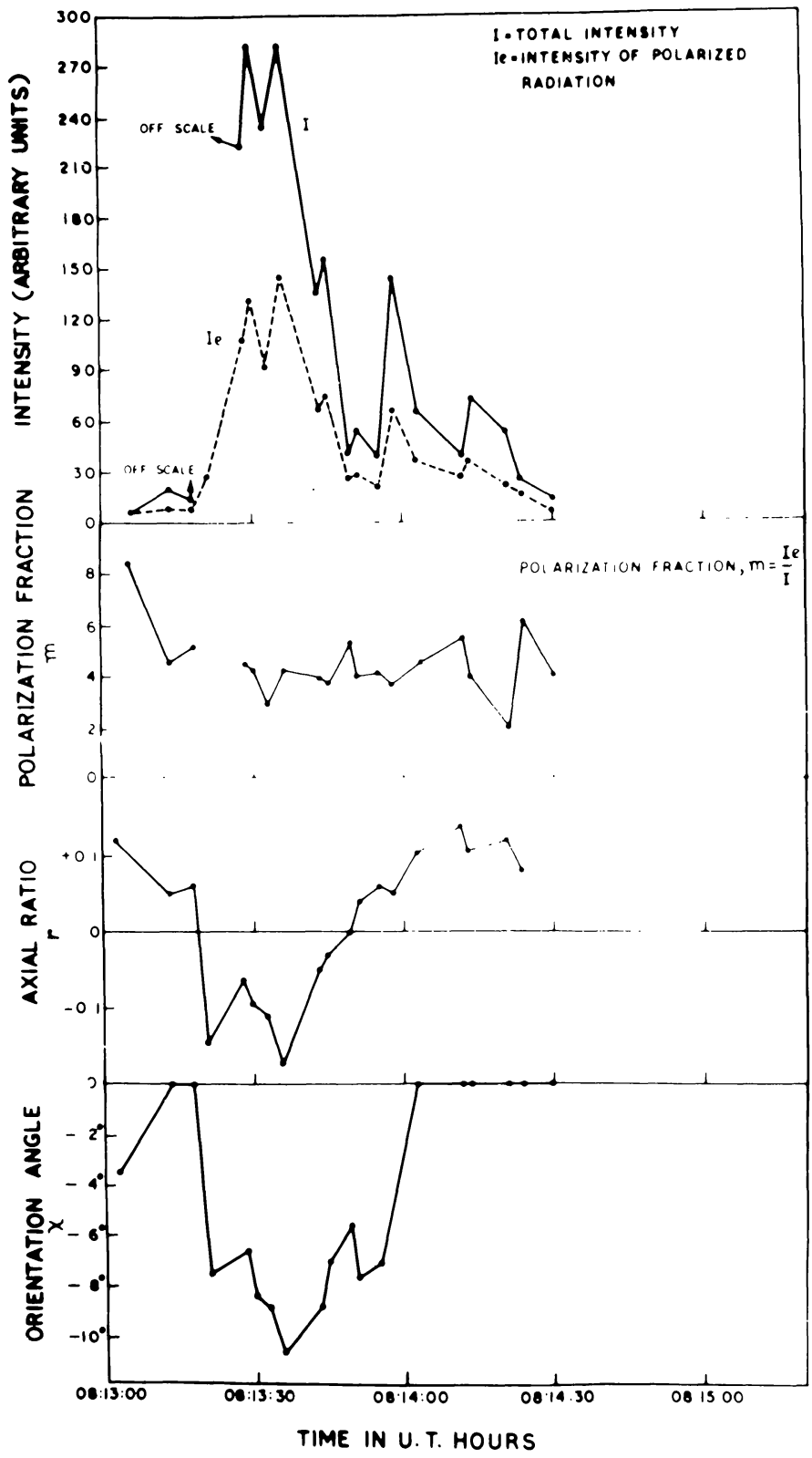

Fig. 15. Various polarization parameter of the decametric continuum and superimposed type III bursts recorded at 25 MHz on 14 July 1969 (from Mattoo *et al.*, 1975).

polarization prevails for type I burst-chains and continuum. They also observed that the degree of polarization of type I burst and chain increases at the initial stage of storm development. Once it attains 100%, it remains at the level till the end of the storm. It is concluded from the study of these two noise storms, that each storm has its own evolution of polarization characteristics which may depend on the magnetic field configuration at the source and its heliographic position.

In the decameter range, high time-resolution spectral measurement along with polarization was started by Warwick and Dulk (1969) and Ellis (1969). Ellis (1969) found that in the case of a 'split pair' both components were polarized in the right handed sense. Fast circularly polarized pulses (100%) were observed by Barrow and Saunders (1972). The 'double bursts' near 25 MHz as reported by Sastry (1972) showed same sense and degree of circular polarization.

No type IIIb burst showed complete circular polarization, though individual stria bursts can be circularly polarized. Like split pair, the sense of polarization of type IIIb should be either right or left handed. In a given type IIIb burst all elements need not be polarized, but if they do, then there exists a predominant sense (R or L) of polarization (de la Noë and Boischot, 1972; Sawant, 1977).

While studying the polarization characteristics of type III bursts at decameter wavelengths (35 MHz), Mattoo and Bhonsle (1974) found that the time profiles of certain short duration bursts observed on two closely spaced frequencies separated by 4 kHz were dissimilar, implying the existence of fine structure in frequency. They found that the Faraday rotation at 35 MHz is of the order of 10^3 radians (Bhonsle and Mattoo, 1973), in agreement with earlier results reported at 34 MHz by Dodge (1972). Out of this, about 80% Faraday rotation was shown to occur near the source and about 10% in the ionosphere. To account for these low values of the total Faraday rotation, Dodge (1972) suggested that mode coupling can take place in the presence of localized variation in directions and magnitude of the magnetic field, since there exists a high probability of a given wave encountering a region of transverse magnetic field that would destroy all the previously acquired Faraday rotation. Mattoo (1973) argued that the observed Faraday rotation should be at times as small as 100 radians as mode coupling can occur anywhere between the source and orbit of the Earth. This is the amount of Faraday rotation suffered by 35 MHz ray in the Earth's ionosphere but such low values for solar bursts have never been observed. Therefore, Bhonsle and Mattoo (1974) suggested that if decametric type II emission occurs predominantly at the second haromonic of the local plasma frequency, then the observed low values ($\sim 10^3$ radians) of Faraday rotation can be explained. On the other hand, Melrose (1975) suggested that the observed small values of the Faraday rotation at 200 MHz (Akabane and Cohen, 1961) and at 35 MHz can be accounted for if corona is inhomogeneous with scale sizes ($\geqslant 100$ km) of irregularities and strong mode coupling is operative near the source. Dodge (1972) calculated high resolution spectra (5 Hz) of the complete polarization parameters of type III bursts across narrow bandwidths (50 Hz). The consequence of the low value of Faraday rotation ($\sim 10^3$ radians) is to definitely increase the probability of

detection of linearly polarized type III bursts since it substantially reduces Faraday dispersion (Bhonsle and Mattoo, 1973). The claim by Grognard and McLean (1973) for the non-existence of linear polarization in type III bursts at 80 MHz is doubted by Bhonsle and Mattoo (1973) because of Grognard and McLeans's instrumental limitations in measuring small values of differential group delays. However, it may be stated that Boischot and Lecacheux (1972) adopted a different approach of detection of linear polarization in the frequency range of 80–20 MHz but failed to observe the presence of linear polarization in type III bursts.

Bhonsle *et al.* (1967) with their digital polarimeter at 26 and 22 MHz with 100 Hz bandwidth and 1 s time resolution reported polarization measurements during three events. They found weak polarization and stable orientation angle for decametric type III bursts. Chin *et al.* (1971) also measured polarization parameters at 25 MHz within a 100 Hz bandwidth and found that the bursts were mostly linear or weakly elliptically polarized.

3. Spectral Information of Decametric Noise Storms

3.1. Decametric continuum

A decametric continuum is characterized by a wide band noise upon which are superimposed large number (thousands) of type III events (Warwick, 1965). Whether the continuum is separately originated in a single plasma process or consists of large number of unresolved type III bursts has not been established so far. The duration of the continuum is from a few hours to maximum of seven days. Short term variability (from a few seconds to a few hours) of the continuum is also observed as that in metric continuum. The observed brightness temperature increases with frequency but the angular size of the decametric continuum decreases with increasing frequency. The movements of source position of decametric type IV continuum with velocities of the order of a few hundred to thousand kilometer per second and their association with transient events have also been reported by Gergely (1974) and Gergely and Kundu (1975) as shown in Figure 16.

From the experiments conducted in space vechicles such as RAE and IMP-6 satellites (Haddock and Graedel, 1970; Fainberg and Stone, 1971), it is found that the emissions around 60 kHz appear as a slowly varying continuum with occasional burst peaks which can be recognized. Concurrent observations with the Clark Lake Radio interferometer at 60–20 MHz have shown the presence of a continuum above the same active region, as that observed by IMP-6, which is presumably responsible for the hectometer type III storms (Gergely, 1974). Hence, it may be considered that the metric continuum serves as a reservoir of energetic electrons for decametric type III storms (Boischot *et al.*, 1970) and decametric continuum in turn serves as a reservoir to a hectometer and kilometer type III storms. The close connection between meter and decameter storms on the one hand, and between decameter continuum and hectometer storms on the other, suggests that all of them are

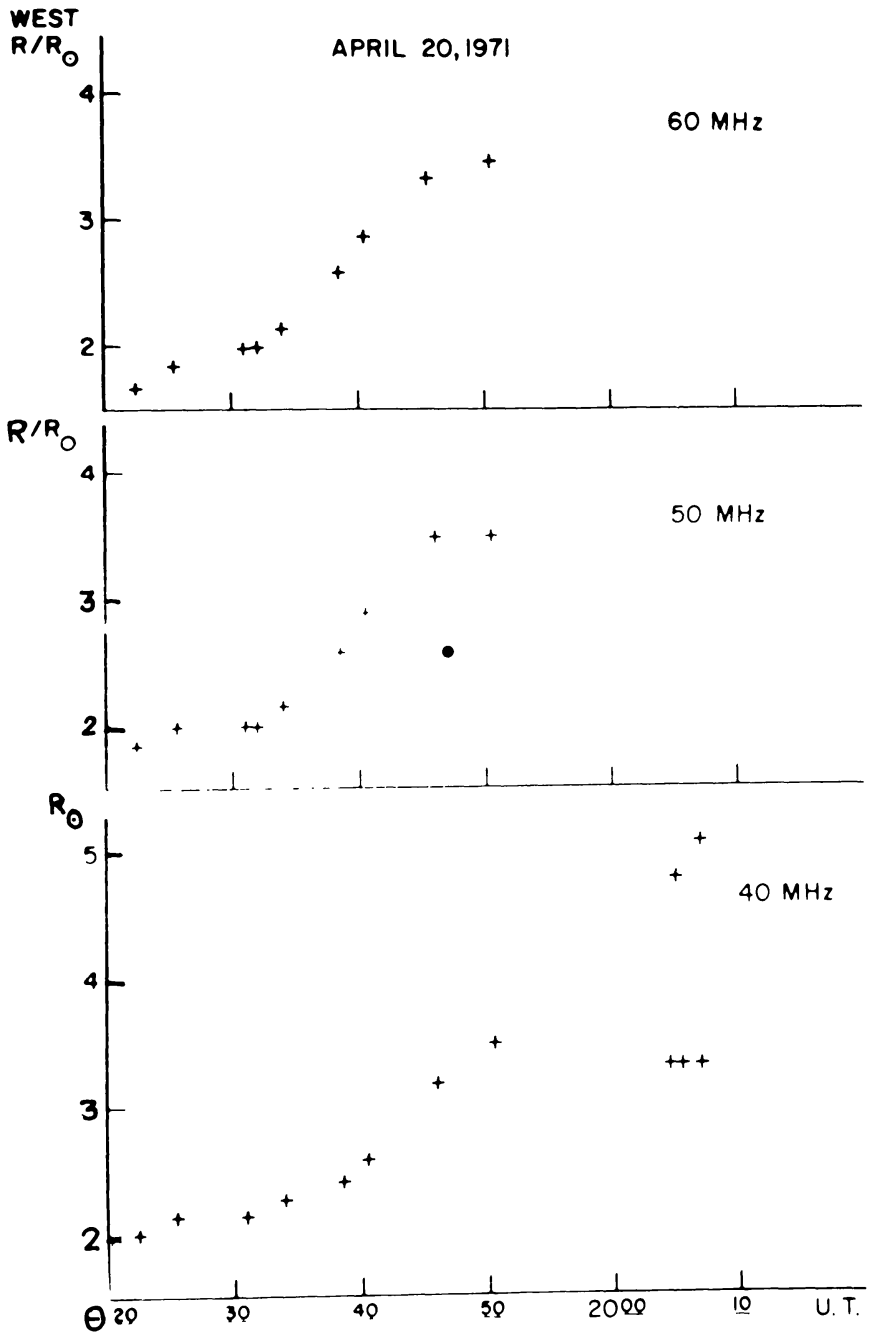

Fig. 16. Positions of type IV burst observed on 20 April 1971 at 60, 70, and 40 MHz. The filled circle indicates the position of type III bursts at 50 MHz (from Gergely and Kundu, 1975).

produced by the same outward streaming energetic electrons (~40 keV) (Aubier *et al.*, 1978). However, as the height of the source increases with decreasing frequency, the decameter continuum is quite a distinct source from that of meter-save continuum (Kundu, 1971; Elgaroy, 1977). The polarization information of decametric continuum is scanty. Mattoo *et al.* (1975) found in one event strong polarization (80%) of the continuum radiation as discussed in Section 2.4.

1979SSRv...24..259B

TABLE IV

High resolution decametric instruments used for solar work

Experimenter	Frenquency MHz	Frequency resolution kHz	Time resolution ms	Angular resolution	Antenna type or gain in dB or effective area	(a) Instrument and (b) comments
Ellis and McCulloch (1967)	24–28 28–36 36–46 46–60	30	20		Fixed double Log periodic	(a) Spectrographs
Ellis (1969)	24–34 27–28 28–34 28–34 28–60	20 2 20 50 50	20 40		Fixed double Log periodic	(a) Spectrographs. In the 28–34 MHz range 20 kHz, and 50 kHz bandwidths are used for polarization and intensity studies respectively. (b) *R–L* polarization
Yoh and James (1967)	38.10 38.15 38.20 38.25 38.30 38.40	16	Not reported		36 dB	(a) Fixed frequency receivers.
Warwick and Dulk (1969)	24-37	60	10		Log periodic 5 dB over a dipole	(a) Spectrograph (b) Linear polarization
Sastry (1972)	Around 25	5, 6 or 13	10		24 dB	(a) Multi-channel receiver. (b) *R–L* polarization
de la Noë and Boischot (1972)	20–40 40–80	15	20		Arecibo Dish	(a) Spectrographs and Fixed frequency receivers

Table IV (Continued)

Experimenter	Frequency MHz	Frequency resolution kHz	Time resolution ms	Angular resolution	Antenna type or gain in dB or effective area	(a) Instrument and (b) comments
	29.3 36.9 60.0	100	10			(b) (i) R–L polarization (ii) Realizable frequency resolution in case of 20 to 40 MHz is 60 kHz (de la Noë, 1975).
Moiser and Fainberg (1974)	10–80 channels 16 channel separation 100 kHz	20	10			(a) Multi-channel receivers.
Baselyan *et al.* (1974)	23.8–35.8 16.0–17.5	10	250 64		1400 m^2 collecting area	(a) Spectrographs and Fixed frequency receivers
	12.25, 12.5 12.7, 14.7 16.7, 24.5 25.0, 25.4	3	40			
Lecacheux (1975)	10–11 channels 50	20	0.1		Two log periodic 12 dB	(a) Multi-channel receivers.
Sawant (1977)	35–34	5	10		(i) Eight element crossed Yagi antenna array (ii) $\pm 16 \pm 1$ dB	(a) Spectograph (b) Simultaneous (20 ms) recording in R and L polarization.

Table IV (Continued)

Experimenter	Frequency MHz	Frequency resolution kHz	Time resolution ms	Angular resolution	Antenna type or gain in dB or effective area	(a) Instrument and (b) comments
Erickson and Kundu (1976)	Tunable (15–120 MHz) (sample frequencies for comparison below)	—				
	40	1	1000	10′.4	13500 m^2	(a) Mills 'Tee' of log periodic elements
	34			12′.4	18700 m^2	
	26			16′.2	32000 m^2	(b) Two dimensional instantaneous planned.
	22			19′.0	44600 m^2	
	20			21′.0	54000 m^2	
Wild (1967)	160	—	1000	1′.9	6000 m^2	(a) Radioheliograph
	80			3′.8	6000 m^2	(b) (i) Two dimensional
	40			7′.6	3000 m^2	(ii) R and L polarization
Warwick (1964)	8–80		1000	10° × 10°	1000 m^2	(a) Sweep frequency interferometer
Erickson and Kuiper (1975)	65–25		1000	5′	16 log periodic antenna each having gain of 9 dB	(a) Sweep frequency interferometer
Chen and Shawhan (1978)	26.5	6	3000	—	Six dipole antennas	(a) Multi-baselaine time sharing interferometer
Dodge (1972)	34	0.005 0.05	8960	—	Orthogonal log periodic antennas	(a) High Resolution Fourier Spectroscopy and Polarimetry
Bhonsle and Mattoo (1974)	35	6	1000	—	Crossed Yagi antenna 8 ± 1 dB	(a) Time sharing two bandwidth radio polarimeter
Radhakrishnan (1976) Sastry (1976)	30	—	—	1° circular	E–W length 1 km N–S length 500 m 'T' shape	(b) Sensitivity 30 Jansky.

3.2. Decametric bursts

High resolution observations of decametric bursts of type I to V and other spectral features are discussed in this section. Resolution in time and frequency comparable to that obtained in the metric band was not realized in the decametre range until recently. We have already listed in Table IV variety of instrumentation used in the decametre range from 1966 onwards. High sensitivity (employing large antennas) coupled with high resolution work in the decametre range was initiated by de la Noë and Boischot (1972). A high resolution spectroscope in the range 35–34 MHz with frequency and time resolution of 5 kHz and 10 ms respectively has started operating at Ahmedabad since 1974 and many new microscopic spectral features have been discovered with this instrument (Sawant *et al.*, 1975, 1976a, b; Bhonsle, 1976; Sawant, 1977). We shall summarize in the following pages the phenomenology of varieties of bursts observed in the decameter range.

3.2.1. *Split Pairs*

'Split Pairs' shown in Figure 17a are bursts mostly observed below 60 MHz with the average duration of 1–2 s (Ellis and McCulloch, 1966). Ellis and McCulloch discovered that split pairs consisted of two parallel short lived bursts sometimes drifting towards low frequency. According to them, two elements of the burst do not usually begin exactly at the same time; the lower frequency element starts on an average earlier than the high frequency one. In general, the high frequency element in a pair is more intense than the low frequency one and in triplets the middle one is more intense than the other two.

The drift rate of each element is of the order of 0.1 MHz s^{-1} and the frequency separation between the two elements increases with frequency, the average value being 0.1 MHz at 25 MHz to 1 MHz at 60 MHz. The bandwidth of the high frequency element is about 50 kHz. These bursts can occur in isolation, in chains and sometimes in association with type III bursts. In about 10% of the observed split pair bursts, triple splitting has been observed (see Figure 17b). In the double chain of bursts, chains were found to be harmonically related, within the frequency range of 60–24 MHz.

3.2.2. *Stria and Diffuse Stria Bursts*

The high sensitivity ($\sim 10^{-22}$ W m^{-2} Hz^{-1}) and high resolution (in time and frequency) observations in the range 40–20 MHz and 80–40 MHz by de la Noë and Boischot (1972) along with the positional information of the storm (de la Noë, 1975) have led to the identification of new types of bursts, viz. stria, diffuse stria and type IIIb. These are described in the next section.

A large number of single bursts, identical to an individual element of split pair (Ellis and McCulloch, 1966) was observed and named as 'stria' bursts (de la Noë and Boischot, 1972). Figure 17c shows an example of stria burst. The drift rate of stria bursts varies from 10–150 kHz s^{-1}. In very few cases (2%), reverse drift rates have

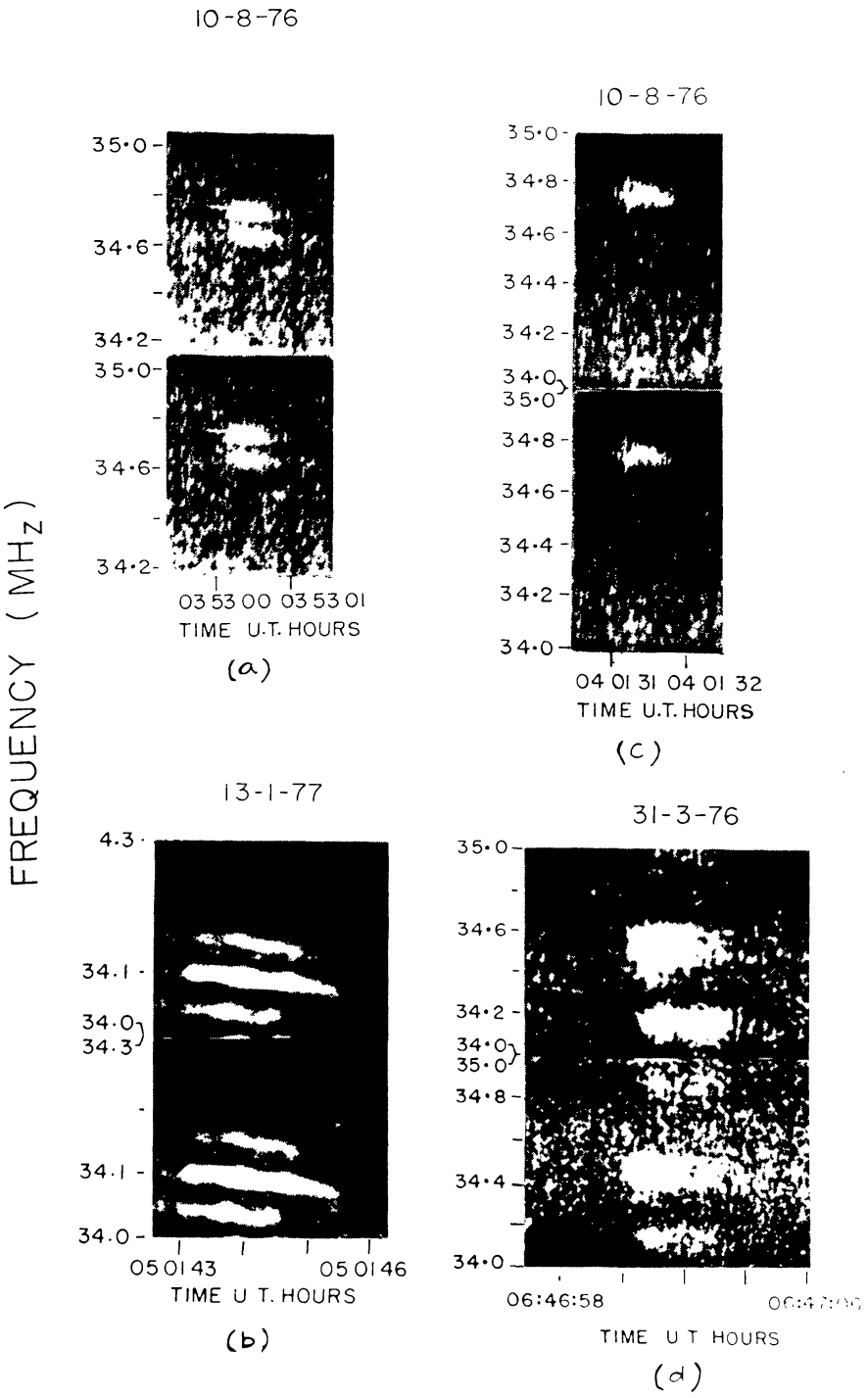

Fig. 17. Examples of decametric bursts observed by High Resolution Spectroscope at Ahmedabad: (a) split pair, (b) long duration triplet, (c) stria burst, and (d) type IIId burst in *R*- and *L*-polarization (from Sawant, 1977).

been observed. The duration of these bursts increases from high to low frequencies, which is 0.6 s at 60 MHz to 1.2 s at 30 MHz (de la Noë, 1975). Of these, about 25% formed split pairs. Figure 17d shows diffuse stria bursts. Essentially diffuse stria bursts are of longer duration and exhibit no frequency drift (Baselyan *et al.*, 1974a, b;

de la Noë, 1975). Average duration of diffuse stria burst at 25 MHz is ~10 s. The instantaneous bandwidth of diffuse stria burst is 1.5 to 2 times larger than that of the ordinary stria bursts (0.12 MHz at 24 MHz). They may be also grouped to form split pair, triplet and chains. Chains of diffuse stria bursts are named as type IIId burst and in general, type IIId burst follows type III burst and the two are related by fundamental-harmonic (F–H) relationship (Baselyan *et al.*, 1974b). No circular polarization is observed for these bursts (de la Noë, 1975; Sawant, 1977).

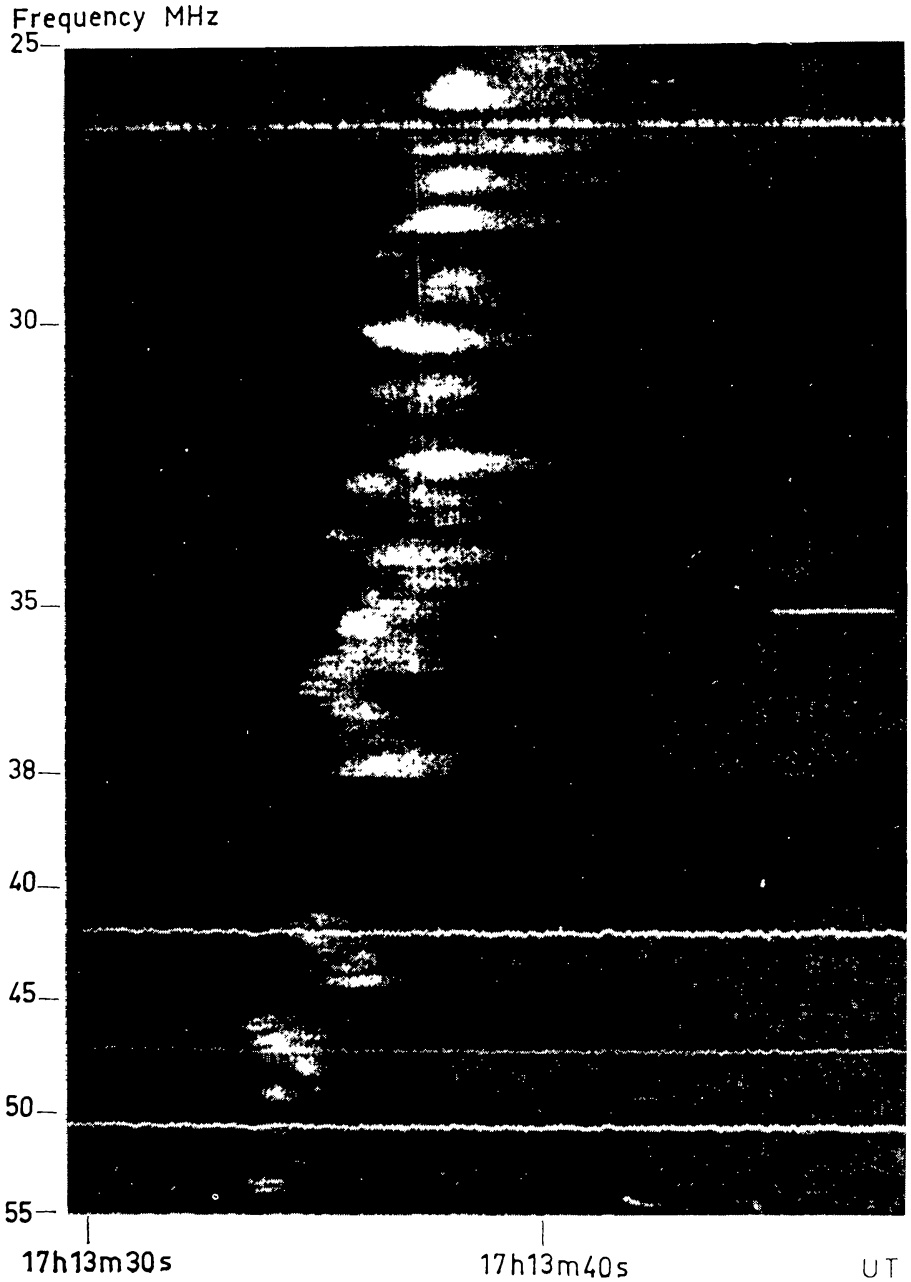

Fig. 18. An example of type IIIb burst observed in the range 55 to 25 MHz (from de la Noë and Boischot, 1972).

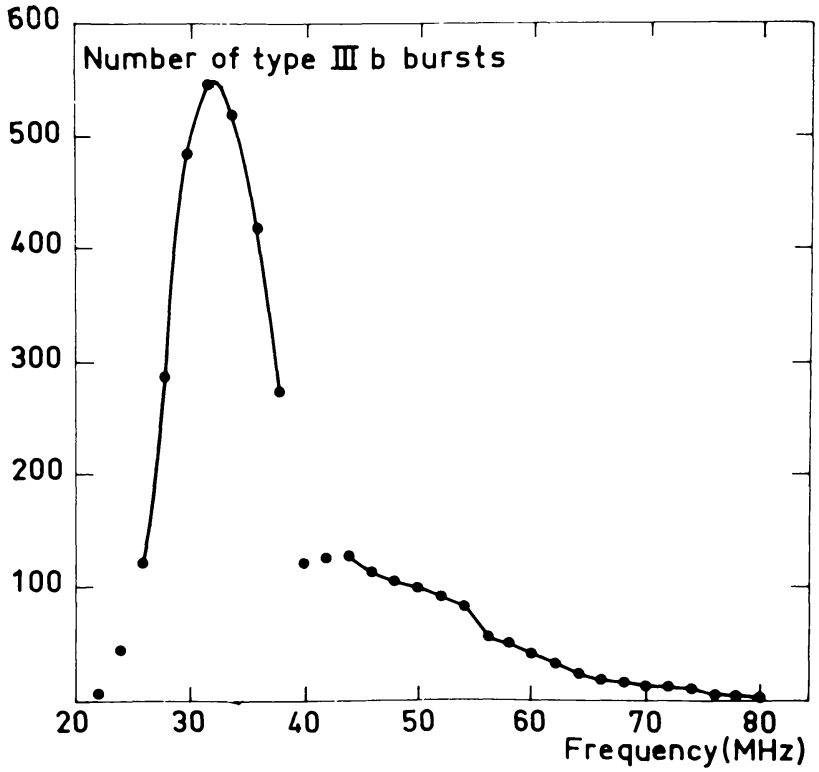

Fig. 19. Plot of number of type IIIb bursts versus frequency observed during July and August 1970. Note the maximum around 30 MHz (from de la Noë and Boischot, 1972).

3.2.3. *Type IIIb Bursts*

Chains of stria, split pairs, and triplets have been named as type IIIb bursts by de la Noë and Boischot (1972), an example of which is shown in Figure 18. Type IIIb bursts are observed in decameter wavelength regions as frequently as type III bursts and rarely in the meter wavelengths (Ellis and McCulloch, 1967; de la Noë *et al.*, 1972; Baselyan *et al.*, 1974 a, b; Takakura and Yousef, 1974). Drift rates of type IIIb bursts are approximately twice the drift rate of type III burst in the same frequency range (Baselyan *et al.*, 1974b). Type IIIb bursts are observed more frequently around 35 MHz (de la Noë and Boischot, 1972) in the frequency 80–20 MHz as shown in Figure 19. The number of elements in type IIIb bursts is found to have longitudinal dependence and is minimum at CMP (de la Noë, 1975) and can be as large as 40 in 80–20 MHz range (Boischot, 1973). In general, the number of elements in type IIIb is small and in the limit stria burst can be a type IIIb burst reduced to a single element.

3.2.4. *Type IIIb–III Bursts*

Intense type IIIb burst is observed 1–5 s before weak and prolonged decametric type III burst as shown in Figure 20 in the range of 75–25 MHz (de la Noë and Boischot, 1972). Detailed analysis of the time delay and frequency ratio between the two related type IIIb (which was earlier referred to as chains of split pairs and triplets) (Ellis and McCulloch, 1967) and type III burst favours the F–H hypothesis (Baselyan

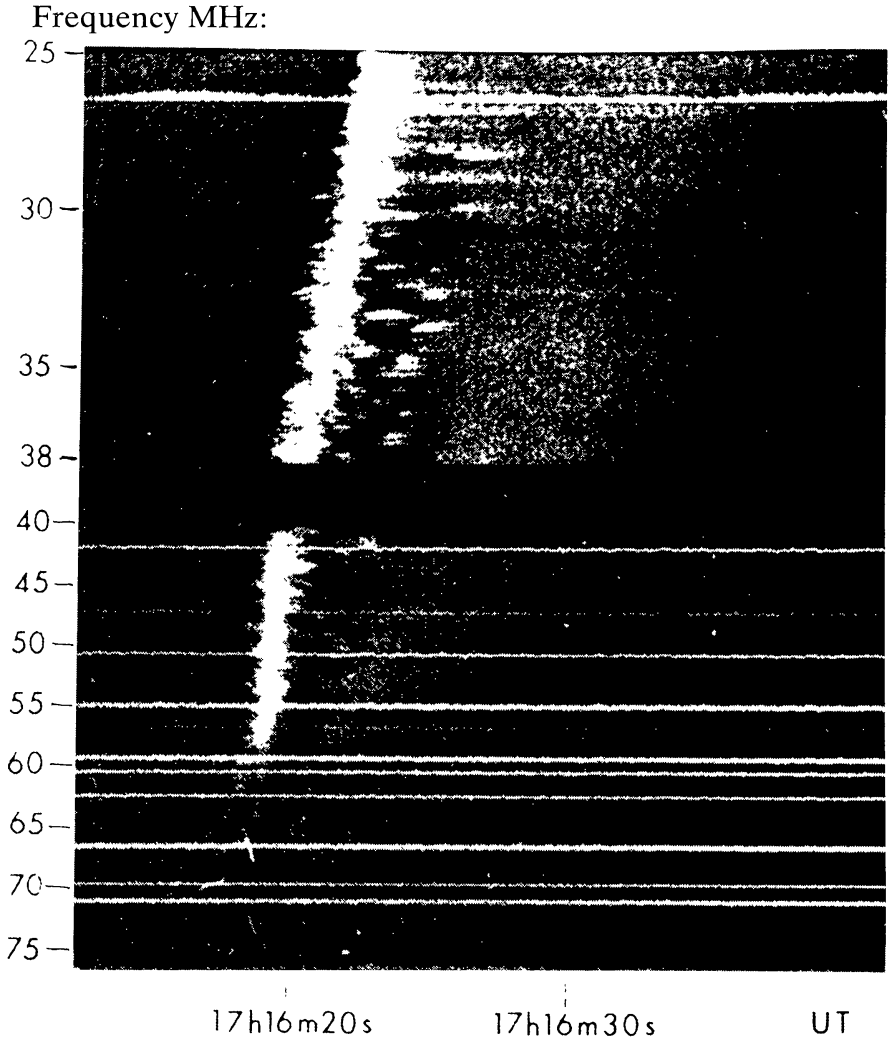

Fig. 20. Type IIIb burst as a precursor of type III burst observed on 8 August, 1970, in the range 80 to 25 MHz. Dispersion of striae along time axis and large number of split pairs in type IIIb should be noted (from de la Noë and Boischot, 1972).

et al., 1974 a, b; Takakura and Yousef, 1975; Moiser and Fainberg, 1975). They found that 33% of type IIIb's were preceded by the normal diffuse type III burst or 27% of the normal type III bursts had type IIIb as a precursor (de la Noë and Boischot, 1972; de la Noë, 1974). From the statistical study de la Noë (1974) concluded that a precursor type IIIb burst is truly associated with a type III burst particularly when they occur beyond 50° solar longitude. They also observed that at a given time the ratio of the mean frequency of type IIIb burst to that of type III burst is on the average 1.75 and is consistent with that obtained by Ellis and McCulloch (1967). This ratio was also found to be comparable to that of harmonic type II bursts (Roberts, 1959) and for a harmonic type III bursts (Stewart, 1962).

de la Noë and Boischot (1972) have suggested that type IIIb is a precursor of the following type III burst and is not likely to be fundamental harmonic (F–H) related pair because (a) on a fixed frequency receiver, records of type IIIb bursts were

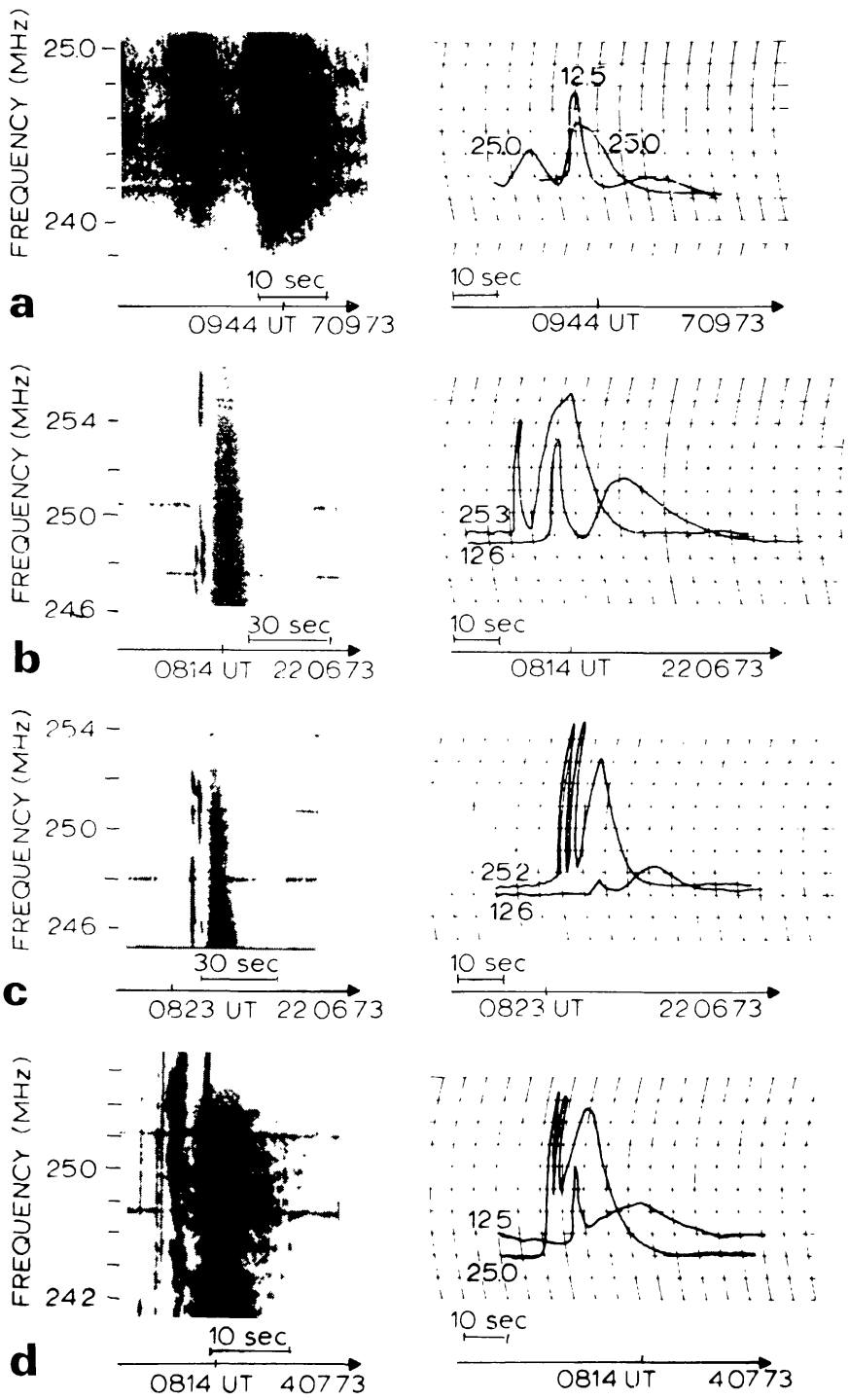

Fig. 21. (a) Normal type III burst with diffusive character of the fundamental and the second harmonic (b, c, d). Show fine structure of type III burst at the fundamental frequency (in the form of stria-burst chains and splitted pairs with echo) and the diffusive second harmonic. Note the gap between fundamental and the second harmonic on the fixed frequency records. This time gap decreases as the drift rate increases (from Baselyan *et al.*, 1974).

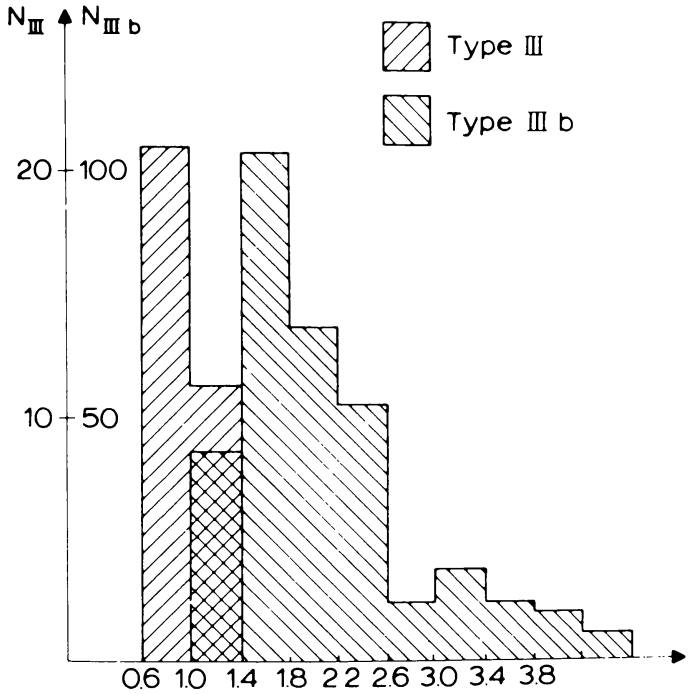

Fig. 22. Dependence of number of bursts on drift rate for the first harmonic of normal type III bursts and type IIIb bursts (from Baselyan *et al.*, 1974).

superimposed on the beginning of type III bursts and no time gap was observed as expected from F–H relationship, and (b) the total energy radiated in a type IIIb burst having many stria is of the same order of magnitude, if not larger, than that in type III burst. But more recent theoretical work by Smith and de la Noë (1976) and experimental evidence that both type IIIb and associated type III (Takakura and Yousef, 1975; de la Noë and Gergely, 1977) originate at the same position supports F-H hypothesis for their generation process.

Baselyan *et al.* (1974 a, b), while observing bursts in the range 25–12.5 MHz, found many examples of distinct time difference between type IIIb and III and also some superposed bursts (IIIb–III) with very small time difference between them on their fixed frequency records (see Figure 21). In some cases, the time difference between IIIb (fundamental) and III (second harmonic) is clearly observed. The superposed time type IIIb–III burst was explained by them as the generation of type IIIb burst at the fundamental frequency and type III at the second harmonic frequency by fast ($0.6c$) exciter beams. The exciters for type IIIb bursts are faster by factor of two than the conventional exciter speeds ($0.3c$) for isolated type III bursts, (as shown in Figure 22) and estimated length of the type IIIb electron stream is $\sim 10^3$ km (Sawant *et al.*, 1978).

Takakura and Yousef (1975) have not only observed type IIIb–III but also type IIIb–IIIb as F–H related pairs. This is shown in Figure 23 as observed on 20 May 1973. A convincing example of F–H related pair of bursts is given by Stewart (1975) in which a conventional inverted 'U' burst observed on 11 May 1974 in the

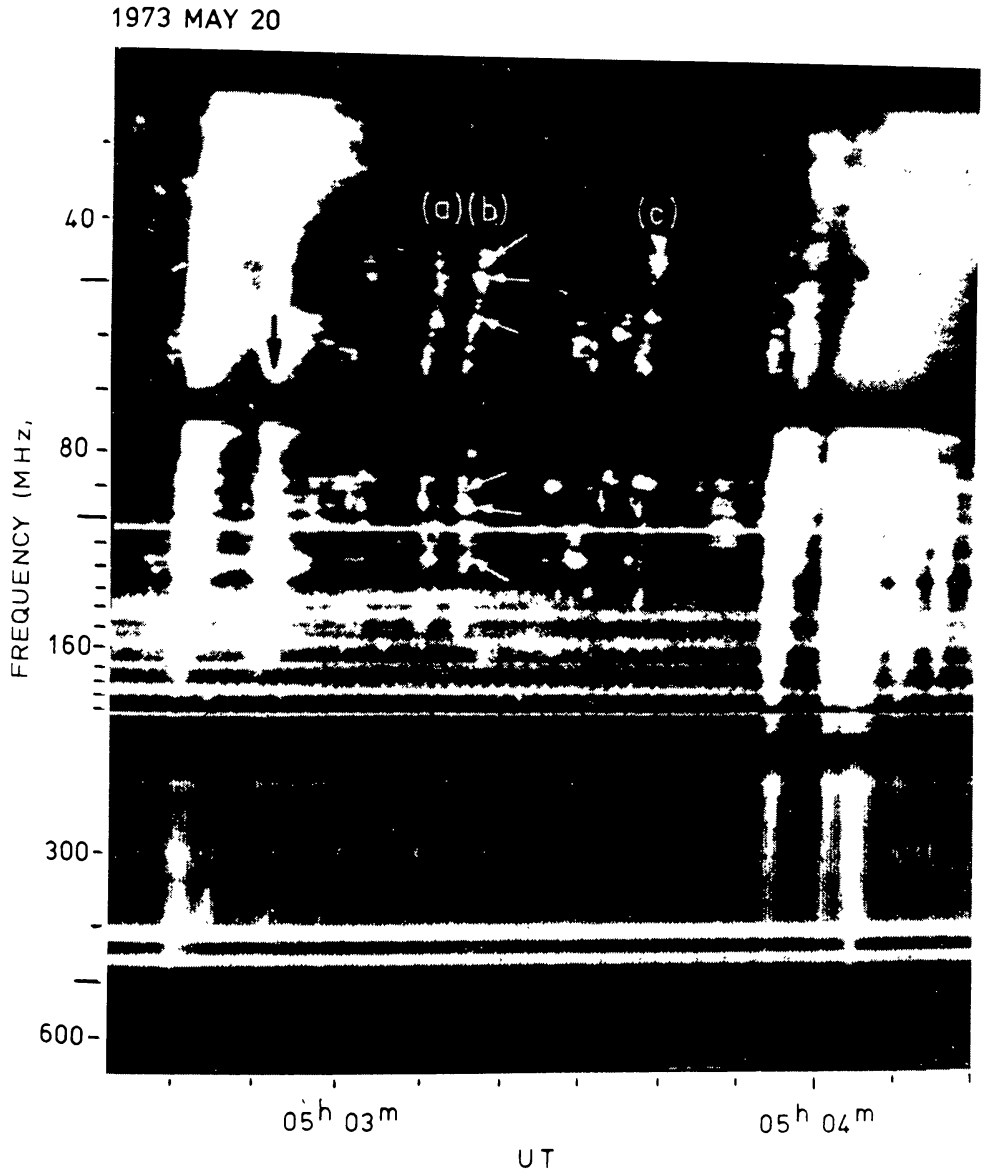

Fig. 23. A group of type IIIb and type III bursts observed on 20 May 1973. Type IIIb are harmonic pairs with 1:2 frequency ratio. Both fundamental and the second harmonic emission show stria. Arrows indicate three sets of harmonic pairs of prominent striae, each harmonic pair is indicated by a pair of parallel arrows (from Takakura and Yousef, 1975).

fundamental shows striations while its second harmonic shows a continuous trace (see Figure 24).

Apart from these commonly observed features, other features such as fast drift storm bursts, hook bursts, drift pair, etc. are also observed. Fast drift storm bursts are observed during decametric noise storm. They occur in groups of 10 to 20 bursts. Drift rates of these bursts are within the range of 1 to 2 MHz s^{-1} and bandwidths 30 kHz. (Ellis, 1969).

3.2.5. *Drift pairs (DP) and their Variants*

Drift pair bursts shown in Figure 25 are bursts appearing in dynamic spectrum as two

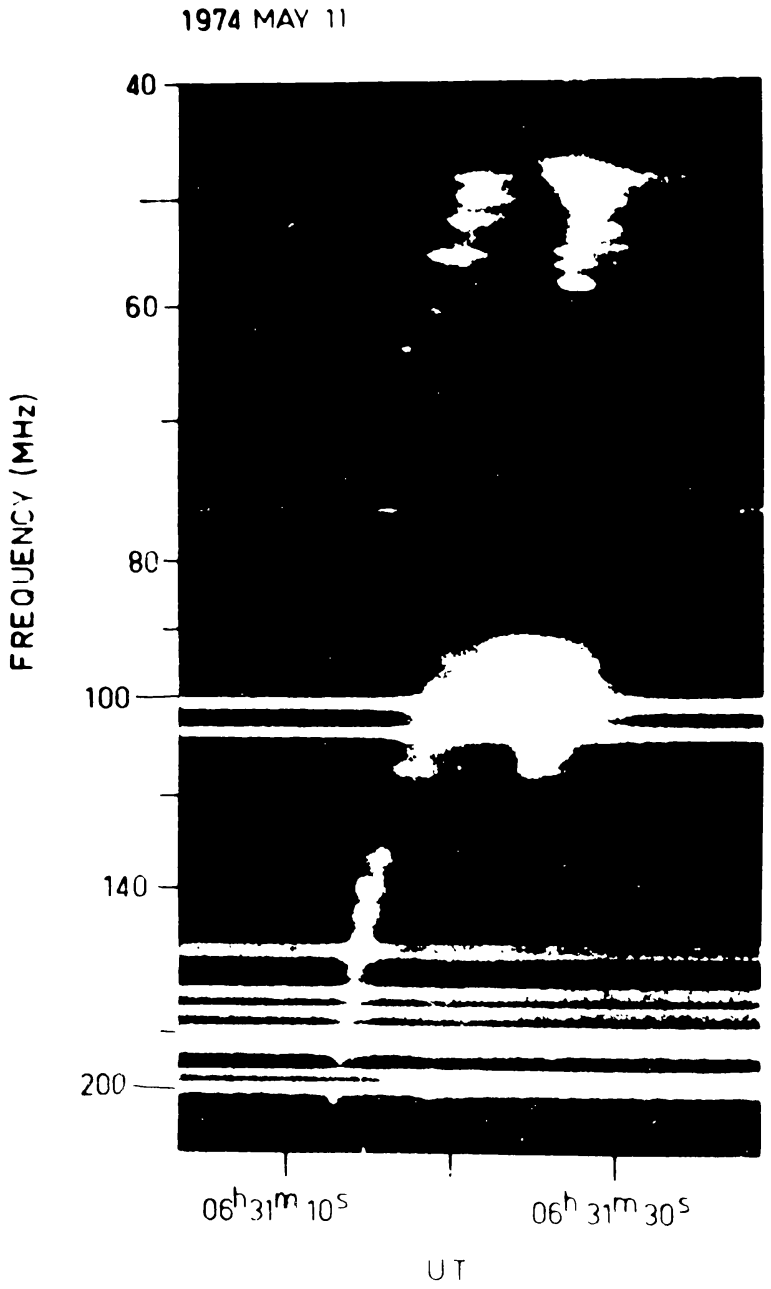

Fig. 24. Inverted U burst recorded by Culgoora spectrograph. On the original spectrogram the brightening at the beginning of the down stroke of the fundamental is seen to consist of two clearly separated striae. Intensity variations observed in the range of 110 to 200 MHz are instrumental origin (from Stewart, 1975).

similar elements drifting in frequency either with positive or negative drift rates and where the second element is the repetition of the first with a time delay of about 1–2 s (Roberts, 1958; Ellis and McCulloch, 1967; Ellis, 1969; de la Noë and Boischot, 1972; Moller-Pedersen, 1974; Moller-Pedersen *et al.*, 1978). Each element has instantaneous bandwidth of about 400 kHz and total duration of about 0.4 s around 30 MHz.

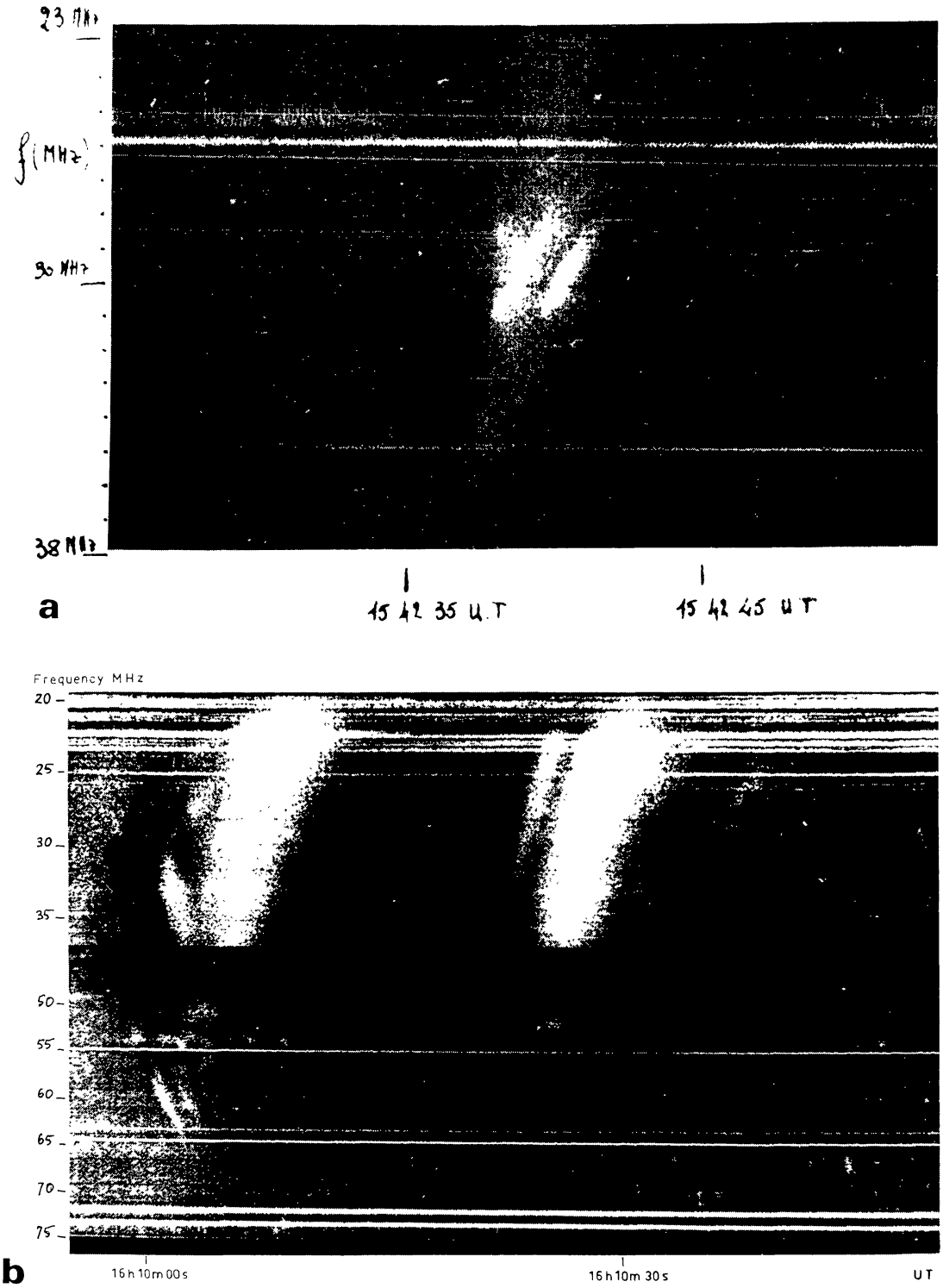

Fig. 25. (a) Forward drift pair superimposed on a weak type III burst observed on 2 August 1970. (b) Reverse drift pair burst situated at the starting frequency of type III burst and the simultaneous fundamental burst occurring at half the frequency of the drift pair observed on 25 July 1970 at 16:10 UT (from de la Noë and Moller-Pedersen, 1971).

The variant of drift pair is a 'hook' burst of which the second component looks like a 'hook'. The drift rate and bandwidths are similar to that of a drift pair but the slope is suddenly reversed, producing a curved trace of increasing frequency. On dynamic spectra, it looks like VLF hooks produced by electron streams in the Earth's magnetosphere (Ellis, 1969).

3.2.6. *'Echo-Type' Bursts*

An echo of solar radio burst is a commonly observed phenomenon in the solar corona. Echoes have been observed in all the spectral features observed in the solar decametric noise storms such as drift pair, split pair, and type IIIb burst as shown in Figure 26 (Ellis and McCulloch, 1967; Baselyan *et al.*, 1974; Sawant *et al.*, 1977). On

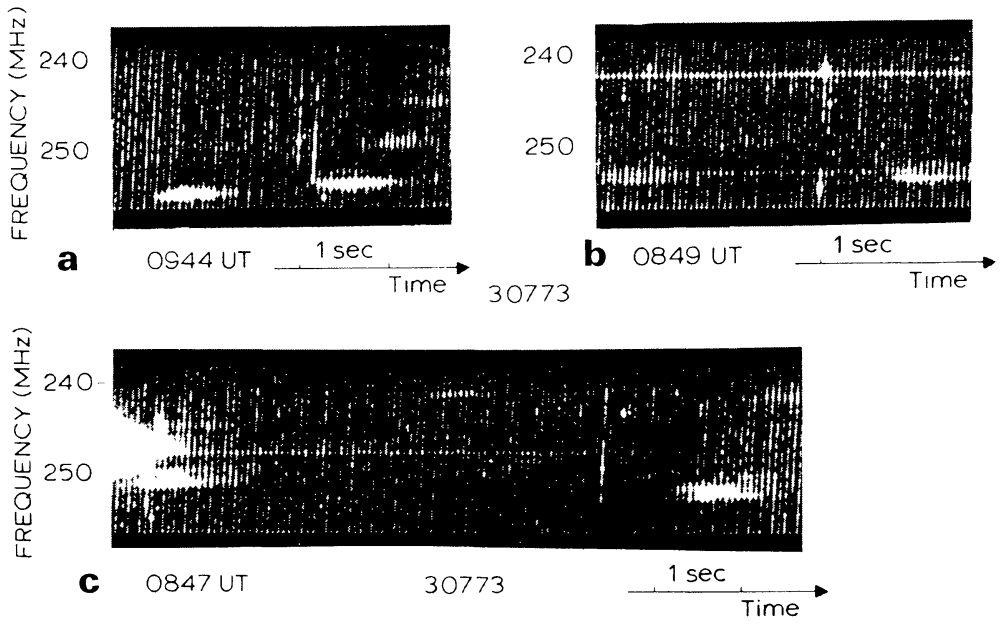

Fig. 26. Examples of echo type events; (a) and (b) show ordinary stria bursts and (c) split pairs (from Baselyan *et al.*, 1974).

an average, the frequency-shift of the reflected component of the burst is of the order of ±10 to 30 kHz and the time delays range from 0.6 to 6 s. It has been observed that the instantaneous bandwidths and frequency drift rates are an order of magnitude less in the case of the echo-type events as compared to those events without an echo. Also in case of split pair, triplet and type IIIb, all the burst elements are not always reflected (Baselyan *et al.*, 1974; Sawant, 1977).

3.2.7. *'Echo-Like' Bursts*

During the noise storms from February 1974 to August 1976, 148 conventional 'echo-type' and 52 'echo-like' bursts were observed. These 'echo-like' bursts differ from 'echo-type' bursts in the magnitude of the central frequency shift and the

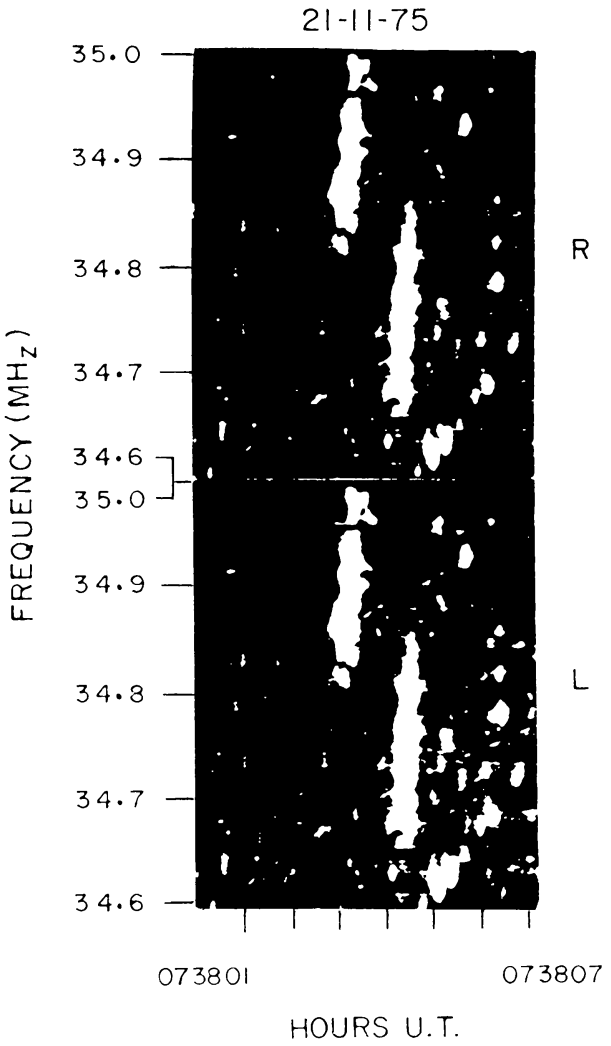

Fig. 27. Dynamic spectra of 'echo-like' reverse drift pairs observed at 07:38:02 UT. In this case the starting frequency of the second element is lower by 150 kHz (from Sawant *et al.*, 1977).

polarization properties (Bhonsle *et al.*, 1977). Some of the important characteristics of 'echo-like' bursts are as follows.

The observed time delays between the first and second component in 'echo-like' event is of the order of 0.6–6 s and the central frequency of the reflected second component is shifted by as much as ±300 kHz or more with respect to the first component (see Figure 27). In 64% of 'echo-like' events, the shift in frequency of the second component was lower ($-\Delta f$) with respect to the first and in 36% it was higher ($+\Delta f$). A convincing example of a microscopic inverted 'U' burst as an 'echo-like' event observed at Ahmedabad on 20 November, 1975 at 0603:30 UT is shown in Figure 28. It may be noted that there is a striking similarity between the two components but for the central frequency shift at the 'turnover' point.

These 'echo-like' events have been explained by Bhonsle *et al.* (1977) assuming two successive exciter electron streams passing through the same moving irregularity and emitting radiation through plasma oscillation process. It is worth noting that

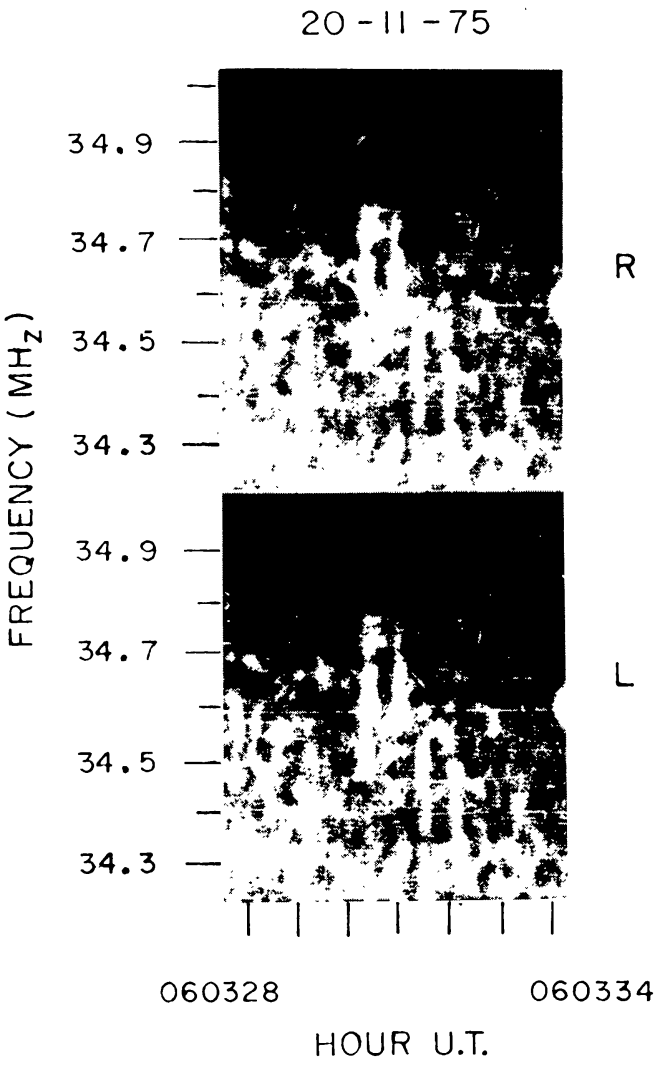

Fig. 28. Dynamic spectra of 'echo-like' inverted 'U' bursts observed at 06:03:30 and 06:03:31.5 UT in *R* and *L* polarization. Frequency range of inverted 'U' burst is 250 kHz (from Sawant *et al.*, 1977).

Elgaroy (1977) and Abranin *et al.* (1977) have also suggested similar independent exciters for 'echo-type' events. The positive or negative shift in the central frequency of these bursts indicates the motion of the irregularity toward or away from the Sun. Knowing the time difference between the central frequencies of 'echo-like' bursts and Δf, the magnitude of the motion of the irregularity has been estimated as 100 to 1000 km s^{-1} away from the Sun and around 2000 km s^{-1} toward the Sun. These values are consistent with the estimates given by Dennison and Hewish (1967) from interplanetary scintillation studies and Ivanov and Livshits (1968) from their studies of motions of irregularities along the field lines.

3.2.8. *'V-shaped' Bursts*

These bursts were first reported by Baselyan *et al.* (1974) in the range 25 to 12.5 MHz. Similar bursts were also observed at Ahmedabad at 35 MHz in 1974.

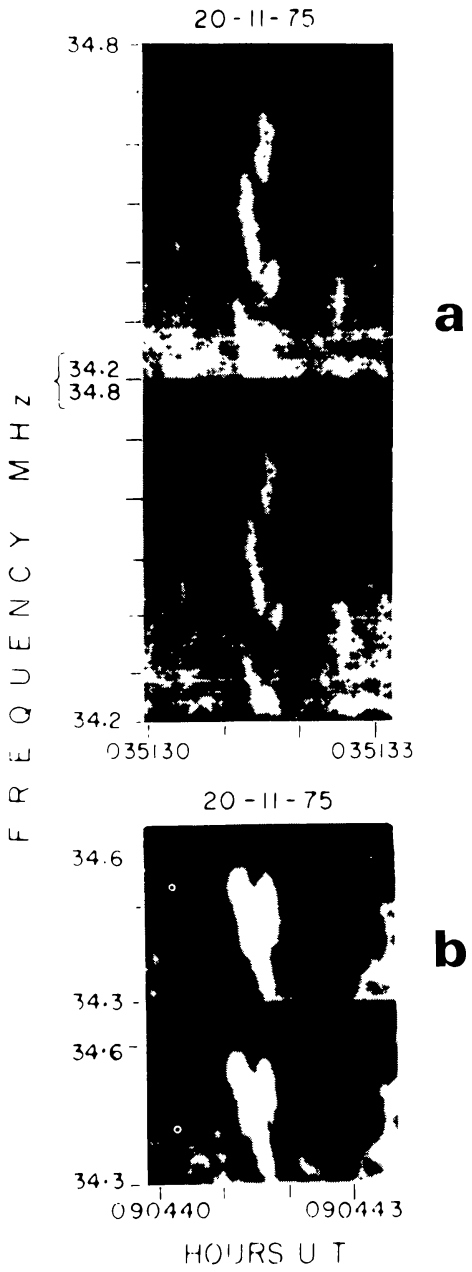

Fig. 29. (a) Chain of V-shaped burst. (b) Isolated V-shaped burst showing no circular polarization (from Sawant, 1977).

Their polarization properties in the range 35–34 MHz were reported for the first time by Sawant (1977). Figure 29 shows an example of this burst and its polarization. No circular polarization was observed in isolated cases of V-shaped burst or in their chains, either in their first or in the second branch. Maximum time delays observed between the first and the second branch of V-shaped burst is about 2 s. Separation between the two branches of the V-bursts is of the order of 300 kHz and is higher than that of the split pairs observed in the same range.

Baselyan *et al.* (1974a) have suggested strong frequency dependent reflection to be responsible for the generation of V-shaped burst. Fomichev and Chertok (1970)

predicted theoretically the change of degree of polarization or reversal of sense of polarization after reflection in echo-type events. In case of V-shaped burst, if the second branch is due to strong frequency dependent reflection, at least occasionally a change of degree of polarization is expected and should have been observed on the second branch of V-shaped burst. But so far no significant change of degree of polarization has been observed (Sawant, 1977).

3.2.9. *New Microscopic Spectral Features*

We now report in the following the characteristics of four new types of microscopic spectral features (near 35 MHz) observed at Ahmedabad during decametric noise

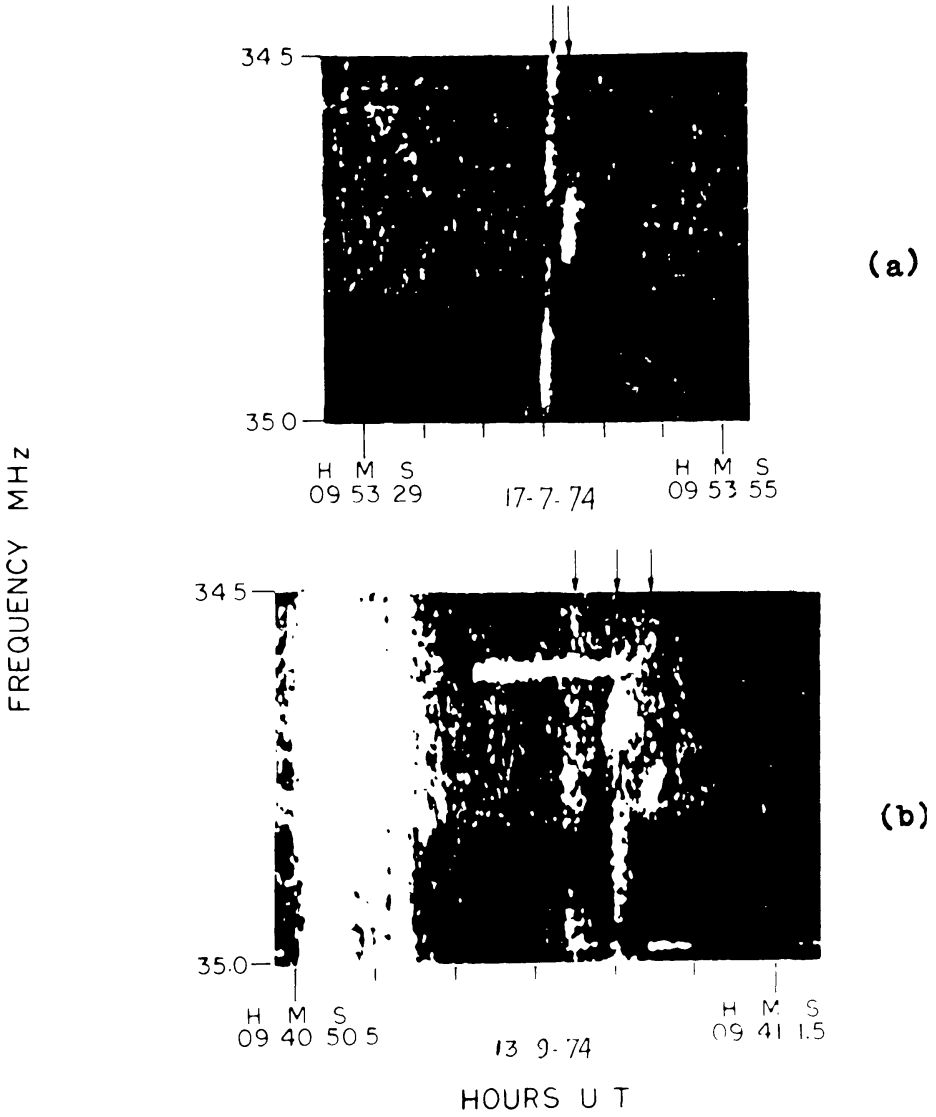

Fig. 30. Dynamic spectra of complementary bursts (C.B.'s) near 35 MHz: (a) Burst on 17 July 1974 showing two components (marked by arrows above), the first with the emission gap around its centre, the second strong and delayed by 0.5 s. (b) Bursts on 13 September 1974. The bright vertical patch is a group of type III bursts. The next event shows three components displaying similar characteristics as the two components as in (a). Horizontal bright line is due to local transmission (from Sawant *et al.*, 1975).

storms from 1974 to 1977 (Sawant, 1975; Sawant *et al.*, 1976a, b; 1977; Sawant, 1977).

3.2.9.1. *'Complementary' Bursts (C.B.'s)*. These bursts essentially consist of two components, each having a duration of ~1 s (see Figure 30). The duration is found to slightly increase as the frequency decreases and the first component shows a weak emission or emission gap over a certain frequency range. These emission gaps can have widths ranging from 30 kHz to 500 kHz. The frequency drift rate of the first component is about 1 MHz s^{-1}. The second component is observed after a certain time delay and its frequency range is approximately equal to that of the emission gap observed in the first component. Generally, the second element is enhanced in itensity and is also of ~1 s duration. The frequency drift rate of the second component is lower than that of the first one. In particular, the drift rates are higher if the time delay between the two components is more. No circular polarization was observed either in the first or in the second component (Sawant, 1977). A histogram of the time delays in seconds between the two components of the C.B.'s against the number of events is shown in Figure 31. It clearly shows two groups of C.B.'s having time delays centered around 1–2 and 10–15 s.

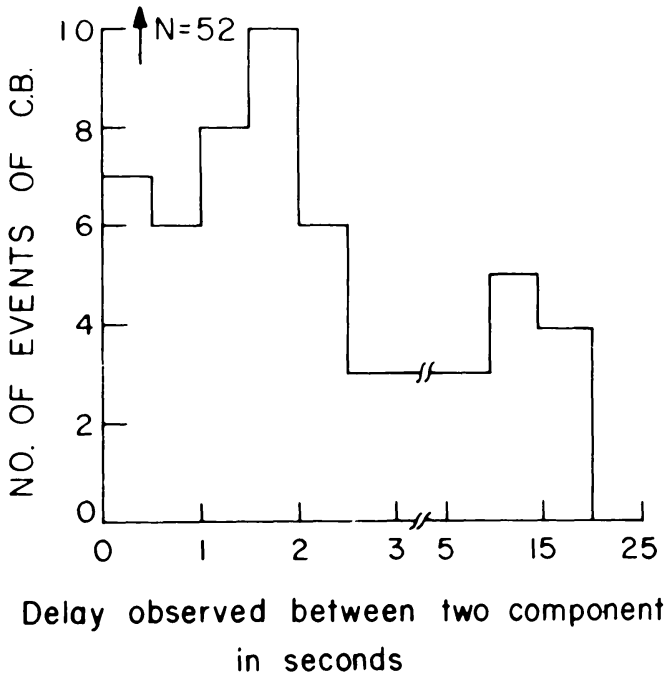

Fig. 31. Histogram showing the number of bursts as a function of time delay between the C.B. components. Total number of 52 C.B. bursts were observed from July 1974 to March 1976. Note the two groups, one around 1–2 s and the other around 10–15 s (from Sawant, 1977).

In storms of November 1975 and March 1976, twelve C.B.'s were observed at Ahmedabad with improved sensitivity and their spectra were recorded in *R*- and *L*-polarization. An example is shown in Figure 32, which was recorded on 9 August

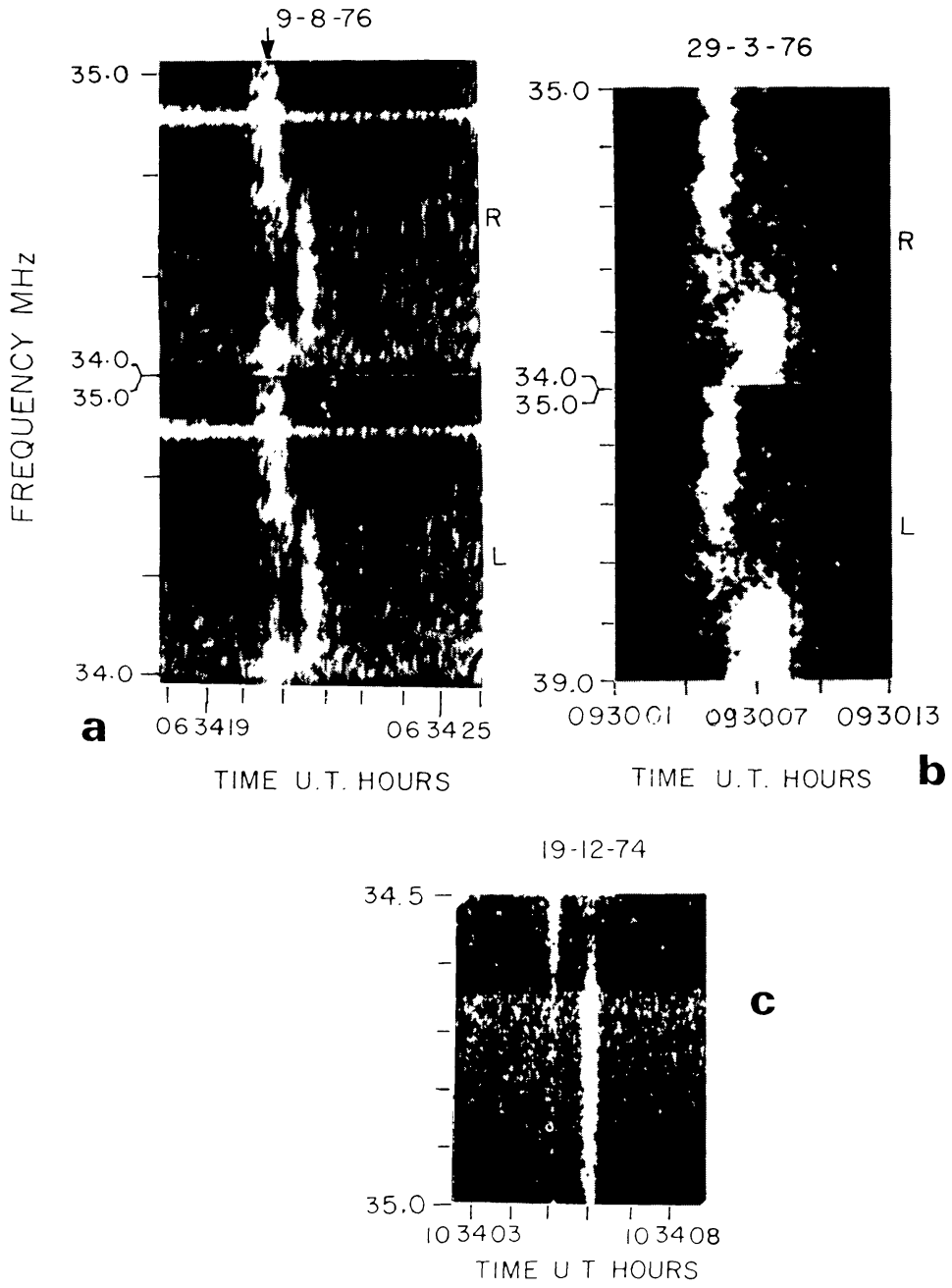

Fig. 32. Dynamic spectra of C.B.'s (marked by an arrow) near 35 MHz observed on 9 August 1976 in *R*- and *L*-polarizations. Horizontal bright line is due to local transmission. (b) and (c) show similar examples of C.B.'s (from Sawant, 1977).

1976 at 06:34:21 UT. A weak emission or gap in emission of the first component occurred after a delay of 0.3 s. Both the components were equally intense in *R* or *L* polarization, which means that they were randomly or linearly polarized. This is true of all the C.B.'s recorded so far.

3.2.9.2. *Bursts showing curvature along frequency axis.* Dynamic spectra of decametric type III bursts (duration 1 s) and normal type III bursts (duration ~ 10 s)

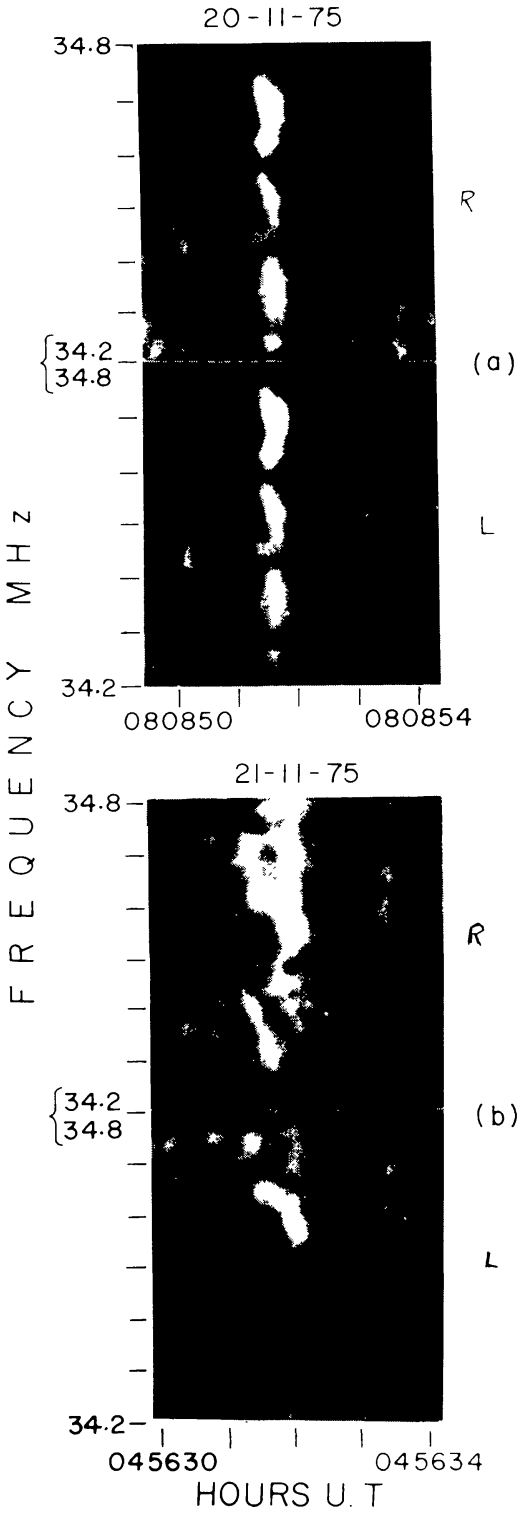

Fig. 33. Dynamic spectra of solar bursts near 35 MHz in *R* (upper) and *L* (Lower) polarization showing: (a) three striae, out of which upper two are curved and lower one is straight; (b) a split pair with a curved upper trace and a straight lower one.

showing curvature along the frequency axis over a certain frequency range were observed at Ahmedabad in almost all storms recorded from February 1974 to August 1977. In case of type IIIb or split pair, curvatures along the frequency axis are sometimes observed (see Figure 33). On macroscopic scale, curvatures along the frequency axis were recorded in drift pair (Roberts, 1958). Average characteristics of these bursts showing curvature in different types of bursts are summarized in Table V. Since curvature along the frequency axis over a certain range of frequencies are observed in varieties of bursts, this effect is not likely to be inherent in the source and so it appears to be due to propagational effects, such as group delays (Sawant *et al.*, 1976a, b).

TABLE V

Characteristics of bursts showing curvature along frequency axis[a]

Type of burst	No. of events	Curvature frequency range, kHz	Delay time w.r.t. extreme frequencies ms
III	(7)	200–500	200–400
III decametric	(13)	100–300	200–300
split pair	(3)	——–200	0–200
IIIb	(4)	——–200	0–200

[a] From Sawant *et al.* (1976b).

3.2.9.3. *Chains of 'dot' emission.* An intense short duration and narrow band solar radio emission defined as 'dot' emission is observed in the frequency range 35 to 34.0 MHz. Often the bandwidths of these narrow band bursts were ~50 kHz and total duration ~300 ms. These 'dot' emissions have a tendency to occur in groups. Most of the properties of chains of 'dot' emissions are similar to those of type IIIb except that (i) no association of chains of 'dot' emission have been observed with type III or type IIIb, (ii) the total duration of chains of 'dot' emissions is at least by a factor of 2 less compared to that of type IIIb; duration of type IIIb burst at 36.9 MHz is 1.0 ± 0.2 s (de la Noë and Boischot, 1972) whereas that of 'dot' emission is 0.3 ± 0.1 s (Sawant *et al.*, 1976a, b), (iii) chains of 'dot' have rarely been observed to cover the entire frequency range (35 to 34.0 MHz) of the spectroscope while type IIIb bursts are usually observed all over the frequency range of the spectroscope. In general, chains of 'dot' extend over a frequency range of 400 to 300 kHz and start and stop at different frequencies as seen within the frequency range of the spectroscope. This is shown in Figure 34. The most common feature of the chains of 'dot' emission is the occurrence of an echo of one of the elements. Echoes of all the elements have never been observed at the same time. Eighty 'dot' emissions recorded from all the noise storms were available at Ahmedabad for the study of instanteous bandwidths.

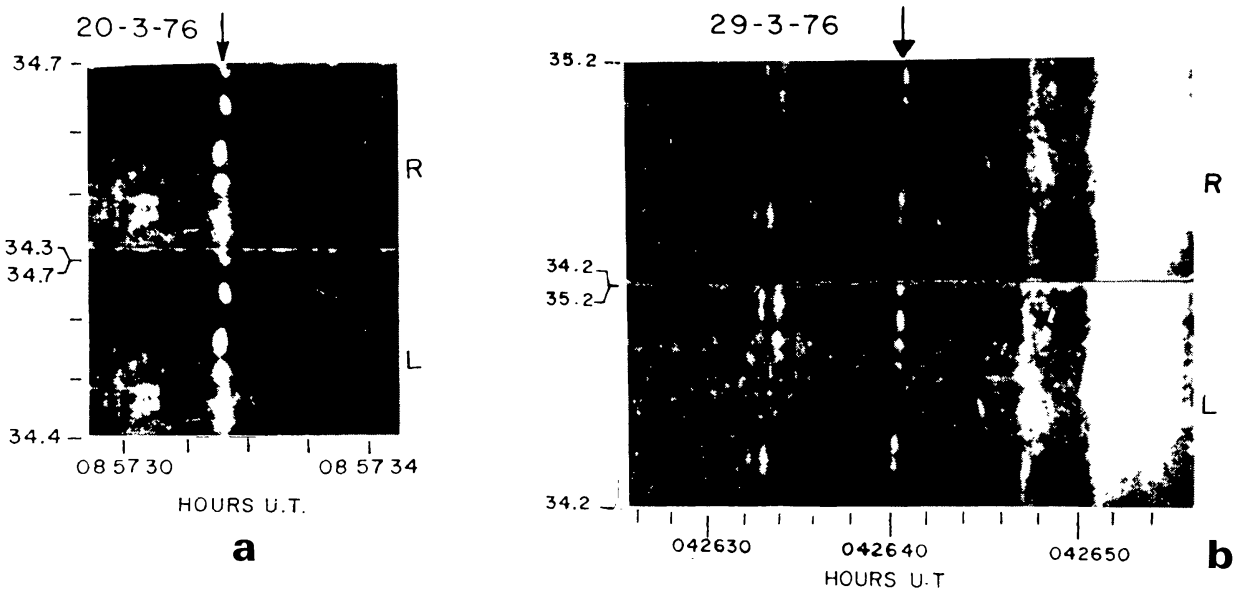

Fig. 34. Dynamic spectra of chains of 'dot' around 35 MHz: (a) chain of 'dots' observed on 20 March 1976, (b) a chain of 'dot' with intermittent emission shown by an arrow. An associated type IIIb-III burst can be seen around 04:26:50 UT (from Sawant *et al.*, 1976).

Within the range of 35 to 34 MHz, instantantaneous bandwidths peak at 50± 10 kHz. Drift rates of 16 chains of 'dot' emissions were measured and were found to be of the order of 1.5 MHz s^{-1}.

3.2.9.4. *Microscopic 'U', inverted 'U' and partial 'U' bursts.* Microscopic 'U', inverted 'U', and partial 'U' bursts were observed at Ahmedabad in November 1975 and March 1976 noise storms. Figure 35 shows the decametric bursts which appear like inverted 'U', 'U' and partial 'U' bursts on microscopic frequency scales. The microscopic 'U' and inverted 'U' bursts are characterized by the total duration of 1 s. The average duration of each branch of families of microscopic 'U' bursts is 0.3 ± 0.1 s and the observed frequency range of these bursts is 0.1–1 MHz. Both or one of the branches of microscopic families of 'U' bursts sometimes show intensity variation along the frequency axis. One of the important properties is that they show enhanced intensity at their 'turnover' points. Both branches of microscopic 'U' burst may show different frequency drift rates. Microscopic 'U' bursts have also been observed to occur in groups. Typical parameters of decametric type 'U' and 'partial U' bursts are given in Table VI. Frequency drift rates of these microscopic 'U' bursts and striations in them may be explained by the change of sign of the local electron density gradient and by their steepness respectively, which the electron exciter beam would encounter as it traverses an individual electron density irregularity. (Sawant *et al.*, 1976a, b; Sawant, 1977).

3.2.10. *Type V Bursts*

So far no fine structures in type V burst have been reported. It is possible that fine

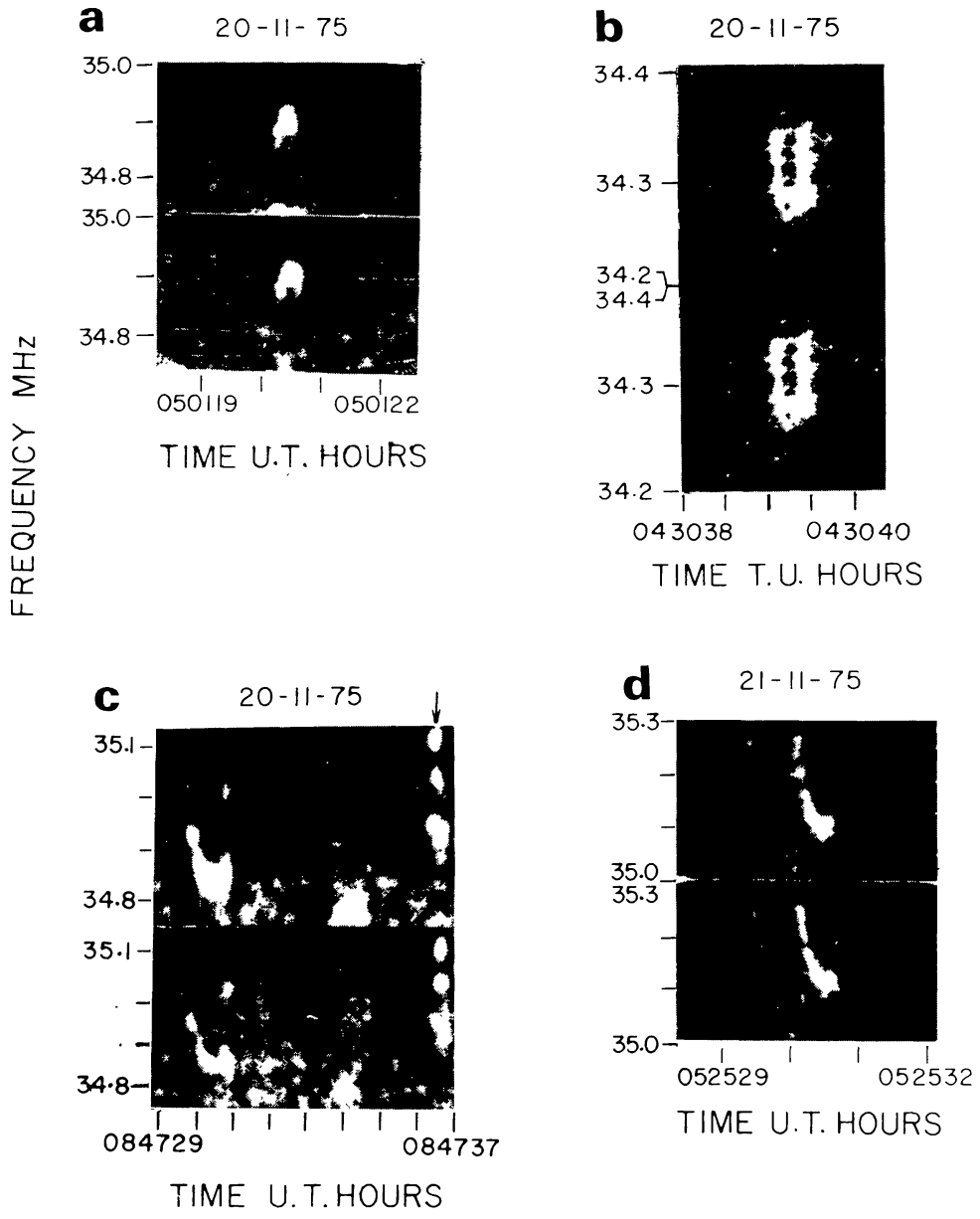

Fig. 35. Dynamic spectra of solar bursts near 35 MHz in R (upper) and L (lower) polarizations: (a) 'Inverted U' burst observed over a range of 150 kHz, (b) 'U' burst observed at 04:30:39 UT, (c) another 'U' burst, and (d) 'partial U' burst (from Sawant *et al.*, 1976).

structures in type V may be revealed if the observations are made with high sensitivity coupled with high resolution.

3.2.11. *High Resolution Observations of Decametric Type II Bursts*

Decametric type II bursts are characterized by slow-drift in the spectral features from high frequency to low frequency with drift rate of 0.05 MHz s^{-1} at 30 MHz (Roberts, 1959; Maxwell and Thompson, 1962). On the plasma hypothesis the frequency drift is found to correspond to the velocity of the order of 10^3 km s^{-1} and moving agency is identified with collisionless MHD shock wave set up as a result of an

TABLE VI

Typical parameters of decametric type 'U', 'inverted U' and 'partial U' bursts near 35 MHz[a]

Burst types & No.	Range of total duration (s)	Approximate frequency range (kHz)	Average drift rate (kHz s^{-1})		Striations
			*1st component	2nd component	
'U' 8	0.6–1.2	400–1000	−250	1200	Yes
'Inverted U' 7	0.5–1	60–700	−1000	700	Yes
'Partial U' 6	0.8	200–400	−400		Yes

* 1st component of the bursts is the one that occurs prior to the time when the frequency drift rate becomes zero.

[a] From Sawant *et al.* (1976b).

explosion at the time of flash phase in a solar flare (Kundu, 1965). Apparently, these MHD shock waves continue their travel in the interplanetary space with little or no deceleration at least up to the orbit of the Earth or even beyond (Dryer, 1975), and occasionally these shock waves are observed (optically) to travel in the transverse direction (Bhatnagar *et al.*, 1978). Earlier work including recent Culgoora observations has been reviewed by Wild and Smerd (1972). The spectacular radio events observed in August 1972 by the ground-based techniques have been reviewed by Bhonsle *et al.* (1976) who have stressed the importance of studying type II/IV bursts as they are linked with the occurrence of proton flares and cause polar cap absorptions and geomagnetic storms on the Earth. In particular, Dodge (1973) reported occurrence of type III, IV, and II bursts on 7 August 1972 from 15:10 to 15:52 UT in the frequency range of 80–20 MHz. As many as four type II bursts were recognizable against type IV continuum with radial velocities of collisionless MHD shocks of 3900, 4900, 1400, and 900 km s^{-1}, (Dodge, 1973a, b) while Maxwell and Rinehart (1974) reported at least two components each having different radial velocity range of 1000–1500 km s^{-1} for the slower component and 2000–3000 km s^{-1} for the faster component. Malitson *et al.* (1973) tracked the same type II shock wave from corona to the Earth's orbit and deduced an average velocity of 1270 km s^{-1} for the shock wave. These wide variations in the inferred radial velocities can possibly be attributed to errors introduced due to difficulty in recognizing drifting spectral features against very intense continuum background radiation on the photographic recording film. It seems, however, swept frequency interferometer such as that of Dodge (1973) gives more detailed information of such complex events as it is relatively easy to identify them. Very scanty high resolution observations of type II/IV in the decameter range are available at present (Aubier and de la Noë, 1971; Lacombe and Moller-Pedersen, 1971; Sawant *et al.*, 1978). About 50% of type II bursts are preceded by a group of type III bursts by several minutes. Often type II bursts show a herring-bone structure of rapidly drifting short duration bursts emerging from drifting bands (Kundu, 1965).

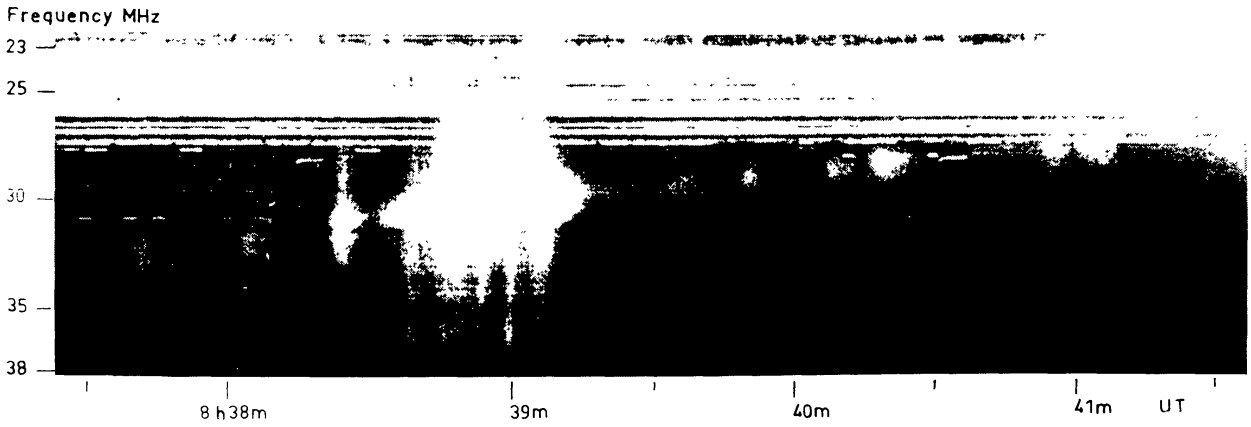

Fig. 36. Interaction between successive type III particle streams and an ascending shock wave observed on 10 March 1970. Intense horizontal lines are due to local interference (from Lacombe and Moller-Pedersen, 1971).

With the help of high resolution spectroscope in the range 40–20 MHz, interaction between fast moving electron streams and ascending slowly moving shock was observed as an enhancement of type III-like burst within the frequency range as shown in Figure 36. The characteristics of type II bursts even after the interaction with type III are not changed, implying very little energy transfer from shock to the exciter of type III bursts. The large frequency bandwidth of superimposed weak type

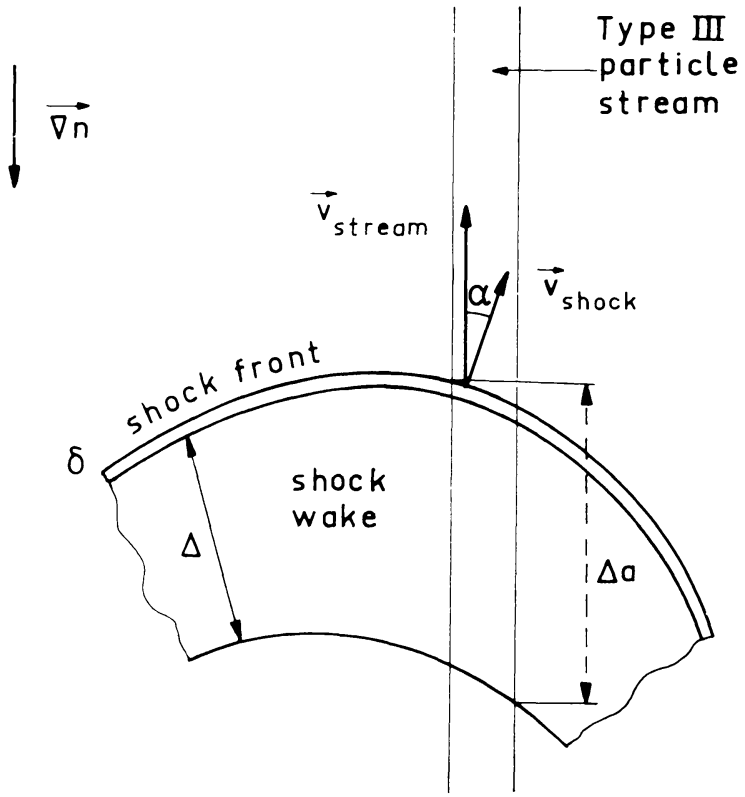

Fig. 37. A schematic putline of the interaction between a type III particle stream and shock wave when their respective velocities are almost parallel (from Lacombe and Moller-Pedersen, 1971).

III bursts can be explained under the assumption of a long wake behind the shock front where a modification of the nonlinear stabilization process of the instability of the stream takes place as shown in Figure 37 (Lacombe and Moller-Pedersen, 1971).

Apart from the above mentioned features, a fine structure in the form of 'bright spots' of emission lasting for a few seconds (0.6 to 2.35 s) and of relatively narrow bandwidth were observed by Aubier and de la Noë (1971). These bright spots are due to the excess of emission caused by the passage of shock front through the electron density irregularities. The sizes of these irregularities turn out to be a few thousand kilometers (Aubier and de la Noë, 1971).

Analysis of twenty type II solar radio bursts observed during 1968–1972 in the frequency range of 240–40 MHz at Ahmedabad has revealed that such bright spots are predominantly observed below 100 MHz. Frequency spread and total duration of these spots are 500 kHz to a few MHz and 0.5 to 4 s respectively (Sawant *et al.*, 1978). Sawant *et al.* (1978) have argued that the upper limit for the shock thickness may also be obtained from the duration of 'bright spots' in type II bursts and is of the order of 10^3–10^4 km in the region of 1.5–$2.5R_\odot$ above the photosphere. It is interesting to note that these values are consistent with theoretical estimates (Dryer, 1975).

3.2.12. *High Resolution Observations of Decametric Type IV Bursts and Coronal Transients*

With the introduction of fast radioheliograph at 160, 80, and 43.25 MHz at Culgoora, it was possible to study the motions of type IV bursts in two dimensions. They have been classified as advancing shock front, expanding magnetic arch and ejected plasma blobs (Wild and Smerd, 1972; McClean, 1974). This radiation is considered to be the synchrotron radiation by relativistic electrons (Boischot and Clavelier, 1968). The flare associated type II events are almost always associated with type IV emission. It is interesting to note that some type III bursts coincided in position with moving type IV source. Further understanding of moving type IV burst came from the work of Gergely and Kundu (1975) in the decameter range. They observed four type IV decametric bursts in the range 65–20 MHz with the help of sweep frequency interferometer at the Clark Lake Radio Observatory. All these bursts were associated with coronal transients (Hansen *et al.*, 1971; Riddle *et al.*, 1973) which are not necessarily associated with type II and had sizes of $0.8R_\odot$ (at 60 MHz plasma level) of the initial source which increased to 1.4–$2.0R_\odot$ (at 40 MHz plasma level) before the source was split into two components. Gergely (1974) does not favour the association of 'advancing shock front' (moving type IV burst) and coronal transients. On the other hand, he is in agreement with Smerd and Dulk (1971) who proposed that both the expanding arch or the isolated source could account for the coronal transient. It has been observed that coronal transients sometimes display homologous tendency with time scales of the order of 18 to 24 hr as was the case for 13 and 14 May 1971 as well as 11 January 1973 events (Gergely, 1974). Gergely *et al.* (1978) reported on the simultaneous observations of coronal

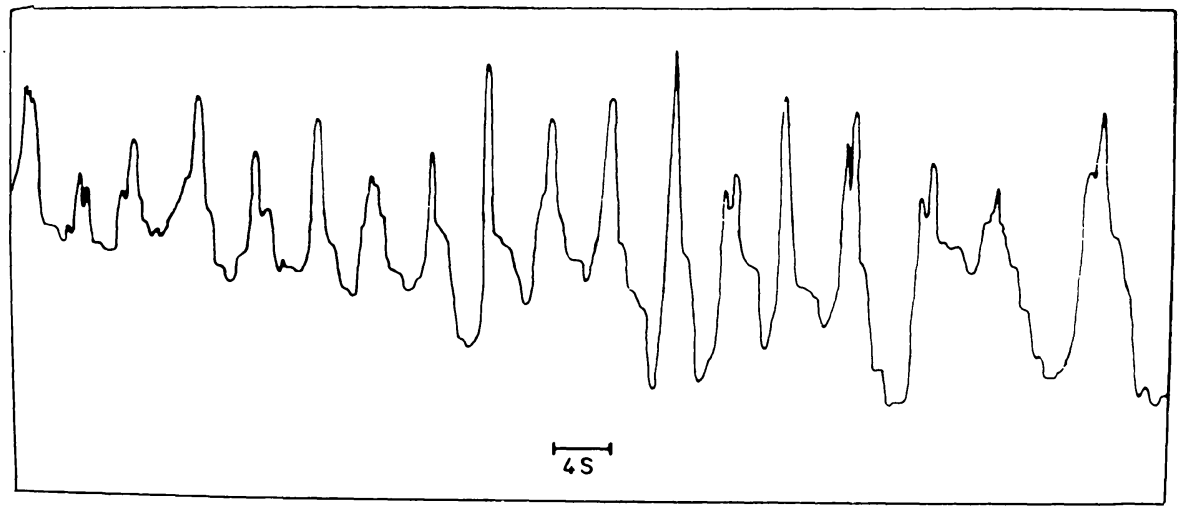

Fig. 38. Micro–photo–metric tracing of the pulsating structures at a frequency of 26 MHz observed on 22 August 1972 around 18:19 UT. The 12 s sub-harmonic is clearly noticeable at least over 3 cycles (from Achong, 1974).

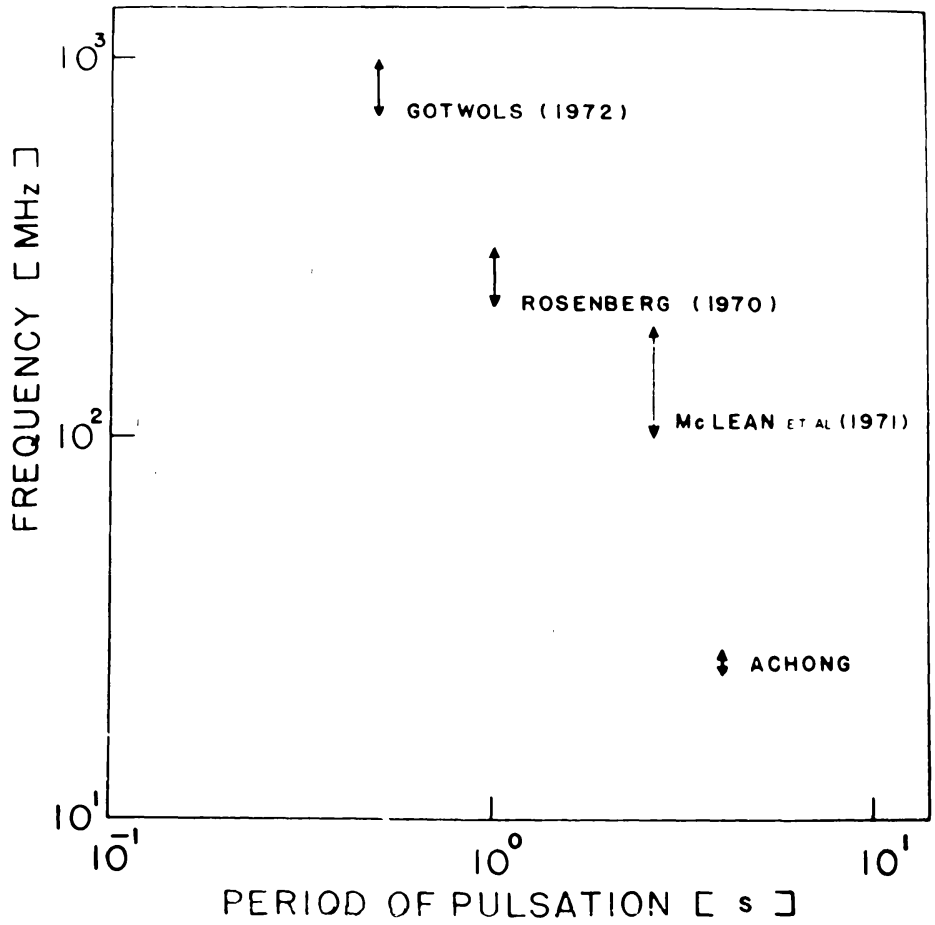

Fig. 39. Pulsation periods obtained by various researchers for different solar events. The observed bandwidths are indicated by double-pointed arrows (from Achong, 1974).

transient on 21 August 1973 in white light from skylab and at decameter wavelengths using two dimensional radio observations with sweep frequency array at Clark Lake. From these observations, they determined thickness of the loop as not less than $0.6R_{\odot}$. Assuming radio emission due to gyrosynchroton mechanism, they estimated magnetic field strength of the order of 1–4 G at $1R_{\odot}$ above the photosphere.

Another frequently observed feature in type IV is the occurrence of pulsations. These pulsations have a period of 4 s and sharp low cut off frequency at 18 MHz were observed with the help of high frequency and time resolution spectroscope in the range 28–18 MHz (Achong, 1974). An example of which is shown by the micro-photometer trace in Figure 38. The periodicity of pulsations observed at other frequencies and their frequency range is given by Figure 39, as reported by various workers. These pulsations can be explained by periodic vibration of magnetic flux tube due to standing hydromagnetic wave (Rosenberg, 1970). As the synchrotron radiation intensity is a sensitive function of magnetic field, periodic fluctuation of the field causes periodic fluctuation in the synchrotron radiation. This model was further elaborated by McLean *et al.* (1971) to be more consistent with observations of pulsations.

3.2.13. *Decametric Type III and Type I-Like Bursts*

Leblanc and Aubier (1977) have observed type III-like decametric bursts associated with metric type I burst. These are shown in Figure 40. They are observed, in the

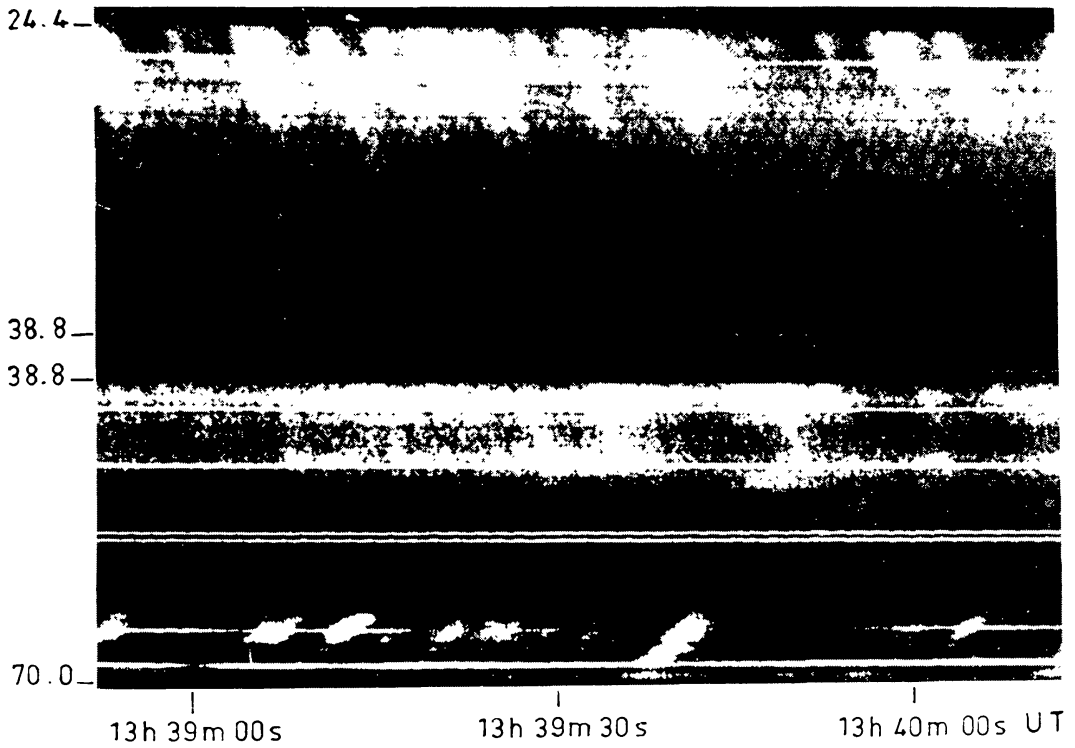

Fig. 40. Type III and type I-like burst observed in the range 50–25 MHz on 29 July 1973 (from Leblanc and Aubier, 1977).

range 70–25 MHz, for type I bursts drift rates 1–2 MHz s^{-1}, which is less than that of type III burst in the same region. They have predominantly negative drifts associated with positively drifting type III bursts in the decametric region. These type III and type I-like decametric bursts have been interpreted in terms of local acceleration at the top of a magnetic arch in the corona. Further they have predicted strong circular polarization of these bursts (Leblanc and Aubier, 1977).

The type IV continuum which is supposed to be smooth has revealed fine structure when observed with high time and frequency resolution. If such observations are made with high sensitivity (using large antenna arrays), many more features may be observed as those observed in metric band (Young *et al.*, 1961; Abranin, 1970; Kuijpers, 1975; Sawant *et al.*, 1978).

4. Heliographic Longitudinal Dependence of Decametric Bursts and Their Parameters

In order to investigate the dependence of the decametric storm bursts and their parameters on the heliographic longitude, the following analysis was carried out.

4.1. Decametric bursts

Decametric noise storms generally consist of varieties of bursts superimposed on continuum radiation. So far as burst component is concerned, the following two classes are considered: (i) Short duration narrow band bursts such as type IIIb, C.B.'s, microscopic families of 'U' burst, chains of 'dot' emission, drift pairs and their variants. It is convenient to denote all the bursts showing fine structure in frequency and time plane as 'BF' type bursts, and (ii) decametric noise storm type III bursts which are smooth in frequency and time plane.

The percentage occurrence 'P' of type III bursts on each day (Moller-Pedersen, 1974) as modified by Sawant (1977) is given by

$$P = \frac{\text{number of type III bursts}}{\text{number of (type III bursts} + \text{'BF' bursts)}} \times 100, \tag{2}$$

where the denominator represents the total number of bursts observed on each day. 'P' was estimated for different noise storms from the data collected over 39 days (Sawant, 1977). Similar analysis was carried out earlier by Moller-Pedersen (1974) in the range 70–24.4 MHz for the noise storms observed from December 1972 to February 1974. Figure 41 shows the Nancay 169 MHz storm center positions and the percentage occurrence 'P' of type III burst as defined above. Following conclusions can be drawn from Figure 41.

(1) Generally, storms evolve starting with 'BF' bursts at large longitudes from CMP. As the storm approaches CMP, the percentage occurrence of type III burst increases and the sequence is reversed when the source crosses the CMP. This can also be seen clearly from Figure 42a, b.

(2) Type III storm centers are mostly situated near CMP but 'BF' burst sources are situated away from CMP.

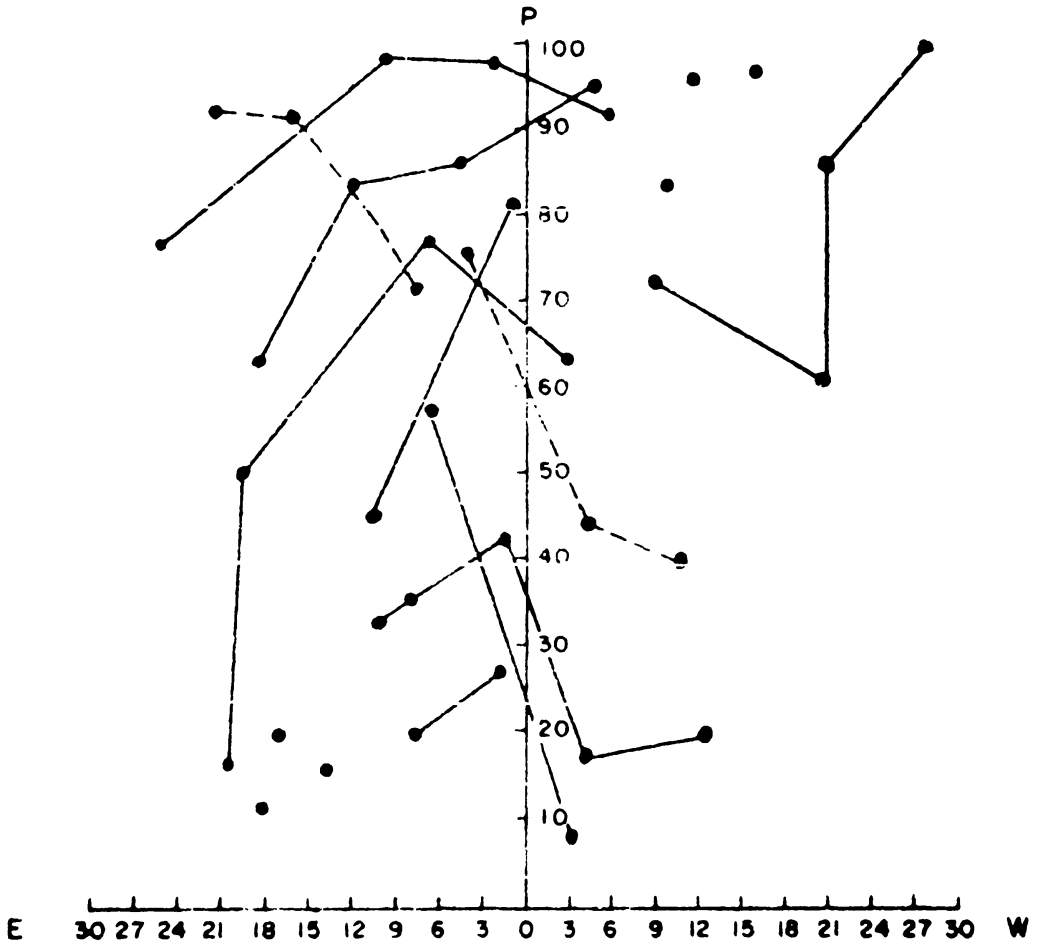

Fig. 41. The 169 MHz storm center positions observed at Nancay and the percentage occurrence 'P' of decametric type III burst at Ahmedabad. Continuous line indicates availability of data on successive days, while broken line indicates the lack of observations for a period of 1 to 2 days (from Sawant, 1977).

Moller-Pedersen (1974) has carried out similar analysis and classified the decametric storms as type IIIb storms, type III storms and type III storms with drift pair (DP) and has shown that type III storms, with or without drift pair bursts, correspond to the active regions close to the central meridian of the Sun. Type III-DP storms have shorter lifetimes of the order 1–2 days than the other storms. To account for the longitude dependence of these bursts, Moller-Pedersen suggested that type III and type IIIb bursts are probably emitted simultaneously but with different directivities and in different directions. This inference needs to be checked by the Solar stereo radio astronomy experiments with spacecraft.

Alternatively, longitudinal dependence of these bursts may be attributed to propagation effects in the intervening medium. But the appearance of type IIIb, and type IIIb in fundamental and second harmonic (Takakura and Yousef, 1975) does not favour this possibility since propagation effects such as absorption or refraction,

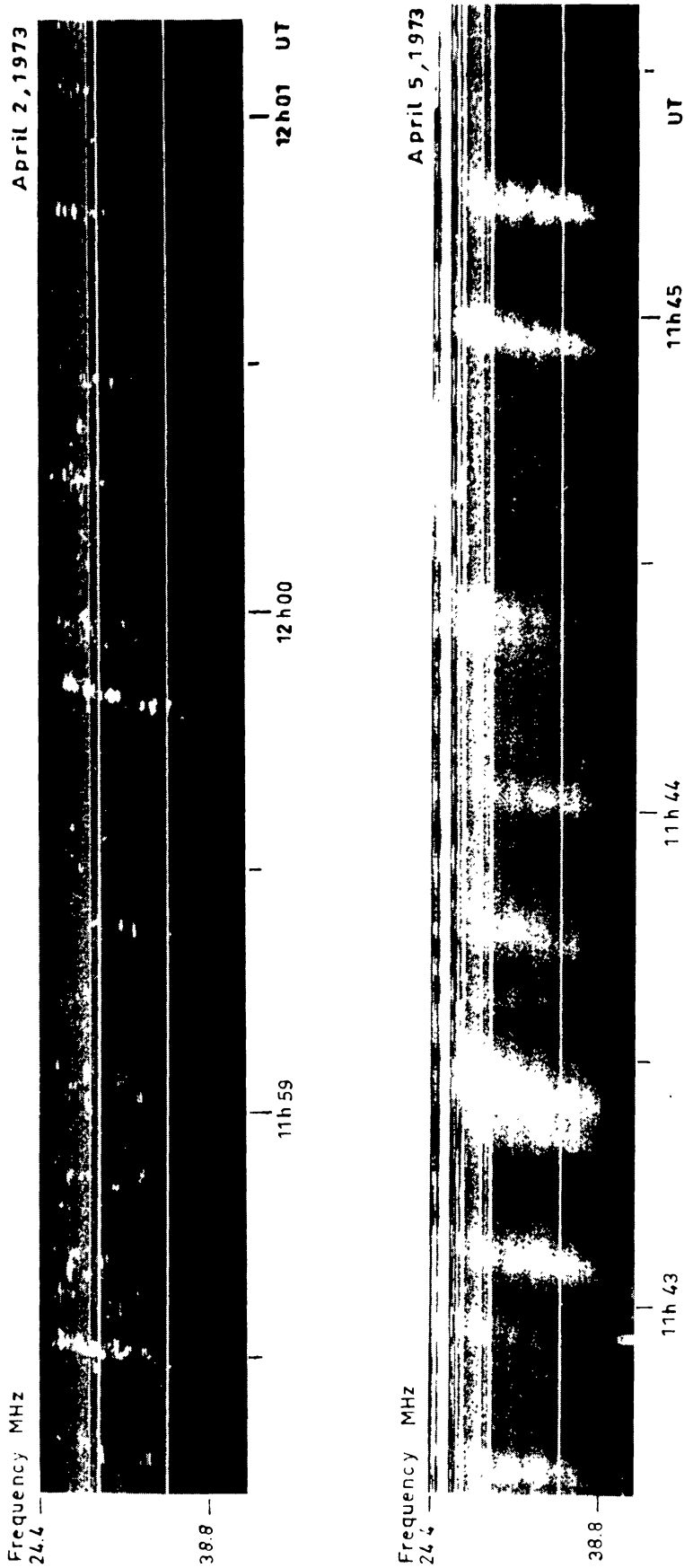

Fig. 42a–b. Evolution of decametric noise storms observed with a sweep frequency receiver in the range 38.8 to 24.4 MHz. (a) Type IIIb storm observed on 2 April 1973, (b) Type III storm observed on 5 April 1973. Intense horizontal lines are of local interference (from Moller-Pedersen, 1974).

being dissimilar at fundamental and second harmonic should make identification of F–H relationship difficult. Further, similarity in positions of type IIIb–type III bursts (Takakura and Yousef, 1975; Abranin *et al.*, 1976, 1977) has to be taken into account in the development of the theory of type IIIb–III burst.

4.2. Decametric burst parameters

Heliographic longitudinal dependence of the spectral parameters of stria, split pair,

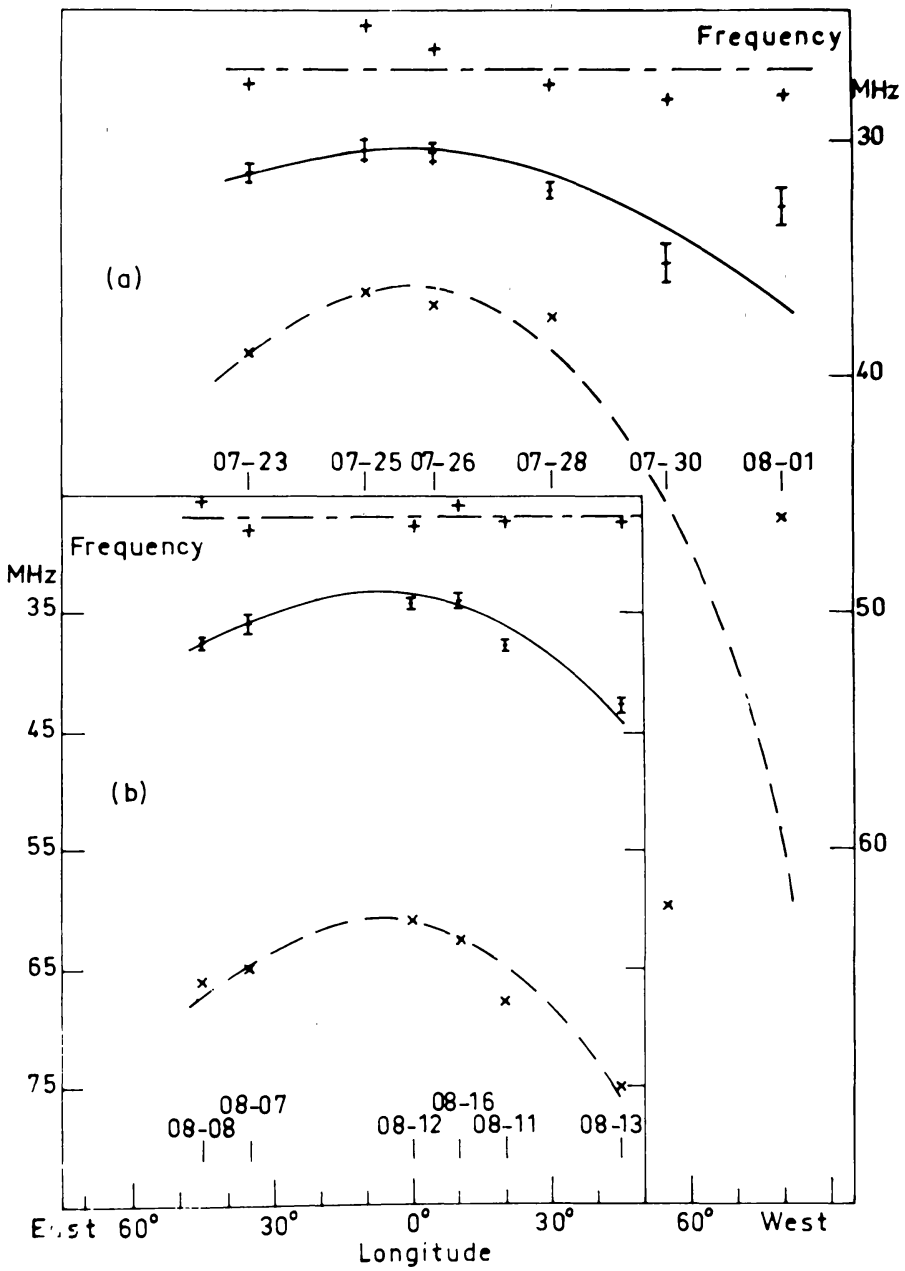

Fig. 43. Average daily frequency of the elements plotted in terms of the average longitude of five regions, for the period of observation: (a) 23 July to 2 August 1970; (b) 7 August to 16 August. +, × represent the daily average frequency for the twenty elements of lower and higher frequency respectively (from de la Noë, 1975).

and triplet all grouped into type IIIb were investigated by de la Noë (1975) and Sawant (1977). The following results came out of the analysis:

(1) The daily average frequency of occurrence in case of stria, split pair, triplets and type IIIb bursts showed minimum when active regions were located near the central meridian of the Sun. This is shown clearly in Figure 43.

(2) The average duration of stria, split pair, triplet and type IIIb increases from high to low frequency and follows an exponential law. This duration is larger for sources near the limb than that at CMP. Figure 44 shows the variations of average

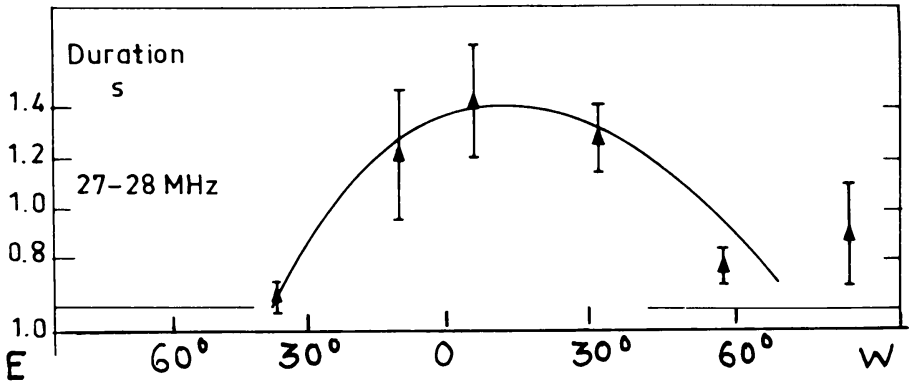

Fig. 44a.

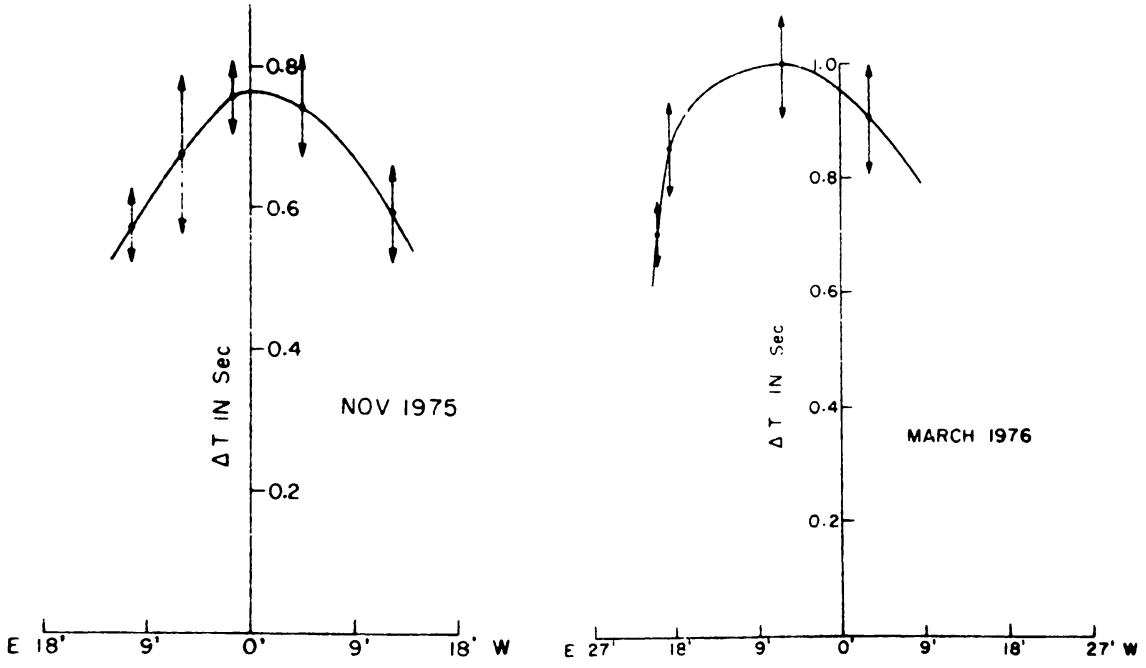

Fig. 44b.

Fig. 44a–b. Daily average duration Δt versus the average longitude of the active regions at different frequencies: (a) for the period of observation 23 July, 1970 to 2 August 1970 in the range 28–27 MHz (from de la Noë, 1975). (b) The Nançay 169 MHz storm center positions and the daily average duration of stria burst observed within the range 35–34 MHz. 90% confidence level is indicated by an arrow (from Sawant, 1977).

duration in the range 28–27 MHz (de la Noë, 1975) and in the range 35–34 MHz (Sawant, 1977).

(3) Average drift rates vary from day to day and it has no systematic variation with average longitude. The average drift rate ranges between 0–150 kHz s^{-1}.

(4) Instantaneous bandwidth of elements in the split pair and triplets and their frequency separation are independent of helio longitude. In split pairs and triplets, the elements have instantaneous bandwidths narrower than those of single stria, the average ratio being 1 : 1.5.

5. Noise Storms at Hectometer and Kilometer Wavelengths

Radio Astronomy Explorer Satellite (RAE 1), launched in 1968 and devoted mainly to solar radio observations at low frequencies, observed for the first time noise storms comprising continuum radiation and thousands of drifting bursts in hectometer and kilometer wavelength ranges (Fainberg and Stone, 1970a, b, 1971a, b; Weber *et al.*, 1971; Malitson *et al.*, 1973a, b). IMP-6 spacecraft observations showed that the source position of continuum component and that of type III burst were the same (Fainberg and Stone, 1974). During a storm, a large number of type III bursts, 1 every 10 s, were observed near 2.8 MHz. They occur in large number when the source moves away from CMP. This effect could either be due to a change in source activity or due to refractive focusing of electromagnetic radiation by the corona in the direction of steepest density gradient.

Simultaneous studies in the range 60–20 MHz (decameter) from the ground and in the range 5 MHz to 300 kHz (hecto- kilometer) from the satellite showed that when the continuum was observed in the decametric range, simultaneous hectometer emission was composed of large fast drifting bursts. These observations have been interpreted by Stone *et al.* (1969) as the localized region of decametric continuum acting as the storage of particles responsible for hectometric drifting bursts.

The noise storm provides an opportunity to estimate the exciter speed independent of coronal electron density models. The August 1968 noise storm was observed over a period of a half solar rotation. Mean frequency drift rate of bursts was found to be varying with longitude, being maximum at CMP. This variation in the drift rate was estimated quantitatively, assuming the path of the outward moving sources from simple geometrical considerations and finite velocity (c) of propagation of radio emission. Then by curve fitting technique, absolute value of the source speed was determined as $0.37c$ to $0.4c$ by Fainberg and Stone (1970b) in general agreement with the accepted value obtained by Wild *et al.* (1959) at metre wavelengths. Further, assuming the emission to be at fundamental, electron densities were derived; but these densities are an order of magnitude higher than that observed in the solar wind. The densities estimated on the basis of second harmonic emission, however, are a factor of 4 higher than the Newkirk's model of the density (1967) for solar minimum as shown in Figure 45. This factor may still be further reduced if refraction and scattering effects are taken into account and hence, it gives an indirect support for

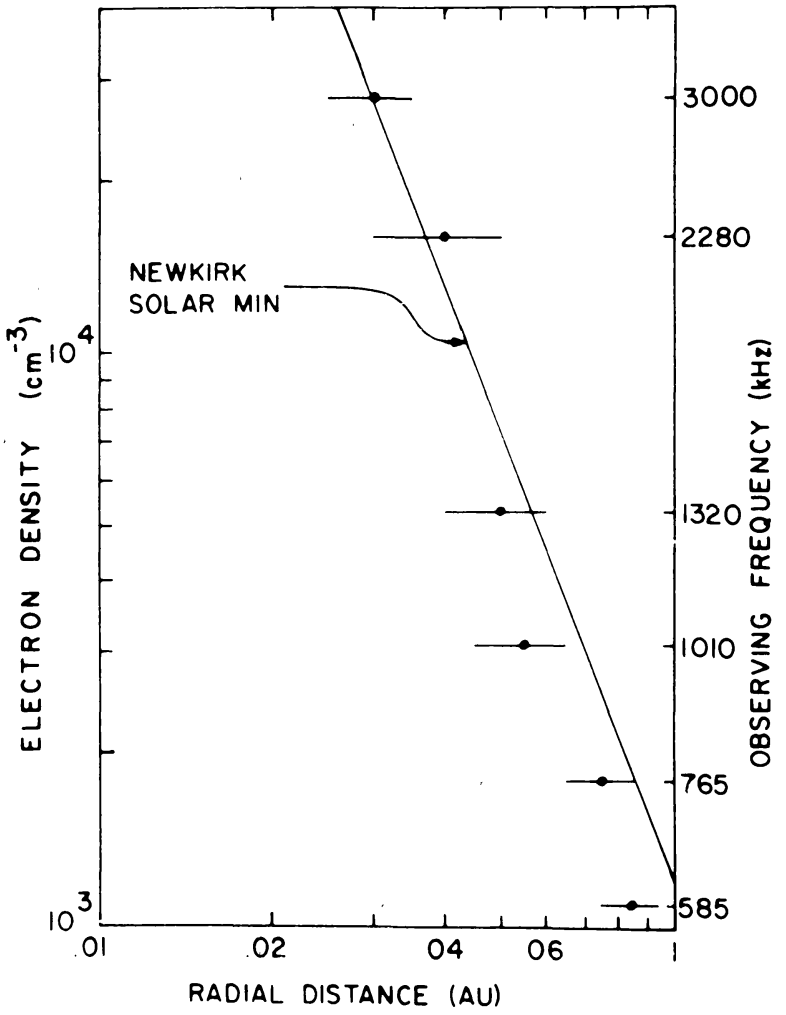

Fig. 45. Estimated electron densities for the 28 March 1976 burst trajectory, using the measured source locations at each observing frequency under the assumption that emission occurs at twice the local plasma frequency. The Newkirk (1967) electron density model is shown for comparison (from Weber, 1977).

emission at hecto- and kilometer wavelengths to occur at the second harmonic of the local plasma frequency. From theoretical considerations also, Steinberg (1972) has shown that hecto–kilometric burst seems to originate at the second harmonic.

With the help of Helios-1 and -2, and RAE-2 satellites, Weber *et al.* (1977) have for the first time determined two dimensional position of the hecto- and kilometric burst sources without assuming any density model, as shown in Figure 46a. Only assumption they made was that the emission is at the second harmonic of the local plasma frequency. They determined burst positions for the 28 March 1976 event, from which they obtained the speed of the slower exciter electrons as $(0.13 \pm 0.03)c$, which is consistent with other measurements of exciter speeds between 0.1 to $0.2c$ for burst peaks (Fainberg *et al.*, 1972; Lin *et al.*, 1973). The positions obtained from direction finding by the spin modulation of Helios-1 and -2 agree well with the arrival time determinations. This shows that corrections due to propagational effects such as

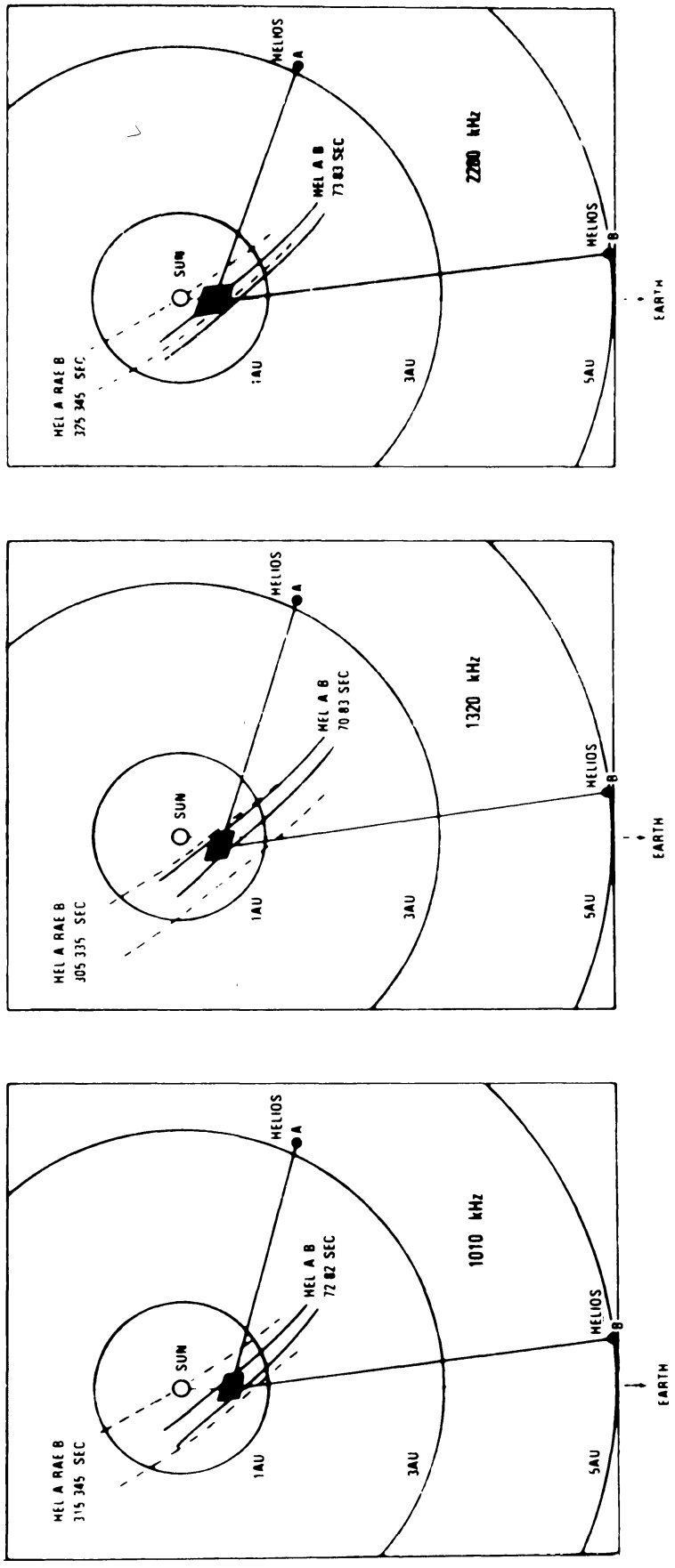

Fig. 46a. Location of burst source regions given by the intersections of the directions measured at HELIOS-A and -B and by arrival time differences at HELIOS-A and -B as well as HELIOS-A and RAE-2. Direction finding and arrival time results are in agreement (from Weber *et al.*, 1977).

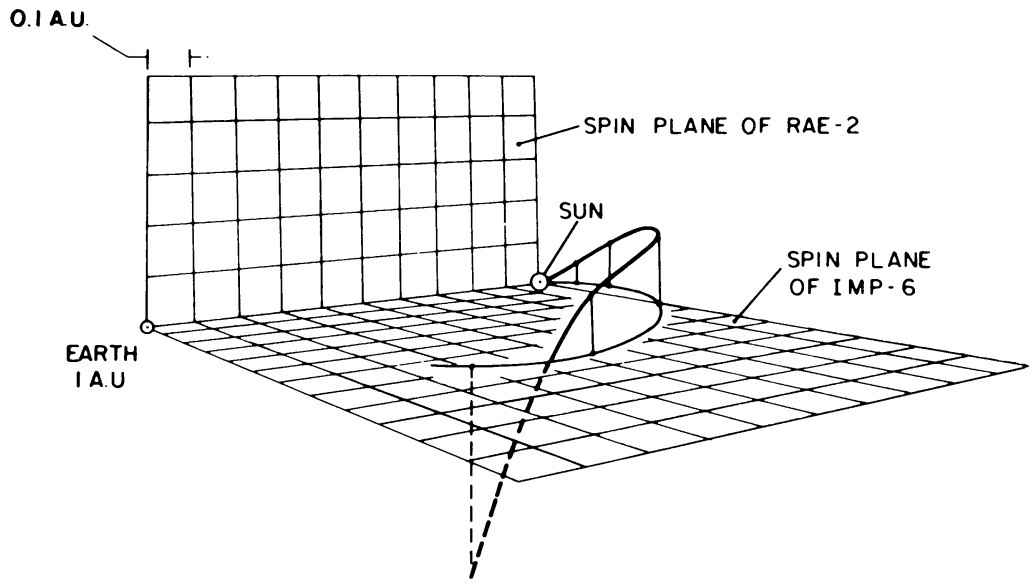

Fig. 46b. Out-of-ecliptic observation of a type III burst trajectory on 23 June 1973 (from Fitzenreiter *et al.*, 1977).

refraction and scattering are not large even if simple geometrical path lengths are assumed.

Using RAE-1 satellite data of hectometer U burst, Stone and Fainberg (1971) have inferred existence of closed magnetic field line extending up to $35R_{\odot}$. Using two spinning spacecraft, IMP-6 and RAE-2, whose spin axis were almost perpendicular to each other, Fitzenreiter *et al.* (1977) mapped a line of force of the interplanetary magnetic field which originated in the northern hemisphere of the Sun. This line of force crossed the ecliptic plane at about 0.8 AU from the Sun and reached a point south of the ecliptic at 20° heliocentric latitude, delineating out-of-ecliptic type III burst trajectory as shown in Figure 46b. More details of hecto- and kilometric burst observations and stereo radio astronomy experiment may be found in Fainberg and Stone (1974) and Steinberg (1977) respectively.

The IMP-6 satellite was the first to provide the observations of high sensitivity and accurate directions of radio sources using spin modulation technique. Accurate aspect information of $>1°$ was obtained from optical sensors. It also provided an opportunity for the simultaneous observations of energetic particles (protons and electrons) and radio emission. An extensive study of IMP-6 and IMP-8 plasma and radio wave data showed that electron plasma oscillations are seldom observed in association with solar electron events and type III radio bursts at 1 AU. (Gurnett and Frank, 1975). These authors have shown that neither the type II radio emissions nor the radiation from the upstream of the bowshock can be adequately explained by the current theory for the coupling of electron plasma oscillations to the electromagnetic radiation. For the first time, a sweep frequency receiver in the range 4–2 MHz with time resolution of 2 s and frequency resolution of 20 kHz was flown on OGO-3, which detected many type III bursts but observations of type I bursts were inconclusive (Haddock and Graedel, 1970).

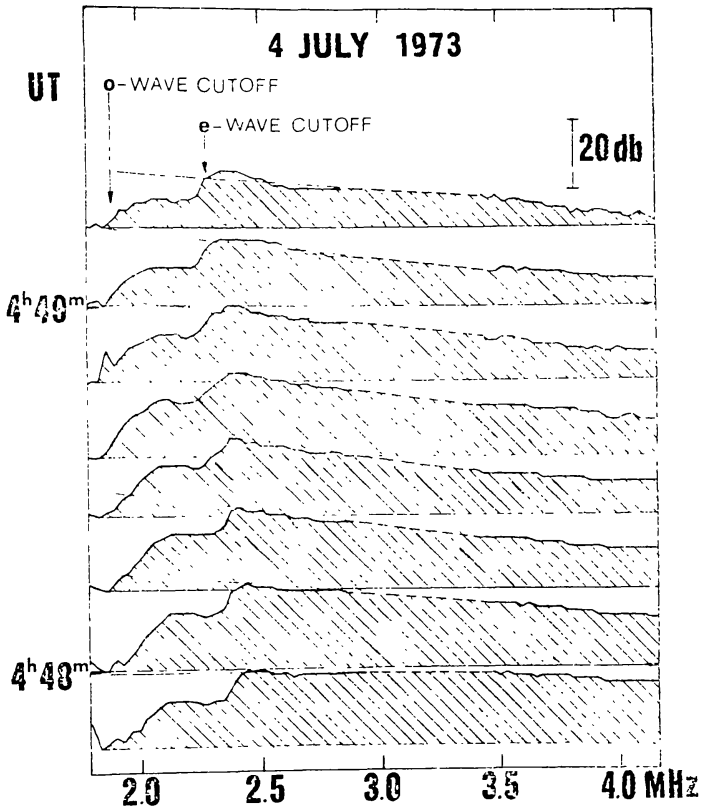

Fig. 47. Dynamic spectrum – in the range of 4–2 MHz – of polarization of type III burst. Hatched indicating high degree of circular polarization recorded on Intercosmos-Kopernick 500. The ionospheric cut off levels are indicated with arrows (from Hanasz *et al.*, 1977).

The Soviet–Polish Inter Cosmos – Kopernik satellite has detected for the first time – high degree of circular polarization (70%) of intense type III burst at 2.3 MHz as shown in Figure 47. Also irregular structure has been discovered in the initial phase of type III burst in the range 6–4 MHz, which has been identified as type IIIb–III burst. A lower limit of type IIIb burst so far observed is found to be 4 MHz (Hanasz *et al.*, 1978).

In the STEREO-5 experiment Poquerusse and Steinberg (1978) have simultaneously observed type IIIb (shown in Figure 48a) and III (shown in Figure 48b) solar radio bursts at 30 and 60 MHz from the Earth (Nancay) and from Planetary Space Probe Mars 7. As seen from Figure 48b the peak intensities of the two records show large differences up to 3 dB even when the angle between probe–Sun–Earth is 3°. This effect is found to be stronger at lower frequency 30 MHz than at 60 MHz. They claim that these observed differences in peak intensity are due to ionospheric scintillations.

Weber *et al.* (1977) reported on first burst directivity measurements of a low frequency burst from two quite different viewing directions, from Helios A and B which were within 20° and 70° away from the source respectively. They observed intensity variation at Helios A and Helios B by an amount 3 to 10 dB as the angle between the spacecraft varied from approximately 60° to 70°. This variation is

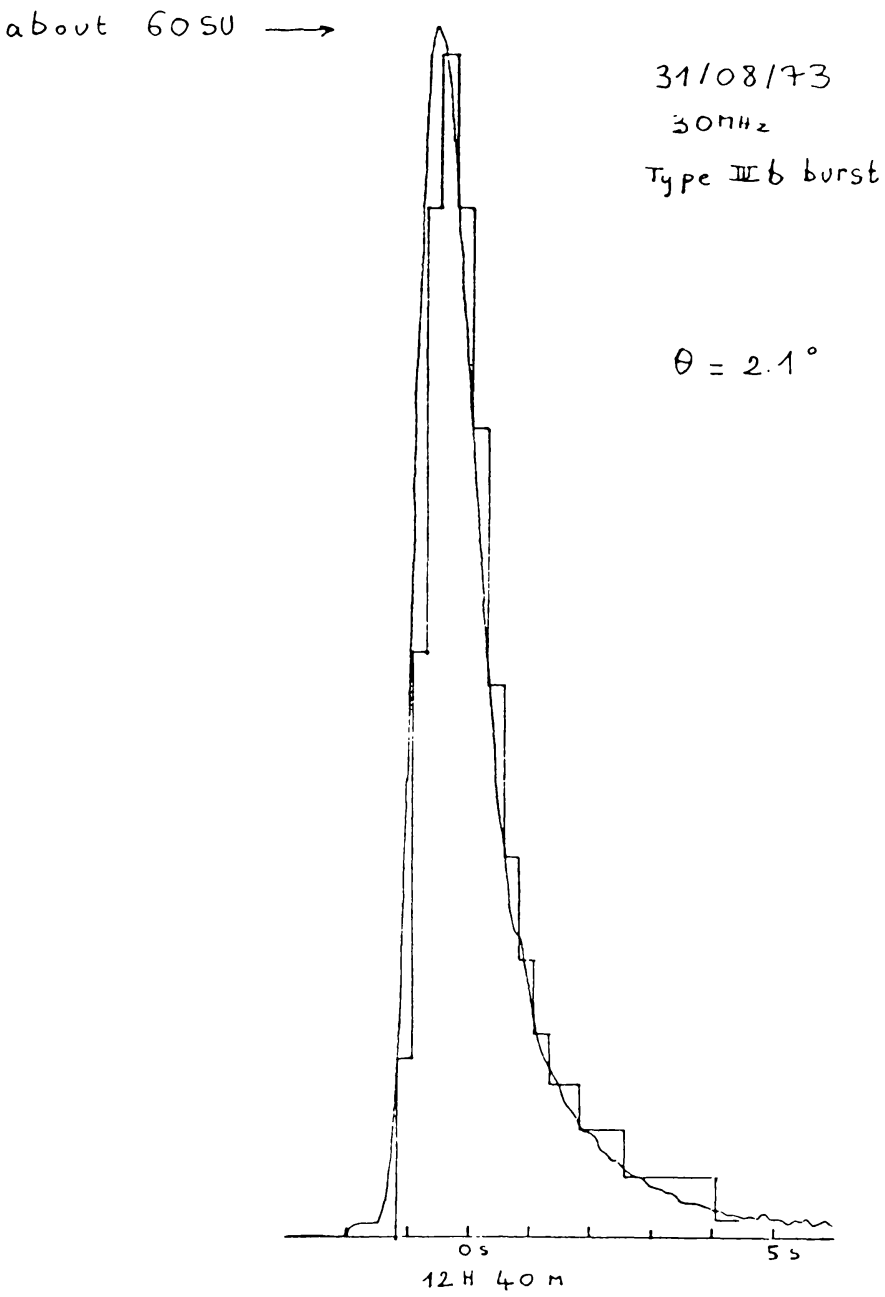

Fig. 48a.

Fig. 48a–b. Simulataneous observations of solar radio bursts at 30 MHz from the Earth (Nançay) and from a planetary space probe (Mars 7). Probe – Sun – Earth angle is (a) Type IIIb burst, and (b) record of type III noise storm portion (from Poquerusse and Steinberg, 1978).

consistent with that observed at 169 MHz by Stereo-1 experiment (Caroubalos *et al.*, 1974).

6. Refraction and Scattering Effects in the Corona

Once electromagnetic waves are generated at the source in the corona they have to propagate through the overlying magneto-ionic medium. Near the source, refraction and scattering effects will dominate and will have to be taken into account for the

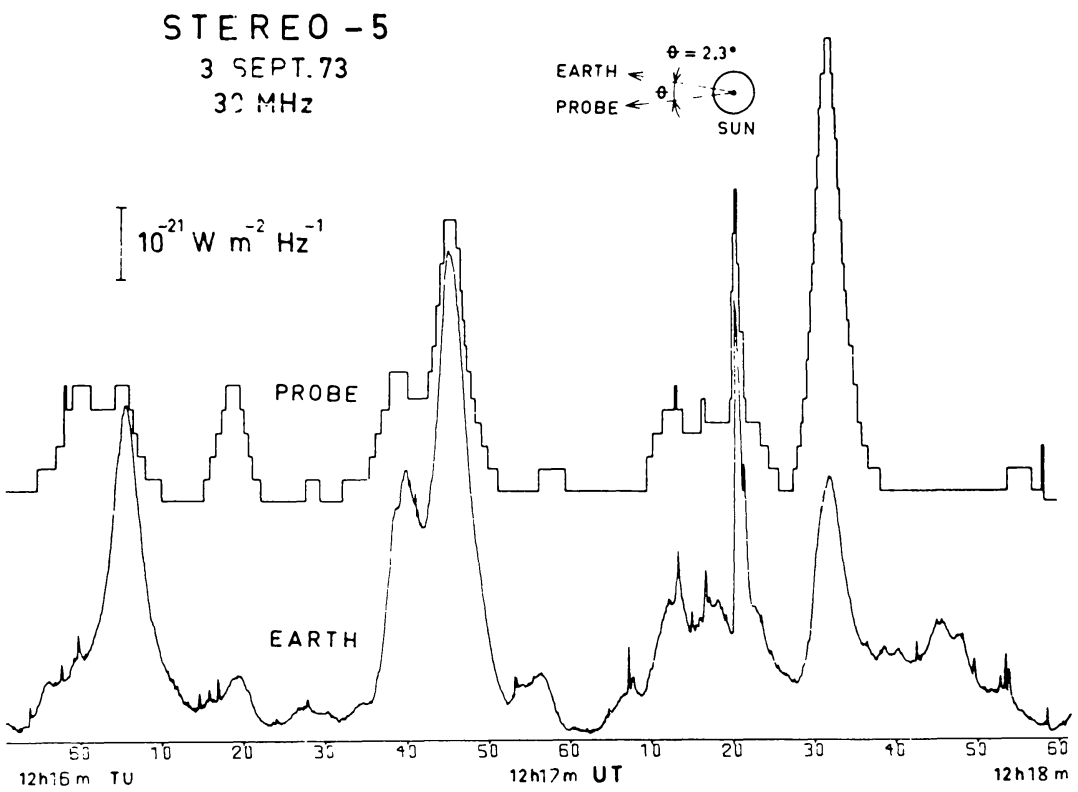

Fig. 48b.

determination of source sizes and their positions. During subsequent propagation, differential absorption, mode coupling, Faraday rotation, dispersion effects will modify the spectral and polarization characteristics of the radiation.

Refraction in the corona arises because of the large scale gradients in the electron density in the corona. Neglecting the effect of magnetic field and collisions, the effect of refraction has been estimated (Fokker, 1965a). It can be shown that the emission which originates close to the limb will appear to be shifted towards the center of the disk, as sketched in Figure 49. On the other hand, for sources close to the center of the disk there will be negligible shifts in position. Also refraction is more for the emission near the plasma level as compared to the scattering effect. Harmonic radiation follows closely the path of unscattered refracted radiation (Fokker, 1965a; Fokker and Rutten, 1967; Steinberg *et al.*, 1971; and Riddle, 1972).

In addition to smooth variation of the electron density small scale density fluctuations are also present in the corona which give rise to scattering. Effects of scattering have been estimated by using numerical approach and assuming spherically symmetrical corona without considering the effect of magnetic field. This was done initially by Fokker (1965) and Fokker and Rutten (1967) assuming isotropic inhomogeneities and neglecting regular refraction, which was taken into account by Steinberg *et al.* (1971). Riddle (1972) extended this treatment to anisotropic inhomogeneities, radially elongated, and computed the effect on the position and size of type III source at 80 MHz with the following conclusions:

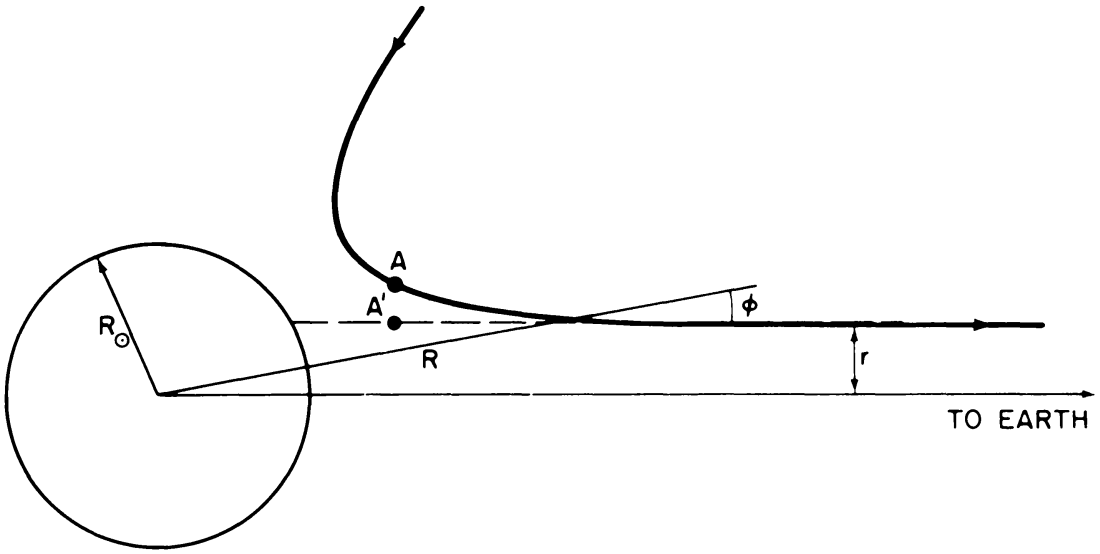

Fig. 49. Coronal refraction of a radio ray on its trajectory to the Earth. 'A' indicates the actual source position, 'A' the apparent position (from Gergely, 1974).

(i) The directivity decreases drastically for the fundamental compared to that of the harmonic radiation.

(ii) In the transverse plane, source size increases but in the radial direction its change is small since in this plane systematic refraction always reduces the apparent source size.

(iii) The effect on sizes of harmonic radiation is obviously small up to 60° longitude from CMP. Beyond 60° longitude they become comparable with that of the fundamental and are large for sources on the limb.

(iv) Position shift of fundamental and second harmonic is shown to be away from the centre and towards the centre respectively due to scattering. But refraction which is dominant at fundamental will shift position of the source towards the centre. Thus, while estimating relative position of fundamental and second harmonic, ray path effects are additive and for isotropically emitting sources, true differences in position of fundamental and harmonic tend to get cancelled out.

(v) Life time of sources will increase since the observed duration is the burst duration plus the scattering duration.

Studies of type III burst made by McLean (1971) and Stewart (1972) are consistent with these conclusions. Riddle (1972) further modified this model without spherical symmetry and studied the influence of a streamer when the source is located in it. Fokker (1971) argued that in the presence of scattering effects, radiation from a point source reaches the observed with different time delays, which should randomize any linear polarization. The current status of the validity of linear polarization is given in Section 2.4.

Recently, Smith and Riddle (1975) have developed a model for type III burst considering the effect of scattering of radiation in the source itself. The most important result is that the scattering in the source does not always hamper the

amplification of the fundamental due to propagation along the fibre-like irregularities in the corona. They have argued that the interpretation of type IIIb–III bursts with their intricate fine structure in the first trace is simple in terms of amplification process in small scale inhomogeneities. This can happen if the source is extremely inhomogeneous and small regions exist with very high level of energy density in plasma waves, this then allows the fundamental to be amplified in spite of scattering and contribute little to emissivity of the harmonic.

As electromagnetic wave propagate out in the corona, other propagation effects will also affect the radiation characteristics. Amplitude of the e.m. radiation can be damped either by collisional damping or in case of plasma waves by collisionless damping (Landau damping) (Aubier and Boischot, 1972; Harvey and Aubier, 1973; Aubier, 1974). Investigation of the damping processes has led to the understanding of the temperature of the corona and the nature of exciter function (Solar Radio Group, Utrecht, 1974; Barrow and Achong, 1975; Achong and Barrow, 1975).

Abranin *et al.* (1976) have measured the source size of stria burst in the range of 26–24 MHz, and have given an upper limit of the order of 10′ of arc. Leblanc (1973) has given the estimates of source sizes at 60 and 30 MHz, which are comparable at both the frequencies. Source size increases in the presence of scattering from 4′ of arc to 5′ of arc respectively as the source moves from CMP to limb. These values are obtained by assuming spherically symmetrical corona. The analysis performed at 80 MHz, for source position on the axis of streamer leads to somewhat smaller values (~2′) than the values obtained by assuming spherically symmetrical corona. This effect will also decrease the predicted source size at 30 MHz (~4′ arc). Investigations of source sizes of type I burst by Kerdraon (1973) and Bougeret and Steinberg (1977) suggest that the scattering should take place near the source, since different source sizes were observed at the same longitudes, considering the effect of scattering within the source itself due to small scale irregularities.

In order to understand core and halo structure of type III burst, Figure 50 shows two models taking into account emission at source and subsequent propagation effects. The first sketch, Figure 50a, shows scattering model for point source and the second, Figure 50b, reflection model for the extended source (Chen and Shawhan, 1978, and references therein). In the case of point source, no significant change takes place by varying the scattering parameters. Results of scattering calculations at different frequencies are summarized in Table VII. It can be seen that the source size increases from the center to the limb at all listed frequencies and also source size becomes larger at lower frequencies.

In the case of extended source reflection model, halo is a natural consequence of extended region, with E–W size determined by electron sector extent at the harmonic plasma level. The core arises from spherical mirror focussing effect which leads to 3 : 1 halo to core size ratio as observed.

Sizes of type I sources as small as 0.7′ are needed in order to account for the measured 25° beamwidth of type I sources (Steinberg, 1977, and references therein), since there exist a relationship between scattered image and the final beamwidth of

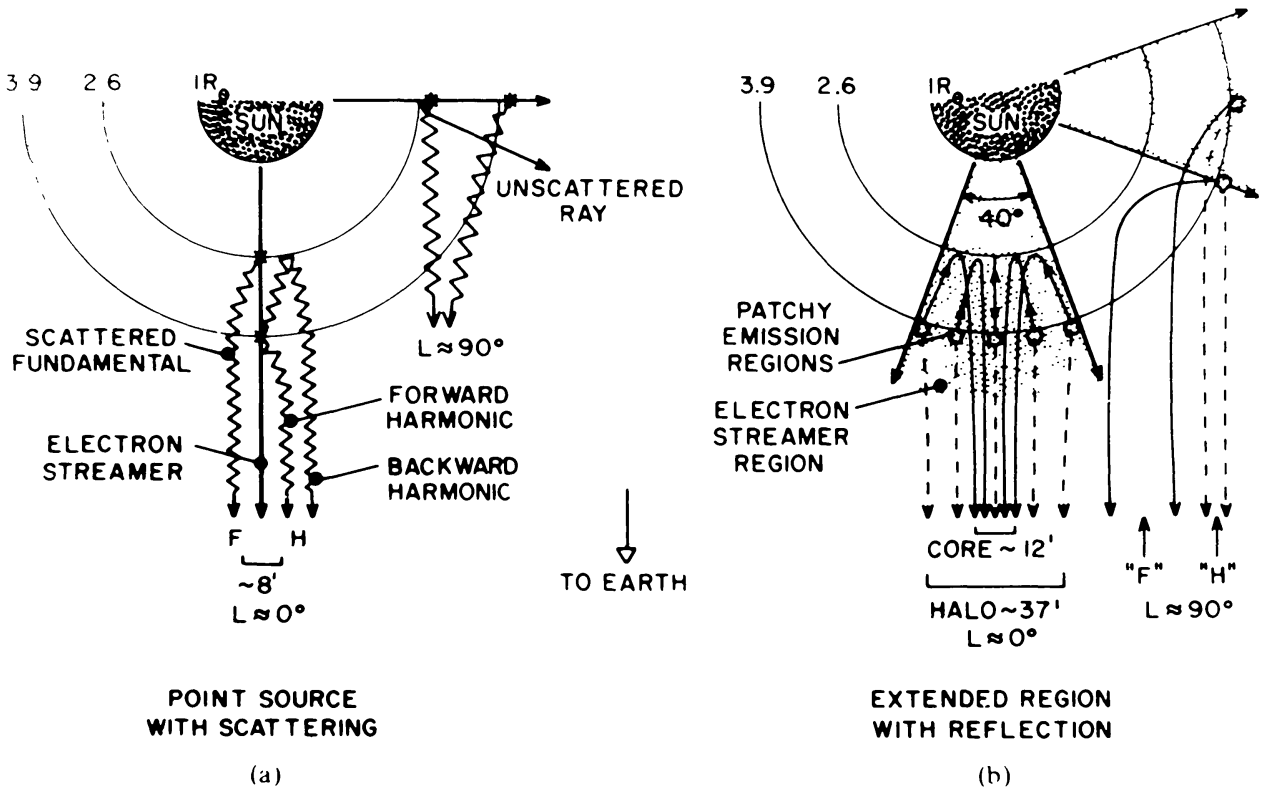

Fig. 50. Pictorial representation of models to explain the source brightness distribution for type III bursts at 26 MHz near the heliographic longitude 0° and 90°; (a) point source with scattering, (b) extended region with reflection (from Chen and Shawhan, 1978).

the observed radiation. Primary sources of 0.7′ are broadened by overdense filaments while preserving its directivity in the plane containing the fibre. Thus, the source sizes as small as 1 to 10 arc sec reported by Takakura and Yousef (1975) and Sawant *et al.* (1976a, b) with excess electron density (~1–2%) around 1 to $2R_\odot$ above the photosphere are plausible.

It is interesting to note that Tyler *et al.* (1977) have observed spectral broadening of radio signals from Viking spacecraft indicating a progressive increase

TABLE VII

Size of scattered image at different frequencies[a]

f(MHz)	f_p/f	n^2/h	Half-power width in min of arc		
			$L=0°$	$L=45°$	$L=75°$
169	0.92	8	3	3.5	4
80	0.975	5	1.8	2	3
60	0.92	8	4	4	5
30	0.92	8	4	4	5

[a] From Elgaroy (1977).

in scale sizes between 1 and 100 km of plasma irregularities from $2R_\odot$ towards the photosphere. They derived this result from the Viking–Solar Corona experiment when the Viking spacecraft was occulted by the Sun in 1976 at solar minimum by observing 3.5 and 13 cm wavelength radio wave scintillations at NASA Space Network.

6.1. Characteristics of small scale coronal density irregularities

The interpretation of the various decametric burst parameters, mentioned in Section 3 suggest the presence of small scale size irregularities (~1″ to 10″ of arc) in the corona at $2R_\odot$ (Melrose, 1974; Takakura and Yousef, 1975; Sawant *et al.*, 1976, 1977; Sawant, 1977). The excess electron density in the irregularity of 1–2% over ambient are predominant, but occasionally irregularities having 1000% excess are also inferred. Scintillation of galactic radio sources due to inhomogeneities in the solar wind also suggest electron density fluctuations of the order of 1 to 5%. (Dennison and Hewish, 1967; Cohen and Gundermann, 1969; Hewish, 1971). 'Echo-like' events suggest fast motions of the irregularities towards and away from photosphere (Bhonsle *et al.*, 1977; Sawant, 1977). Estimated high velocities (−1000 to +2000 km s^{-1}, away and towards the photosphere respectively) of the irregularities deduced from 'echo-like' events are in agreement with the suggestion of Parker (1958) and Ivano and Livshit (1968). Also observations of Dennison and Hewish (1967) suggest the increase in velocities of irregularities as one approaches towards the Sun.

The generation of small irregularities (10^2–10^4 km) with fluctuations in electron density 1–4% and with life time ~1 s is discussed by Baikov and Lotova (1970) and Melrose (1975) by considering different plasma instabilities generated due to anisotropy in temperature and magnetic field. 'Slipping instability' is considered responsible for the generation of such small inhomogeneities within $R_\odot \sim 30$ (Baikov and Lotova, 1970).

The structure of the Sun's corona has been observed over a large range of electromagnetic spectrum for example, in X-rays (Vaiana *et al.*, 1973a, b) and Neupert *et al.* (1974); in UV (Withbroe *et al.*, 1971; Withbroe, 1972), in EUV (Brueckner and Barotoe, 1974); in short radio waves (Kundu, 1971; Butz *et al.*, 1975); and in long radio waves (Leblanc, 1970; Sheridan, 1970; Aubier *et al.*, 1971). All these observations imply the existence of magnetic loop structure at $R_\odot \sim 2$, which are unresolved. Observational resolution limit on the above mentioned observations is 2000 km in UV including EUV suggesting existence of still finer structure.

The observations of the quiet Sun and burst component in the decameter range also support the existence of small scale irregularities. The low values of brightness temperatures (0.6×10^6 K) deduced from the observations of the quiet Sun can be accounted for by considering the effects of scattering by small scale irregularities.

7. Energetics of Noise Storms

At meter wavelengths, typical maximum flux densities of single storm bursts (type I) are estimated to be about 5×10^{-21} W m^{-2} Hz^{-1} (Wild, 1951; Hauge, 1956; Fokker, 1960; Kundu, 1965; de Groot, 1966; Steinberg *et al.*, 1974). Following Elgaroy (1977), for a typical source size (5×10^3 km), energy density of the electromagnetic wave and of the Langmuir wave, assuming plasma hypothesis and conversion efficiency for $1 \rightarrow t$ process of the order of 10^{-6} (Wild *et al.*, 1963), turns out to be $E_{em} = 10^{-12}$ erg cm^{-3} and $E_l = 10^{-6}$ erg cm^{-3}, respectively. For typical plasma parameters in the corona such as magnetic field $H = 3.5$ G (Kai, 1970), electron density $N_e = 10^8$ cm^{-3} and temperature $T = 10^6$ K, magnetic (E_{em}) and thermal E_{th} (nKT) energies are 0.5 erg cm^{-3} and 0.1 erg cm^{-3} respectively. Thus, it is seen that the energy in the burst component (E_{em}) is quite small and so also is the energy in the background continuum as compared to the magnetic and thermal energies in the source region. Though the noise storm is a long duration phenomenon, the energy released in storms is only a fraction of the energy stored in large coronal volumes in the form of magnetic and thermal energy. Even if all the burst energies are combined, they are still much less compared to the magnetic and thermal energies available in the corona. Obviously, energetics of noise storms alone are not sufficient to formulate a theory for the observed burst intensities but theories should be consistent with energetics of the processes involved.

Following classification for electron acceleration phenomena is proposed by Boischot (1974), (i) associated with flash phase flare, (ii) non-associated with flare, and (iii) acceleration in the wake of shock and in front of the shock. In case of flash phase of the flare an impulsive acceleration with duration of a few seconds to minutes may give rise to 1–100 keV electrons. In case of large flares a second phase of acceleration, more gradual and lasting longer (minutes to hours), takes place giving rise to 100 keV to a few MeV electrons and occasionally these electrons get trapped into a special moving structure giving rise to moIV burst. These bursts may also occur due to possible acceleration in the wake of the moving shock. In case of type II burst, acceleration can take place in front of the shock or in the wake of a shock wave. Non flare acceleration is likely to be responsible for noise storms. So far as decametric noise storms are concerned, Boischot (1974) has pointed out that there is no sufficient information on the number and energy of the accelerated electrons. Because of the long duration of decametric noise storms, one must look for a quasi-continuous acceleration process. It is difficult to think of such a process in association with a flare which is essentially a transient phenomenon. Hence, it is essentially a transient phenomenon. Hence, it is almost certain that the source of energetic electrons of long duration must lie in the corona.

8. Salient Features of Theories

8.1. Noise storms

Noise storms which consist of burst component and continuum radiation are

characterized by high intensity ($T_b \sim 10^9$ K), high degree of circular polarization (0-mode), source sizes of a few minutes of arc, and high directivity of emission. Denisse (1960) first proposed a plasma mechanism to explain the origin of continuum radiation. Properties of continuum radiation are similar to type IVmB burst (Boischot, 1974). Many attempts have been made to explain the origin of burst components; type I at metric wavelengths and type III at decametric wavelengths (Elgaroy, 1977).

Several theories have been put forward explaining type I bursts observed in the meter wavelength region and their chains (Takakura, 1963; Trakhtengerts, 1966; Fung and Yip, 1966; Zaitsev and Fomichev, 1973; Sy, 1973; Vereshov, 1974; Manganey and Veltri, 1976a, b). Interpretation of noise storms proceeded along two lines, invoking either gyrosynchrotron or plasma process. Zaitsev and Fomichev (1973) proposed a theory for the generation of type I and type III storm radiation. This theory assumes that the same electron stream, ascending in the solar corona can generate successively type I and type III bursts. An attractive feature of this theory is that since emission occurs at a frequency well above the plasma frequency, diffuse type III bursts 'growing out' of chains of type I bursts at the decametric wavelengths may be explained as plasma emission from accelerated electrons escaping along open field lines. The theory explains type I bursts and their chains by a single mechanism and also all other observed properties of type I bursts such as short duration, frequency drift, polarization, narrow bandwidths, and frequency splitting. Recently, Aubier *et al.* (1978) extended Mangeney and Veltri's (1976a, b) theory of type I storms and accounted for chains of type I bursts and associated decametric type III bursts, as described in Section 8.5.

The change in the characteristics of a decametric noise storm from those of metric noise storm may be due to change of magnetic field configuration from closed field lines to open field lines in the region $R_\odot \sim 1.5$ to 2 above the photosphere due to the solar wind pressure exceeding the magnetic pressure. In the decametric range, type III bursts and their fine structure constitute the burst component ('BF') of noise storms. In particular, dominating fine structure of type III is type IIIb. Chains of stria or split pair or triplets may constitute type IIIb burst. Hence, it is expected that any theory of type IIIb burst should also explain the individual element of these chains.

8.2. 'BF' TYPE BURSTS

It is generally known that plasma hypothesis which is basic to any theory of 'BF' type bursts involves a beam of fast electrons moving out in the corona exciting longitudinal plasma oscillations which are subsequently converted to electromagnetic radiation by scattering on local inhomogeneities. In what follows, we shall briefly give theories of different varieties of 'BF' type bursts.

8.2.1. *Split Pairs*

Ellis and McCulloch (1967) and Ellis (1969) suggested that frequency splitting observed in split-pairs might be attributed to plasma frequency and upper hybrid resonances as suggested earlier by Sturrock (1961) and further developed by Tidman

et al. (1966). This suggestion is supported by an appearance of 'triplets' and increase of frequency separation between their elements with increase in frequency in the burst spectra. Also the observation of harmonically related pair of type III bursts and appearance of bursts showing frequency splitting, both in fundamental and harmonic chains, provides further evidence in its favour. This theory implies that the frequency interval between the middle element and lower and higher frequency elements should not be equal. However, the experimental evidence does not support this theoretical prediction (de la Noë, 1975).

Yip (1973) suggested that in a strongly nonisothermal plasma, thermal fluctuations of the electron density will produce emission at two frequencies and subsequent conversion would generate two pairs near fundamental and second harmonic radiation. But strong circular polarization and triplet bursts cannot be explained by Yip's theory.

8.2.2. *Type IIIb Bursts*

Takakura and Yousef (1975) have developed a theory to explain most of the observed features of type IIIb bursts. This theory with some modifications has been adopted by Sawant *et al.* (1976) to explain the observed microscopic spectral features of decametric bursts. According to Takakura and Yousef, as the stream of electron passes through the corona, and if it happens to traverse a slightly overdense ($\leqslant 10\%$ above the ambient density) filament, its density gradient is first decreased and then increased. In that case, effective interaction length of the source is increased, which will enhance the radiation and opposite will be the effect when the stream of electrons leaves the filament. This will generate a stria in a type IIIb burst. Further, Takakura and Yousef have used estimates of Melrose (1974) for brightness temperatures observed in case of fundamental and in second harmonic emission assuming the process of induced scattering for the conversion of Langmuir waves to transverse waves. In that case, fundamental emission will grow exponentially with the effective interaction length (of a source) which is inversely proportional to the density gradient and second harmonic radiation will be linearly proportional to the effective interaction length. Even if the brightness temperature within the filament is much larger than that outside the filament, the cross-section of the filament may be much smaller than the total cross section of the electron exciter beam. It follows that the contrast between the emission from the filament and from ambient corona will make the burst appear as type IIIb, or type III. This interpretation explains most of the observed features of type IIIb burst such as:

(i) F–H relationship observed in case of type IIIb-type III;

(ii) Appearance of type IIIb at both the fundamental and second harmonic frequency; and

(iii) Similarity in positions and of source sizes of type IIIb and associated type III burst.

Daigne and Moller-Pedersen (1974) compared peak intensities observed at two harmonic frequencies with the theoretical model of Melrose (1974) and concluded

that the latter model requires certain assumptions regarding the source structure to explain F–H pairs. However, any conclusion drawn on the basis of measurements of burst intensities carried out on the Earth should be considered as tentative in view of the effect of ionospheric scintillations on the burst intensities as reported from Stereo-5 experiment (Poqueresse and Steinberg, 1978).

8.2.3. *Type IIIb–III Relationship*

(1) According to de la Noë and Boischot (1972), type IIIb is a precursor i.e., first a stream of fast electrons propagates outwards in the relatively smooth corona, where the conversion of plasma waves into electro-magnetic waves is not very efficient. They excite only sporadic emissions or stria bursts, or no emission at all, but presumably create turbulence along their path. This paves the way for the following stream to give the usual featureless type III burst. If this were the case, every type III burst would have to be preceded by a type IIIb burst and also one does not understand why on some occasions only type IIIb's are observed and on some other occasions only type III's are observed. If one accepts the mechanism of plasma oscillations for the generation of type IIIb–III bursts, then they can be explained as F–H related pairs (Takakura and Yousef, 1975). Melrose and Sy (1972) have considered the plasma emission by taking into account the effect of a weak magnetic field ($\omega_{pe} > \omega_H$) on the conversion process of *l*-wave to *t*-wave. They have shown that the emission at the fundamental frequency can be 100% polarized in the sense of 0-mode which is generated near the plasma frequency, when it is restricted to frequencies below the cut-off for X-mode. This condition will be satisfied if the magnetic field in the filament is stronger or temperature of the filament is lower than that of the ambient plasma (Takakura and Yousef, 1975). According to this theory, if type IIIb–III bursts are F–H related, then the type IIIb–III, and type IIIb bursts should be more strongly polarized than the isolated type III. This prediction appears consistent with observations.

(ii) Smith and de la Noë (1976) have proposed a theory of type IIIb bursts by considering the space time evolution of an electron beam injected into the corona. The strong beam-plasma interaction occurs at the leading edge of the beam, giving rise to the amplification of a quasi-monochromatic large amplitude plasma wave that stabilizes itself by trapping the beam particles. The oscillation of trapped particles in the wave troughs amplifies main electrostatic waves with sidebands, which subsequently decays into electromagnetic waves through the parametric decay instability. The elementary stria bursts can be produced by this process which may repeat at a finite number of discrete plasma levels, producing chains of bursts. These authors have shown that this theory accounts for all the observed spectral properties of type IIIb bursts (de la Noë, 1975, but they have also remarked that understanding of the three individual processes such as beam-plasma interaction, the parametric sideband intensity and the parametric decay instability is not yet complete and the sequential evolution of these three processes has not yet been observed in laboratory

plasmas. Further work on theoretical and experimental aspects of these instabilities is necessary.

(iii) Baselyan *et al.* (1977) have investigated the collisionless deceleration of electron streams which are responsible for type IIIb bursts. They have shown that the electron streams with initial velocities of the order of $0.8c$–$0.4c$ undergo deceleration up to $0.35c$ between 25 and 6.25 MHz plasma levels and after that deceleration stops. The deceleration is caused by the induced scattering of plasma waves which produce energy losses through collisionless mechanism of the fast electron streams. The deceleration stops when a quasi-linear expansion of the stream takes place. Thus, according to Baselyan *et al.*, the mean velocity of streams responsible for type IIIb burst generation is about $0.46c$ between 25 and 12.5 MHz plasma levels and $0.38c$ between 12.5 and 6.25 MHz plasma levels.

8.3. Microscopic spectral features

(i) Theoretical basis for C.B.'s were explained by Sawant *et al.* (1975) in the following manner. The radiation is assumed to be generated by a plasma process throughout the source region. Emission gap of the first component may be explained by the trapping of the electromagnetic radiation over the corresponding frequency range. The occurrence of the delayed second component may then be attributed to the subsequent release of the electromagnetic radiation trapped in duct-like structures or cavities in the corona. The escape of radiation from the duct may be triggered by some secondary disturbance, destroying the condition of trapping of the radiation. The enhancement of the intensity observed in the second component can be attributed to the wave particle interaction in the trapping region. Fokker (1960) has invoked existence of such cavities to explain the production of type I burst. The narrow bandwidth of the trapped radiation in the first component implies that these duct-like structures or cavities are highly selective with Q ($=f/\Delta f$, where Δf is the observed emission gap in the first component and f is the centre frequency of the emission gap) is of the order of 100 to 1000, a rather stringent condition (Sawant, 1977).

Takakura (1977) suggested that if the radiation is generated at fundamental and the radiation corresponding to the gap propagates through an electron density irregularity whose cross-section is less than the linear extent of the source, then the generation of C.B.'s can be explained. This suggestion was pursued further for quantitative studies of C.B.'s by Sawant (1977). The delays of the order 1–10 s observed in the second component are explained if the size of irregularities are of 10^3–10^4 km with excess electron density of 1–4% over the ambient.

(ii) The curvatures observed in different types of bursts along the frequency axis of their dynamic spectra may be attributed to large group delays suffered by different parts of the bursts. The group delays experienced by different frequencies in a given 'striation' are determined by the transverse gradient and orientation of the coronal electron density irregularity in the propagation path.

Now using the relationship between the group path delay and columnar electron density (Lawrence *et al.*, 1964), for typical difference of delay of about 100 ms

between the middle and extreme frequencies of a striation, the radiation would have to traverse a density irregularity containing $\sim 10^{17}$ electrons cm^{-2} column. In order to permit transmission at 35 MHz through such an irregularity one can put an upper limit of $\sim 10^7$ cm^{-3} on the electron density, assuming that the burst generation occurred at the second harmonic of the local plasma frequency. The group path length corresponding to the delay of 100 ms, then turns out to be 9×10^4 km. This is the lower limit on the linear scale of the irregularity in the propagation path.

(iii) The observed bandwidths (50 kHz ± 10 kHz) of 'dot' emissions provide an evidence that they might indeed be generated by the process of induced scattering of plasma waves as they are in good agreement with the theoretically predicted value given by $\Delta f = 10^{-3} \times f$, where Δf is the instantaneous bandwidth and f in MHz is the center frequency of the 'dot' emission (Kaplan and Tystovich, 1969; Melrose, 1974).

(iv) Frequency drift rates of the microscopic 'U' bursts are explained by the change in the sign of the local electron density gradients which the exciter electron beam would encounter as it traverses an individual electron density irregularity (Sawant *et al.*, 1976). Now, following Melrose (1974) who has assumed the process of induced scattering of Langmuir waves by thermal ions to be responsible for their conversion into electromagnetic waves, the spatial variation of brightness temperature T_1, of the fundamental type III emission is given by

$$T_1 = T_1(0)(e^{\mu L} - 1), \tag{2}$$

where $T_1(0)$ is the minimum brightness temperature at the source required for the induced scattering process to dominate over the spontaneous scattering and is equal to 10^9 K, μ is the amplification factor, and L is effective interaction length. (Kaplan and Tystovich, 1969; Melrose, 1974).

The effective interaction length, L, over which the induced scattering of plasma waves will take place,, is inversely proportional to the density gradient (Takakura and Yousef, 1975). As a result the intensity of these bursts at their 'turnover' points is enhanced. This may be due to longer interaction length which the exciter encounters at the crest or trough of a coronal electron density irregularity, where the density gradient is negligible with consequent amplification of radiation (Melrose, 1974).

Computed coronal interaction lengths where microscopic 'U' and 'inverted U' bursts originate turn out to be $\sim 10^4$ km, assuming an exciter velocity of $0.3c$ (where c is the velocity of light) and burst duration of about 1 s. These scales of interaction length are one order of magnitude greater than the minimum length required for induced scattering of Langmuir waves (Melrose, 1974) and shown to be consistent for striations in type IIIb bursts (Takakura and Yousef, 1975).

The 'inverted U', 'U', and 'partial U' bursts show intensity variation with frequency, which may be indicative of density gradients smaller in spatial extent than those required for type IIIb striations. Thus, the emission gaps observed in these events could be caused by extremely small interaction lengths corresponding to very high density gradients. Furthermore, the interaction length can be used to estimate the excess electron density in the coronal region, which comes to about 2–3% over the ambient (Sawant *et al.*, 1976).

8.4. Drift pairs (DP)

(i) The original hypothesis by Roberts (1958) is that a DP represents the direct radiation and reflected radiation from underlying corona at the harmonic frequency. However, only on a few occasions, single trace was observed at the fundamental and hence cannot be taken as a general evidence for the DP to occur at second harmonic (de la Noë and Moller-Pedersen, 1971). Riddle (1974) pointed out the difficulty in maintaining the identity of the two traces of a DP due to different scattering effects of the two rays and this adds further difficulty to Roberts' hypothesis. Theories based on magnetic splitting of the ray are also not realistic since observations show that the displacement of the second trace in a DP is a true time delay.

(ii) In the 'hill' theory proposed by Zheleznyakov (1965) a stream of electrons encounters a hump in the plasma density curve, which is untenable because of the large size hump of the order of $1R_{\odot}$ required to explain the observed reduction in the frequency drift and the duration of DP. In addition, this theory does not explain the origin of the two traces and the constancy of the observed characteristics of DP's from one storm to another.

(iii) Moller-Pedersen *et al.* (1978) have worked out a theory to explain most of the features observed in DP bursts. Here, the two components of DP are explained by the presence of two shock fronts propagating through identical low-β regions on either side of the symmetrical streamer. The forward moving shock gives the first component of the DP. The shock moving in the reverse direction passes through the streamer and gives the second component after traversing the neutral sheet (high-region) where no emission takes place. Typical time delays of the order of 1–2 s of DP's can be explained by assuming for the thickness of the streamer and the velocity of the shocks inferred from other measurements.

(iv) Elgaroy (1977) and Abranin *et al.* (1977) have suggested different fast electron streams to explain echo events and also drift pairs (which may be considered as echo-type events) or even multiple events. Bhonsle *et al.* (1977) have similarly explained 'echo-like' events on the basis of independent exciters.

8.5. Type I–III bursts

Gordon (1971) has proposed a mechanism for the acceleration of electrons which give rise to type I bursts initially and subsequently type III's by a nonlinear process. Aubier *et al.* (1978) have extended the theory of Manganey and Veltri (1976) for explaining the metric type I and decametric type III bursts on the basis of transformation of perpendicular momentum of the electrons, after generating type I burst, to parallel momentum as the exciter moves out along decreasing magnetic field lines. Type III emission then occurs when the parallel velocity component reaches a critical value. This model which is consistent with observations is discussed later.

8.6. Collective modes of oscillations in plasma

It must be remembered that the solar flare and noise storm phenomena are normally

treated in the framework of linear or quasi-linear plasma physics. Of late, there is growing realization of the fact that a great solar flare with a time constant of the order of minutes to hours involves large volume of space and energy and hence it is very likely to be a highly non-linear phenomenon of high density and high temperature plasma in a strong magnetic field. The theory shows that these parameters lead to the excitation of strong collective modes of oscillation. Such modes have been invoked recently to explain some of the microstructures in the radio spectrum of the Sun (Pratap, 1974a, b).

Prasad (1976) proposed a mechanism for the coherent emission of radio waves from a warm uniform plasma by the process of coherent Raman Scattering of plasma waves. The intensity of enhanced emission at twice the plasma frequency, its directivity and the threshold condition have been computed and found to be in agreement with the laboratory observations of radiation output from DC discharges in argon gas and from a helium theta-pinch plasma. It would be interesting to extend Prasad's ideas to explain some of the observed characteristics of solar bursts from millimeter to kilometer wavelengths.

9. Models of Noise Storm Sources

Various models have been proposed to explain observational features of noise storms. Common to all models is magnetic loops or arches extending up 1 to $2R_{\odot}$ in the solar corona above the active regions of opposite polarity (Kai, 1970; Lantos and Jarry, 1970; McLean and Sheridan, 1972; Stewart and Labrum, 1972; Wild and Smerd, 1972; Kai and Sheridan, 1974; Kai and Nakajima, 1974). Gergely and Kundu (1975) have given an empirical model showing association of centimeter and decimeter continuum and type I burst as shown in Figure 51. They have shown the position of decametric continuum radiation above of closed field lines. 'On-fringe' bursts are generated from the same place as decametric continuum radiation. 'Off-fringe' bursts are generated from the place where particles generated in chromospheric flares have direct access to open field lines.

Kai (1970) with the availability of positional and polarization observations of type I and type III burst at 80 MHz suggested that type I sources are often bipolar and type III sources are unipolar. The type III sources tend to avoid the centers of type I activity, which originate in strong magnetic fields whereas type III sources originate in the region of weak magnetic field along open field lines. Wild and Smerd (1972) proposed a model for the generation of type III, V and inverted 'U' bursts based on the position, angular size measurements at 80 MHz and the possible magnetic field configuration. Combining radioheliograph, spectral and optical observations of radio emission at 80 MHz and related active centers, Stewart and Labrum (1972) put forward a model for the first time to explain type I–type III relationship; the type III burst starts at the low frequency side of type I burst. Their suggested model is shown in Figure 52. In this model, the type III bursts originate at the local plasma frequency level along the open field lines above stable dark filaments which indicate the

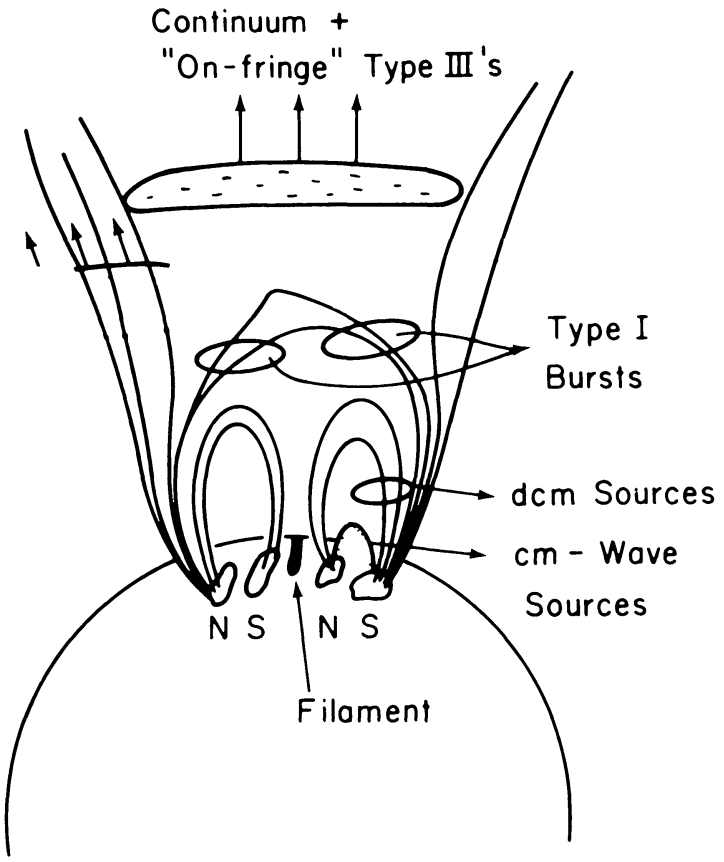

Fig. 51. Empirical model of noise storm region indicating position of storm type 'On-fringe' and 'Off-fringe' type III burst, together with noise storm activity in other regions (from Gergely and Kundu, 1975).

presence of neutral magnetic sheet high up in the corona. Filaments are associated with the reversal of the longitudinal photospheric magnetic field (Howard, 1959). A correlation between plage, filaments and type III bursts has been reported by Mercier (1973). Type I sources are embedded in a closed loop configuration and also at lower heights than that of type III burst. This explains the observed type I–type III frequency relationship. However, Aubier *et al.* (1978) re-examined the data used by Stewart and Labrum (1972) and found that type I and type III bursts were not associated as these bursts were originated from different active regions. The displacement of positions of type I and type III shown by Stewart and Labrum (1972) in their model is questioned by Aubier *et al.* (1978), who, in turn, proposed a model as shown in Figure 53. In this model, the positions of type I–type III sources are shown almost identical since according to their theory the same electron stream is responsible for both. The observed features of type I–type III bursts can be explained fairly satisfactorily by this model.

Observations carried out during the period 19 October to 2 November 1972 by the Culgoora radio-heliograph have further increased our understanding from the simultaneous observations of multiple sources of type I bursts and random shifts of their source positions. A model for the multiple sources of type I bursts has been

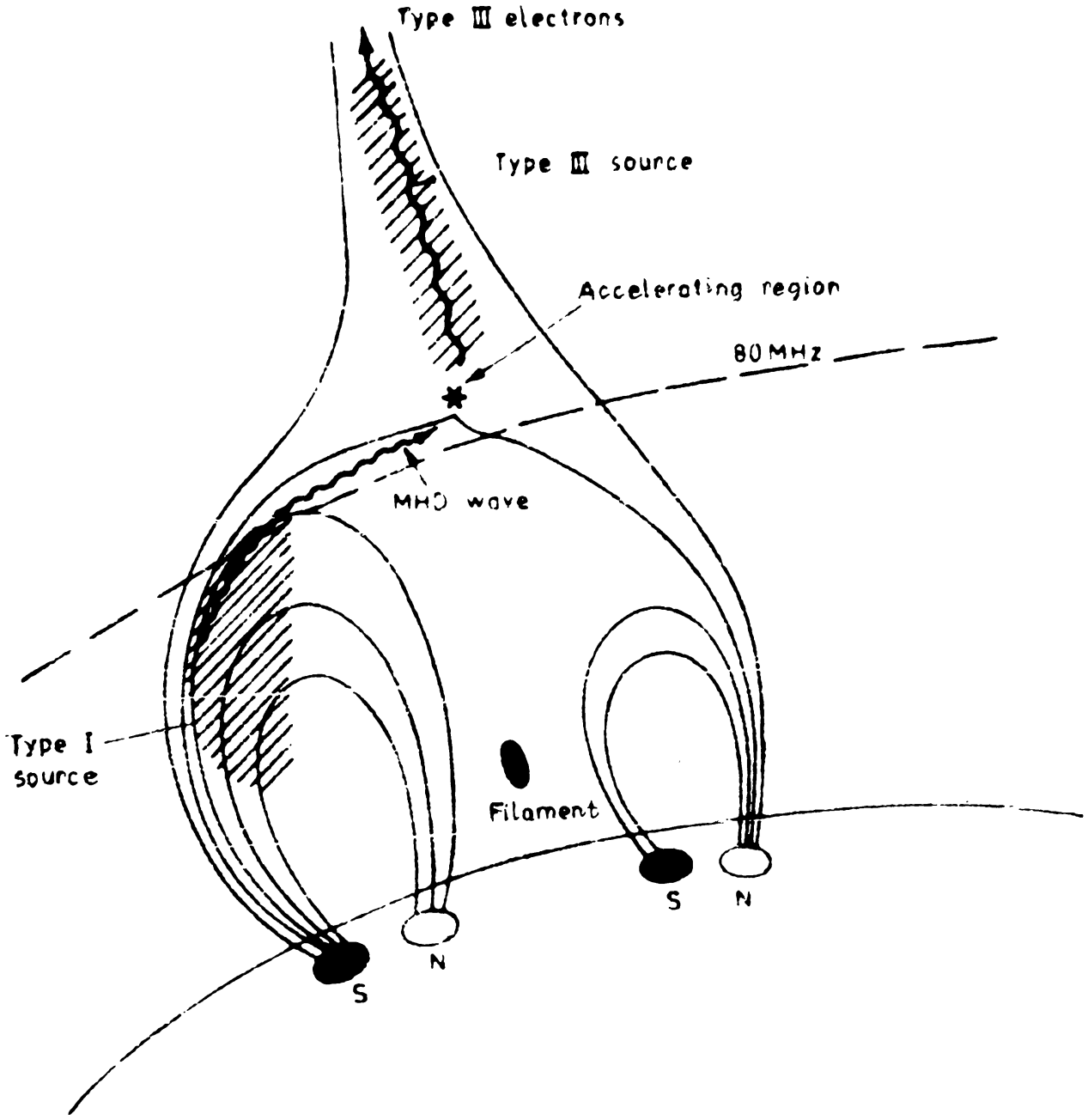

Fig. 52. Model showing observed relationship of type I and type III burst (from Stewart and Labrum, 1972).

proposed by Kai and Sheridan (1974) who have shown that type I sources occur in magnetic loops formed by closed magnetic field lines associated with a particular sunspot group. Observed random shifts in positions of type I bursts may be because of the complex nature of the magnetic fields of multiple sunspot groups.

10. Models of Decametric Noise Storm (Bursts)

In the frequency range 60–20 MHz, transition of metric type I burst to decametric

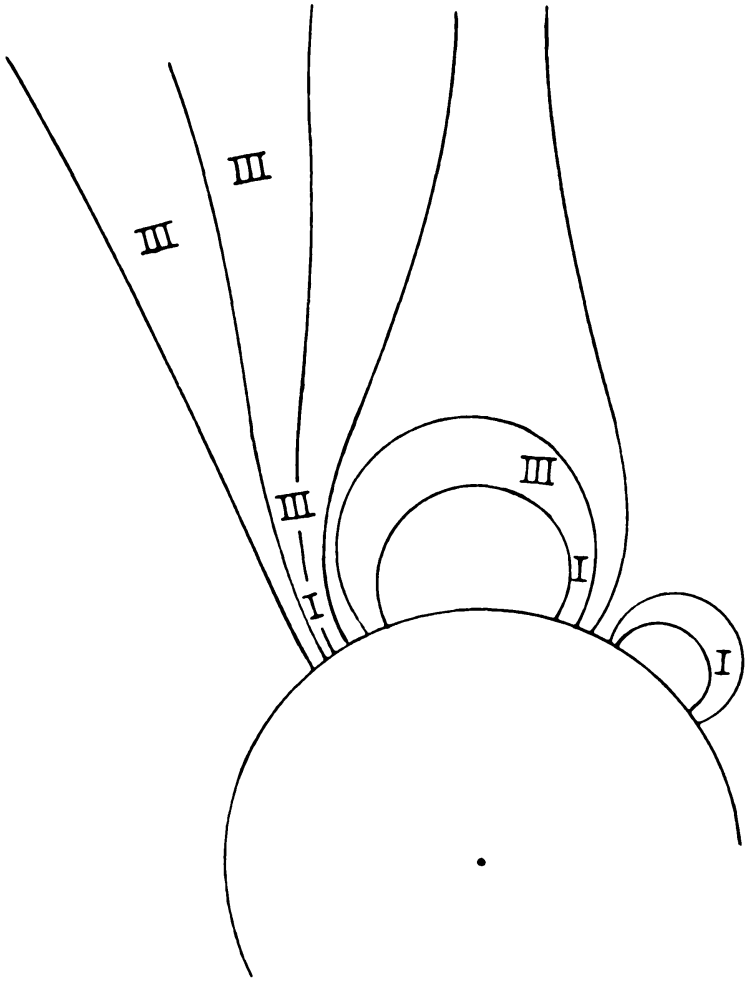

Fig. 53. Schematic representation of the magnetic field configurations in the source regions, showing when type I and or type III storms take place (from Aubier *et al.*, 1978).

type III burst takes place. It is also confirmed that decametric noise storms are always associated with metric noise storms.

Some of the 'BF' type spectral features originate in the source region itself such as chains of 'dot' emission, microscopic families of 'U' burst, type IIIb burst, etc. While some of the fine structure showing curvature along the frequency axis and C.B.'s appear to be propagational effects imposed on the original radiation while propagating from the source to the observer. A model to explain decametric III and 'BF' type bursts proposed by Sawant *et al.* (1978) is shown in Figure 54. Closed magnetic loop structures are observed up to 1 to $1.5R_{\odot}$ above the photosphere, beyond which the magnetic field lines are generally open. Energetic electrons required for generation of decametric type III bursts and for 'BF' type bursts are assumed to be accelerated by MHD waves (Takakura, 1963; Trakhtengerts, 1966; and Zaitsev and Fomichev, 1973). Consistent with smith and Pneuman's (1972) suggestion, the most likely place for energetic electrons to travel is along the edges of the streamer rather than the center of the streamer. The sources of bursts are density irregularities with excess

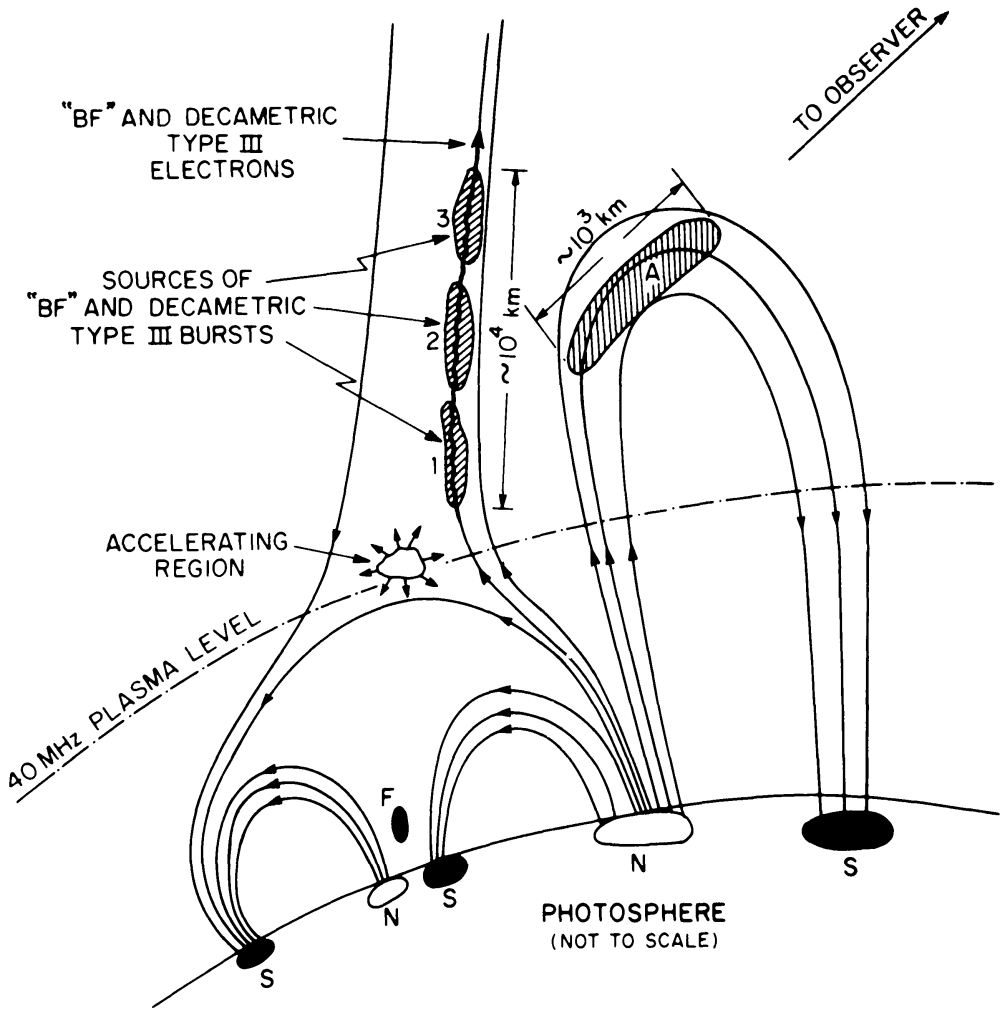

Fig. 54. Empirical model for decametric noise storm (burst component). F – represents the filaments. Thin hatched 1 to 3 sections show the source region of decametric bursts with excess electron density of 1–2% over the ambient. 'A' represents dense irregularity in the line of sight between the source and the observer, which is responsible for propagational effects (from Sawant *et al.*, 1978).

density of 1–2% and sizes of 10^3 to 10^4 km which are assumed to lie along the path of the exciter and are shown by hatching in Figure 54. For generation of burst radiation, plasma hypothesis is assumed. Induced scattering process is assumed for the conversion of Langmuir waves to transverse waves. Bursts are assumed to be generated at fundamental of the local plasma frequency. Depending upon the scale length of irregularity (L) and density gradient $\delta N/\delta\rho$: (i) chain of 'dot' emission ($L \approx 10^3$ km, $\delta N/\delta\rho = 0$), (ii) stria burst ($L \sim 10^4$ km, $\delta N/\delta\rho = 0$), and (iii) families of microscopic 'U' burst (more than three irregularities with $L = 10^3$ km and having $\delta N/\delta\rho \gtrless 0$) are generated. Following Takakura and Yousef (1975) the relative magnitude of the area of the beam and the area of the irregularities determine whether type IIIb or III bursts are genrated even though two different exciters travel along the same path. This also explains same observed positions for type IIIb and type III burst. The complexity of magnetic field lines (loops) connecting different active centers situated

nearby and far away from each other on the solar disk is observationally supported and different models depicting the same have been proposed by Lantos and Jarry (1970), McLean and Sheridan (1972), Kai and Nakajima (1974), and Kai and Sheridan (1974). For simplicity one such loop connecting other active centers little away from the main active center is shown in the same figure. An irregularity (shown by 'A') occasionally may delay part of the radiation generated in the nearby source region giving rise to group delay effect observed on burst profile as curvature along the frequency axis.

11. Concluding Remarks and Suggestions for Future Work

This review paper emphasizes the significance of high resolution solar decametric observations for the exploration of solar corona. The latest high sensitivity measurements of the decametric quiet Sun at different frequencies have enabled the determination of spectral index and existence of the slowly varying component. The occurrence of decametric noise storms and bursts provides an important link between metric phenomena on the one hand and hecto-kilometric phenomena on the other. This gives credence to the idea that just as the metric continuum serves as the energy reservoir for the decametric noise storm bursts, similarly the decametric continuum serves as the energy reservoir for the hecto-kilometric noise storm bursts. Recent work on the details of the decametric burst component has improved our understanding of different physical processes including the role of electron density irregularities intrinsic to the source and along the propagation path. These results support the mechanism of induced scattering of plasma waves on thermal ions together with the interaction of energetic electron beams with small scale irregularities for the generation of decametric bursts. Salient features of existing theories and models for type I–III bursts have been reviewed. A plausible model that incorporates generation of 'BF' type burst is suggested.

Having reviewed the high resolution observations obtained in recent years regarding noise storms and the varieties of bursts in the decameter range, their interpretations and theories, we come to the conclusion that more concerted efforts are necessary to obtain as complete information on these enigmatic solar phenomena as possible both on short term and long term basis in order to arrive at better quantitative understanding than has been possible so far. Specifically:

(i) In the coming years, it would be desirable to organize intense efforts on global scale, to make spectral and polarization observations in a systematic manner of decametric noise storms and bursts with high resolution in time, frequency coupled with high angular resolution and sensitivity. The decametric radio heliographs similar to those at Culgoora (Australia) and Clark Lake (U.S.A.) with high time resolution and operating over a wide frequency range will definitely help in delineating the morphology of the burst sources and their dynamics in the solar corona where the solar wind builds up. Such heliographs need to be established in different parts of the globe in order to achieve continuous surveillance of the solar activity.

(ii) Although some work on polarization at decameter wavelengths has been carried out, there is pressing need to incorporate polarimeters on satellites as almost no information is available at present on the polarization properties of hecto- and kilometric storms and bursts.

(iii) It would be worthwhile to confirm small scales (1–10 arc sec) of the irregularities in the vicinity of the Sun by long baseline interferometry (LBI) in the decametric range.

(iv) In order to verify the low frequency limit of type IIIb bursts, sweep frequency receiver with adequate frequency resolution should be included on future space missions.

(v) It would be desirable to track type II shock waves, in the vicinity of the Sun, using wide band decametric spectroscopy and, in the interplanetary medium, using interplanetary scintillation technique to study 3-dimensional evolution of interplanetary shock waves.

(vi) Systematic observations of the quiet Sun and the slowly varying component in the decameter range have just begun to appear. Hence, they need to be carried out for at least one complete solar cycle in coordination with high resolution optical studies of the Sun.

(vii) On theoretical front, since there are many gaps in our understanding of the coronal plasma processes, it appears that still there is scope for development of satisfactory theory of type III solar radio bursts and their variants over the entire meter to kilometer wavelength range, taking into consideration non-linear plasma instabilities in turbulent warm and hot plasma.

Acknowledgements

The present review would not have been possible but for the enthusiastic response of large number of solar radio astronomers the world over to our request to send preprints, reprints and photographs, for which we express our grateful thanks.

We sincerely thank Prof. K. R. Ramanathan, Emeritus Professor, Physical Research Laboratory (PRL) for his keen interest in this work. It is a great pleasure to acknowledge enthusiastic support and encouragement received from Prof. D. Lal, Director, PRL, for the Solar Radio Astronomy Programme at PRL. Assistance from M/s. A. H. Desai, N. V. Dalal, H. T. Ali, and D. Stephen in the preparation of the manuscript is highly appreciated.

This work is supported by the Department of Space, Government of India.

References

Abranin, E. P., Baselyan, L. L., Goncharov, N. Yu., Zaitsev, V. V., Zinichev, V. A., Rapoport, V. O., and Tsybko, Ya. G.: 1976, *Soviet Astron.* **19**, 602.

Abranin, E. P., Baselyan, L. L., Goncharov, N. Yu., Zaitsev, V. V., Zinichev, V. A., Levin, B. N., Rapoport, V. O., and Tsybko, Ya. G.: 1977, *Astron. J.* (*Russian*) **54**, 146.

Abranin, E. P., Baselyan, L. L., Goncharov, N. Yu., Zaitsev, V. V., Zinichev, V. A., Rapoport, V. O., and Tsybko, Yu. G.: 1978, *Solar Phys.* **57**, 229.
Achong, A.: 1974, *Solar Phys.* **37**, 477.
Achong, A. and Barrow, C. H.: 1975, *Solar Phys.* **45**, 467.
Akabane, K. and Cohen, M. H.: 1961. *Astrophys. J.* **133**, 258.
Aubier, M. G.: 1974, *Astron. Astrophys.* **32**, 141.
Aubier, M. and Boischot, A.: 1972, *Astron. Astrophys.* **19**, 434.
Aubier, M., Leblanc, Y., and Boischot, A.: 1971, *Astron. Astrophys.* **12,** 435.
Aubier, M., Leblanc, Y., and Moller-Pedersen, B.: 1978, to appear in *Astron. Astrophys.*
Babcock, H. D.: 1959, *Astrophys. J.* **130**, 364.
Baikov, I. S. and Lotova, N. A.: 1970, *Soviet Astron. A. J.* **13**, 823.
Barrow, C. H. and Saunders, H.: 1972, *Astrophys. Letters (GB)* **12**, 211.
Barrow, C. H. and Achong, A.: 1975, *Solar Phys.* **45**, 459.
Baselyan, L. L., Goncharov, N. Yu., Zaitsev, V. V., Zinichev, V. A., Rapoport, V. O., and Tysbko, Ya. G: 1974a, *Solar Phys.* **39**, 213.
Baselyan, L. L., Goncharov, N. Yu., Zaitsev, V. V., Zinichev, V. A., Rapoport, V. O., and Tsybko, Ya. G.: 1974b, *Solar Phys.* **39**, 223.
Baselyan, L. L., Goncharov, N. Yu., Zaitsev, V. V., Zinichev, V. A., Rapoport, V. O., and Tsybko, Ya. G.: 1977, *Solar Phys.* **52**, 141.
Bhatnagar, A., Ballabh, G. M., Rajmal Jain, Rao, S. S., Bhonsle, R. V., and Sawant, H. S.: 1977, *Proc. COSPAR Symp. B.*, Tel Aviv, Israel, p. 341.
Bhonsle, R. V.: 1976, *Proc. Symp. Solar Planetary Phys.*, 20–24 Jan. 1976, *Ahmedabad, India* **1**, 15.
Bhonsle, R. V., Fejfar, A., and Lusignan, B. B.: 1967, *Astrophys. J.* **146**, 595.
Bhonsle, R. V., Degaonkar, S. S., and Sawant, H. S.: 1973, *World Data Center A for Solar-Terrestrial Phys.*, Report UAG, 28, Part I, p. 234.
Bhonsle, R. V., Sawant, H. S., Degaonkar, S. S., and Alurkar S. K.: 1977, *Proc. COSPAR Symp. B.*, Tel. Aviv, Israel, p. 321.
Boischot, A.: 1974, in Gordon Newkirk, Jr. (ed.), 'Coronal Disturbances', *IAU Symp* **57**, 423.
Boischot, A. and Clavelier, B.: 1968, *Ann. Astrophys.* **31**, 445.
Boischot, A. and Lecacheux, A.: 1975, *Astron. Astrophys.* **40**, 55.
Boischot, A., de la Noë, J., and Moller-Pedersen, B.: 1970, *Astron. Astrophys.* **4**, 159.
Bougeret, J. L. and Steinberg, J. L.: 1977, *Astron. Astrophys.* **61**, 777.
Brueckner, G. E. and Bartoe, J. D. F.: 1974, *Solar Phys.* **38**, 133.
Butz, M., Furst, E., Hirth, W., and Kundu, M. R.: 1975, *Solar Phys.* **45**, 125.
Caroubalos, C. and Steinberg, J. L.: 1974a, in Gordon Newkirk, Jr. (ed.), 'Coronal Disturbances', *IAU Symp.* **57**, 239.
Caroubalos, C. and Steinberg, J. L.: 1974b, *Astron. Astrophys.* **32**, 245.
Chernov, G. P.: 1976a, *Soviet Astron.* **20**, 449.
Chernov, G. P.: 1976b, *Physica Solnechnoy Atkivnosty*, Sb. Statey, Nauka, p. 110.
Chernov, G. P., Chertok, I. M., Fomichev, V. V., and Markeev, A. K.: 1972, *Solar Phys.* **24**, 215.
Chen, Henry Sha and Shawhan, Stanley D.: 1978, *Solar Phys.* **57**, 205.
Chin, Y. C., Fung, P. C. W., and Lusignan, B. B.: 1971, *Solar Phys.* **16**, 135.
Chiuderi, C., Chiuderi Drago, F., and Noci, G.: 1972, *Solar Phys.* **26**, 343.
Cohen, H. Marshal: 1958, *Proceedings of I.R.E. Radio Astronomy*, Issue 172.
Cohen, M. H.: 1959, *Astrophys. J.* **130**, 22.
Cohen, M. H. and Fokker,, A. D. : 1959, *Paris Symposium on Radio Astronomy*, p. 252.
Cohen, M. H. and Gundermann, E. J.: 1969, *Astrophys. J.* **155**, 645.
Daigne, G. and Moller-Pedersen, B.: 1974 *Astron. Astrophys.* **37**, 355.
de Groot, T.: 1966, *Rech. Astr. Obs. Utrecht* **18**, 1.
de Groot, T., Loonen, J. P., and Slottje, C.: 1976, *Solar Phys.* **48**, 321.
de la Noë, J.: 1974, *Solar Phys.* **37**, 225.
de la Noë, J.: 1975, *Astron. Astrophys.* **43**, 201.
de la Noë, J. and Boischot, A.: 1972, *Astron. Astrophys.* **20**, 55.
de la Noë, J. and Gergely, T.: 1977, *Solar Phys.* **55**, 195.
de la Noë, J. and Moller-Pedersen, B.: 1971, *Astron. Astrophys.* **12**, 371.

de la Noë, J., Boischot, A., and Aubier, M.: 1972, in R. Ramaty and G. R. Stone (eds.), *High Energy Phenomena on the Sun Symposium Proceedings*, Sept. 28–30, p. 602.
Denisse, J. E.: 1960, Inf. Bull. Solar Radio Obs. No. 4, and URSI 13th General Assembly, London 1960.
Dennison, P. A. and Hewish, A.: 1967, *Nature* **213**, 343.
Dodge, J. C.: 1972, Thesis, University of Colorado, 'High-Resolution Fourier Spectroscopy and Polarimetry of Solar Radio Emission at 34 MHz'.
Dodge, J. C.: 1973a, Rep. UAG-28, Part I, WDC-A, p. 242.
Dodge, J. C.: 1973b, Rep. SN-1, Dept. Astro-Geophys., Boulder.
Dulk, G. A. and McLean, D. J.: 1978, *Solar Phys.* **57**, 279.
Dulk, G. A. Sheridan, K. V., Smerd, S. F., and Withbroe, G. W.: 1977, *Solar Phys.* **52**, 157.
Elgaroy, O.: 1959, in R. N. Bracwell (ed.), *Paris Symposium on Radio Astronomy*, Stanford University Press, Stanford, p. 248.
Elgaroy, O.: 1961, *Astrophys. Norv.* **7**, 123.
Elgaroy O.: 1965, in J. Aarons (ed.), *Solar System Radio Astronomy*, Plenum Press, New York, p. 201.
Elgaroy, O.: 1977, *Solar Noise Storms*, Pergamon Press, Oxford.
Elgaroy, O. and Ugland, O.: 1970, *Astron. Astrophys.* **5**, 372.
Ellis, G. R. A.: 1969, *Austrialian J. Phys.* **22**, 177.
Ellis, G. R. A. and McCulloch, P. M.: 1966, *Nature, London* **211**, 1970.
Ellis, G. R. A. and McCulloch, P. M.: 1967, *Australian J. Phys.* **20**, 583.
Erickson, W. C., Gergely, T. E., Kundu, M. R., and Mahoney, M. J.: 1977, *Solar Phys.* **54**, 57.
Fainberg, J. and Stone, R. G.: 1971a, *Solar Phys.* **17**, 392.
Fainberg, J. and Stone, R. G.: 1971b, *Astrophys. J.* **164**, L123.
Fainberg, J. and Stone, R. G.: 1974, *Space Sci. Rev.* **16**, 145.
Fainberg, J., Evans, L. G., and Stone, R. G.: 1972, *Science* **178**, 743.
Fitzenrater, R. J., Fainberg, J., Weker, R. R., Alvarez, H., Haddock, F. T., and Potter, W. H.: 1977, *Solar Phys.* **52**, 477.
Fokker, A. D.: 1960, Doctoral Thesis, University of Leiden.
Fokker, A. D.: 1965a, *Bull. Astron. Inst. Neth.* **18**, 111.
Fokker, A. D.: 1965b, in J. Aarons (ed.), *Solar System Radio Astronomy*, Plenum Press, New York.
Fokker, A. D.: 1965c, *Bull. Astron. Inst. Neth.* **11**, 118.
Fokker, A. D. and Rutten, R. J.: 1967, *Bull. Astron. Inst. Neth.* **19**, 254.
Fomichev, V. V. and Chertok, I. M.: 1970, *Soviet Astron. AJ* **14**, 216.
Fung, P. C. W. and Yip, W. K.: 1966, *Australian J. Phys.* **19**, 759.
Gergely, T. E.: 1974, Ph.D. thesis, University of Maryland, U.S.A., 'Decameter Storm and Type IV Radiation'.
Gergely, T. E. and Erickson, W. C.: 1975, *Solar Phys.* **42**, 467.
Gergely, T. E. and Kundu, M. R.: 1975, *Solar Phys.* **41**, 163.
Gergely, T. E., Kundu, M. R., Poland, A. L., and Munro, R. H.: 1978, COSPAR XXIst Meeting, Innsbruck, Austria, 29 May–10 June 1978, p. 59.
Gorden, I. M.: 1971, *Astrophys. Letters* **5**, 251.
Gurnett, D. A. and Frank, L. A.: 1975, *Solar Phys.* **45**, 477.
Grognard, R. J. M. and McLean, D. J.: 1973, *Solar Phys.* **29**, 183.
Haddock, F. T. and Graedel, T. E.: 1970, *Astrophys. J.* **160**, 293,
Hanasz, J.: 1966, *Australian J. Phys.* **19**, 635.
Hanasz, J., Aksenov, V. J., Komrakov, G. P., Schreiber, R., Welnowski, H., and Wikierski, B.: 1978, Private communication.
Hansen, R. J., Garcia, C. J., Grognard, R. J. M., and Sheridan, K. V.: 1971, *Proc. Astron. Soc. Australia* **2**, 57.
Harvey, C. C. and Aubier, M. G.: 1973, *Astron. Astrophys.* **22**, 1.
Harvey, G. A. and McNarry, L. R.: 1970, *Solar Phys.* **11**, 467.
Hauge, O.: 1956, *Astrophys. Norv.* **5**, 227.
Hewish, A.: 1971, in C. P. Sonnett, P. J. Coleman, Jr., and J. M. Wilcox (eds.), *Solar Wind Asilomar Conf.*, p. 477.
Hey, J. S., Parsons, S. J., and Phillips, J. W.: 1948, *Monthly Notices Roy. Astron. Soc.* **108**, 354.
Howard, R.: 1959, *Astrophys. J.* **133**, 983.

Ivano, K. G. and Livshits, M. A.: 1968, *Geomagnetic Aeronomy* **1**, 128.
Kai, K.: 1970, *Solar Phys.* **11**, 456.
Kai, K. and Nakajima, H.: 1974, *Astron. Soc. Japan* **26,** 379.
Kai, K. and Sheridan, K. V.: 1974, *Solar Phys.* **35**, 181.
Kaplan, S. A. and Tsytovich, V. N.: 1969, *Soviet Phys. Usp.* **12**, 42.
Kerdraon, A.: 1973, *Astron. Astrophys.* **27**, 361.
Korolev, O. S.: 1974, *Soviet Astron.* **17**, 518.
Korolev, O. S.: 1975, *Soviet Astron.* **19**, 747.
Kruger, A.: 1972, *Physics of Solar Continuum Radio Burst*, Akademic-Verlag, Berlin.
Kruse, U. E., Marshall, L., and Platt, J. R.: 1956, *Astrophys. J.* **124**, 601.
Kuiper, J. N.: 1975, *Solar Phys.* **44**, 173.
Kundu, M. R.: 1965, *Solar Radio Astronomy*, John Willey & Sons, New York, p. 5.
Kundu, M. R.: 1971, *Solar Phys.* **21**, 130.
Kundu, M. R. and Erickson, W. C.: 1974, *Solar Phys.* **36**, 179.
Kundu, M. R., Gergely, T. E., and Erickson, W. C.: 1977, *Solar Phys.* **53**, 489.
Labrum. N. R.: 1971, *Australian J. Phys.* **24**, 193.
Lacacheux, A. and Rosolen, C.: 1975, *Astron. Astrophys.* **41**, 223.
Lacombe, C. and Moller-Pedersen: 1971, *Astron. Astrophys.* **15**, 406.
Lantos-Jarry, M. F.: 1970, *Solar Phys.* **15**, 40.
Lawrence, R. S., Little, C. G., and Chivers, H. J. A.: 1964, *Proc. IEEE, U.S.A.* **52**, 4.
Leblanc, Y.: 1970, *Astron. Astrophys.* **4**, 315.
Leblanc, Y.: 1973, *Astrophys. Letters* **14**, 41.
Leblanc, Y. and Aubier, M. G.: 1977, *Astron. Astrophys.* **61**, 353.
Lin, R. P.: 1973, in R. Ramaty and R. G. Stone (eds.), *NASA Symposium on High Energy Phenomenon on the Sun*, Symp. Proceedings, 28–30 September 1972.
Lin, R. P., Evans, L. G., and Fainberg, J.: 1973, *Astrophys. Letters* **V4**, 191.
Malinge, A. M.: 1963, *Ann. Astrophys.* **26**, 97.
Malitson, M. H. and Erickson, W. C.: 1966, *Astrophys. J.* **144**, 337.
Malitson, M. H., Fainberg, J., and Stone, R. G.: 1973, *Astrophys J.* **183**, L35.
Malville, J. M.: 1962, *Astrophys. J.* **136**, 266.
Mangeney, A. and Veltri, P.: 1976a, *Astron. Astrophys.* **47**, 165.
Mangeney, A. and Veltri, P.: 1976b, *Astron. Astrophys.* **47**, 181.
Mattoo, S. K.: 1973, Ph.D. thesis, Gujarat University, Ahmedabad, India, 'Studies in Radio Astronomy'.
Mattoo, S. K., Bhonsle, R. V., and Alurkar, S. K.: 1975, *Indian J. Radio Space Phys.* **4**, 116.
Maxwell, A. and Rinehart, R.: 1974, *Solar Phys.* **37**, 437.
Maxwell, A. and Thompson, A. R.: 1962, *Astrophys. J.* **135**, 138.
McLean, D. J.: 1971, *Australian J. Phys.* **24**, 201.
McLean, D. J.: 1974, in G. Newkirk, Jr. (ed.), 'Coronal Disturbances', *IAU Symp.* **57**, 301.
McLean, D. J. and Sheridan, K. V.: 1972, *Solar Phys.* **26**, 176.
McLean, D. J., Sheridan, K. V., Stewart, R. T., and Wild, J. P.: 1971, *Nature* **234**, 140.
Melrose, D. B.: 1974, *Solar Phys.* **35**, 441.
Melrose, D. B.: 1975, *Solar Phys.* **43**, 79.
Melrose, D. B. and Sy, W. N.: 1972, *Australian J. Phys.* **25**, 387.
Mercier, C.: 1973, *Solar Phys.* **33**, 177.
Moller-Pedersen, B.: 1974. *Astron. Astrophys.* **37**, 163.
Moller-Pedersen, B., Smith R. A., and Mangency, A.: 1978, *Astron. Astrophys.*, (in press).
Moiser, S. R. and Fainberg, J.: 1975, *Solar Phys.* **40**, 501.
Murray Dryer: 1975, *Space Sci. Rev.* **17**, 277.
Neupert, W. M., Thomas, R. J., and Chapman, R. D.: 1974, *Solar Phys.* **34**, 349.
Newkirk, G. Jr.: 1967, *Ann. Rev. Astron. Astrophys.*, 213.
Newkirk, G. Jr.: 1971, in P. Macris (ed.), *Physics of the Solar Corona*, D. Reidel Publ. Co., Dordrecht, Holland, p. 66.
Newkirk, G. Jr.: 1974, in G. Newkirk, Jr. (ed.), 'Coronal Disturbances', *IAU Symp.* **57**.
O'Brien, P. A.: 1953, *Monthly Notices Roy. Astron. Soc.* **113**, 597.
Parker, E. N.: 1958, *Astrophys. J.* **128**, 664.

Payne-Scott, R. and Little, A. G.: 1951, *Australian J. Sci. Res.* **A4**, 508.
Prasad, B.: 1976, *Phys. Fluids* **19**, 464.
Pratap, R.: 1974a, *Il Nuovo Cimento* **19B (1)**, 44.
Pratap, R.: 1974b, *Pramana* **2(2)**, 327.
Radhakrishnan, V.: 1976, *Bull. Astron. Soc. India* **4**, No. 3, 57.
Riddle, A. C.: 1972, *Proc. Astron. Soc. Australia* **2**, 98.
Riddle, A. C.: 1974, *Solar Phys.* **35**, 153.
Riddle, A. C., Tandberg-Hansen, E., and Hansen, R. T.: 1973, in G. Newkirk, Jr. (ed.), 'Coronal Disturbances', *IAU Symp.* **57**, 335.
Roberts, J. A.: 1958, *Australian J. Phys.* **11**, 215.
Roberts, J. A.: 1959, *Australian J. Phys.* **12**, 327.
Rosenberg, H.: 1970, *Astron. Astrophys.* **9**, 159.
Sastry, Ch. V.: 1972, *Astrophys. Letters* **11**, 47.
Sastry, Ch. V.: 1976, paper presented at 3rd Meeting of Astronomical Soc. of India, Nainital, India.
Sawant, H. S.: 1977, Ph.D. Thesis, Gujarat Univ., 'Studies in Solar-Terrestrial Physics'.
Sawant, H. S., Alurkar, S. K., and Bhonsle, R. V.: 1975, *Nature* **253**, 329.
Sawant, H. S., Alurkar, S. K., and Bhonsle, R. V.: 1976a, *Proc. Symp. Solar Planetary Phys.*, 20–24 January, 1976, *Ahmedabad, India* **2**, 1.
Sawant, H. S., Bhonsle, R. V., and Alurkar, S. K.: 1976b, *Solar Phys.* **50**, 481.
Sawant, H. S., Bhonsle, R. V., Degaonkar, S. S., and Alurkar, S. K.: 1977, *Proc. COSPAR Symp. B.*, Tel-Aviv, Israel, p. 313.
Sawant, H. S., Degaonkar, S. S., Alurkar, S. K., and Bhonsle, R. V.: 1978a, (Abstract), *Bull. Astron. Soc. India* **6**, 52.
Sawant, H. S., Degaonkar, S. S., Alurkar, S. K., and Bhonsle, R. V.: 1978b, (Abstract), *Bull. Astron. Soc. India* **6**, 52.
Sawant, H. S., Degaonkar, S. S., Alurkar, S. K., and Bhonsle, R. V.: 1978c, (Abstract), *Proc. COSPAR XXIst Meeting*, Insbruck, Austria, p. 60.
Sawant, H. S., Degaonkar, S. S., and Bhonsle, R. V.: 1978d, (Abstract), paper presented at the *Plasma Phys. Symp.*, November 1978, Ahmedabad, India.
Shin, C. A. and Higgins, C. S.: 1959, *Austrialian J. Phys.* **12**, 357.
Sheridan, K. V.: 1970, *Proc. Astron. Soc. Australia* **1**, 304.
Smerd, S. F. and Dulk, G. A.: 1971, in R. Howard (ed.), *Solar Magnetic Fields*, D. Reidel Publ. Co., p. 616.
Smith, D. F.: 1974, *Space Sci. Rev.* **16**, 91.
Smith, R. A. and de la Noë, J.: 1976, *Astrophys.* **207**, 609.
Smith, D. F. and Pneuman, G. W.: 1972, *Solar Phys.* **25**, 461.
Solar Radio Group Utrecht: 1974, *Space Sci. Rev.* **16**, 45.
Steinberg, J. L.: 1972, *Astron. Astrophys.* **18**, 382.
Steinberg, J. L.: 1977, *Proceedings of the L. D. de Feiter Memorial Symposium on STIP*, Tel-Aviv, Israel, June, 1977.
Steinberg, J. L., Aubier Giraud, M., Leblanc, Y., and Boischot, A.: 1971, *Astron. Astrophys.* **10**, 362.
Steinberg, J. L., Caroubalous, C., and Bourgeret, J. L.: 1974, *Astron. Astrophys.* **37**, 109.
Stewart, R. T.: 1962, *Report on Radio Phys.*, Discussion, CSIRO, Australia.
Stewart, R. T.: 1972, *Proc. Astron. Soc. Australia* **2**, 100.
Stewart, R. T.: 1975, *Solar Phys.* **40**, 417.
Stewart, R. T. and Labrum, N.: 1972, *Solar Phys.* **27**, 192.
Stone, R. G. and Fainberg, J.: 1971, *Solar Phys.* **20**, 106.
Stone, R. G., Fainberg, J., and Fitzenreiter, R. J.: 1969, Programme and abstracts of URSI 1969 Spring Meeting, Washington, D. C., U.S.A., 21–24 April 1969, p. 55.
Sturrock, P. A.: 1961, *Nature* **192**, 58.
Suzuki, S.: 1961, *Ann. Tokyo, Astron. Obs.* **7**, 75.
Sy, W. N.: 1973, *Proc. Astron. Soc. Australia* **2**, 215.
Takakura, T.: 1963, *Astron. Soc. Japan* **15**, 462.
Takakura, T., Shahinaz Yousef: 1975, *Solar Phys.* **40**, 421.
Thiessen, G.: 1952, *Nature* **169**, 147.

Tidman, D. A., Birmingham, T. J., and Stainier, H. M.: 1966, *Astrophys. J.* **146**, 207.
Trakhtengerts, V. Yu.: 1966, *Soviet Astron. AJ* **10**, 281.
Tyler, L. G., Brenkle, J. P., Komarek, A. T., and Zygielbaum, T. A.: 1977, *J. Geophys. Res.* **82**, No. 28, 4335.
Vaiana, G. S., Davis, J. M., Giacconi, R., Krieger, A. S., Silk, J. R., Timothy, A. F., and Zombeck, M.: 1973a, *Astrophys. J.* **185**, L47.
Vaiana, G. S., Krieger, A. S., and Timothy, A. F.: 1973b, *Solar Phys.* **32**, 81.
Vereshkov, G. M.: 1974, *Soviet Astron.* **18**, 152.
Warwick, J. W.: 1965, *Solar System Radio Astronomy*, 131.
Warwick, J. W. and Dulk, G. A.: 1969, *Astrophys. J.* **158**, L123.
Warwick, J. W., Dulk, G. A., and Riddle, A. C.: 1975, Report PRA No. 3 Radio Astronomy Observatory of the University of Colorado.
Weber, R. R., Alexander, J. K., and Stone, R. G.: 1971, *Radio Sci.* **6**, 1085.
Weber, R. R., Fitzenreiter, R. J., Novaco, J. C., and Fainberg, J.: 1977, *Solar Phys.* **54**, 431.
Weiss, A. A.: 1963, *Australian J. Phys.* **16**, 240.
Wild, J. P.: 1951, *Australian J. Sci. Res.* **A4**, 36.
Wild, J. P.: 1957, in H. C. van de Hulst (ed.), 'Radio Astronomy', *IAU Symp.* **4**.
Wild, J. P.: 1967, *Proc. Inst. Radio Electron. Eng. (Australia)* **28**, 277.
Wild, J. P. and Sheridan, K. V.: 1958, *Proc. IRE* **46**, 160.
Wild, J. P. and Smerd, S. F.: 1972, *Ann. Rev. Astron. Astrophys.* **10**, 159.
Wild, J. P., Sheridan, K. V., and Neylan, A. A.: 1959, *Australian J. Phys.* **12**, 369.
Wild, J. P., Smerd, S. F., and Weiss, A. A.: 1963, *Ann. Rev. Astron. Astrophys.* **1**, 291.
Withbroe, G. L.: 1972, *Solar Phys.* **25**, 116.
Withbroe, G. L., Dupree, A. K., Goldberg, L., Huber, M. C. E., Noyes, R. W., Parkinson, W. H., and Reeves, E. M.: 1971, *Solar Phys.* **21**, 272.
Yip, W. K.: 1973, *Solar Phys.* **30**, 513.
Yoh, P. and James, J. C.: 1967, *Astrophys. J.* **149**, 441.
Zaitsev, V. V. and Fomichev, V. V.: 1973, *Soviet Astron.* **16**, 666.
Zheleznyakov, V. V.: 1965, *Soviet Astron.* **9**, 191.
Zheleznyakov, V. V.: 1970, *Radio Emission of the Sun and Planets*, Pergamon Press, Oxford.